



EYE-CLIMA

Verifying emissions
of climate forcers

Second Report on CO₂ and CH₄ Satellite Datasets: TROPOMI, GOSAT and GOSAT-2 XCH₄ Comparison

DELIVERABLE 1.2

Author(s):	T. Hilbig, O. Schneising-Weigel, M. Hilker, H. Bösch
Date of submission:	19-09-2024
Version:	1.0
Responsible partner:	University of Bremen
Deliverable due date:	31-08-2024
Dissemination level:	Public

Call:	HORIZON-CL5-2022-D1-02
Topic:	Climate Sciences and Responses
Project Type:	Research and Innovation Action
Lead Beneficiary:	NILU - Norsk Institutt for Luftforskning



Document History

Version	Date	Comment	Modifications made by
0.1	16-09-2024	First Draft	H. Boesch, T. Hilbig, M. Hilker
0.2	17-09-2024	Internal review	R. Thompson
0.3	18-09-2024	Final version	H. Boesch
0.4	19-09-2024	Formatting	B. Modalen
1.0	19-09-2024	Submitted to Commission	R. Thompson



Summary

This is the second report on the assessment of the CH₄ column data from satellites. The first report covers the TROPospheric Monitoring Instrument (TROPOMI) on board the Sentinel-5 Precursor satellite while this report focusses on the GOSAT and GOSAT-2 sensors. This second report is an update of the first report and we included the first report as part of this report to allow intercomparisons between TROPOMI and GOSAT.

Three TROPOMI XCH₄ data products have been inter-compared and assessed against ground-based reference data from the TCCON network. The datasets include the operational, reprocessed data product RPRO version 02.04.00, the SRON RemoTeC-S5P XCH₄ scientific product version 19.446 and the University of Bremen WFM-DOAS data product version 1.8. For GOSAT, the NIES full physics, the RemoTeC full physics and proxy, the FOCAL full physics and proxy and UoL-FP full physics and proxy datasets have been included. For GOSAT-2, the same retrievals have been used except that no UoL-FP data is available for GOSAT-2. The assessment of all datasets has been carried out globally and for the European domain.

For TROPOMI, we find that the operational and the SRON data products agree very well with each other. This is expected as both are based on the same retrieval algorithm. The WFMD dataset also overall agrees well with the two other datasets globally. There is a pronounced difference in coverage and number of data points with the WFMD product usually showing higher data volume and better coverage. Differences in the retrieved CH₄ values between WFMD and the two other datasets are more pronounced for the European domain than globally. Thus, it can be expected that surface flux inversions on a European domain will differ depending on the chosen dataset. Differences between the WFMD and the operational dataset are also noticeable when observing emission plumes in single overpasses. Here, the often-better coverage of WFMD offers better opportunities for detection of emission plumes. Also, the magnitude of CH₄ in the columns of these single overpasses can differ which can then lead to differences in the quantification of emissions.

The comparison to European TCCON sites of the TROPOMI datasets shows high correlation coefficients and low biases for all three datasets, with lowest biases obtained for the WFMD dataset (2.8 to 12.2 ppb) and the highest for the operational dataset (8.3 ppb to 17.2 ppb). The relative accuracy is similar for the three retrievals. Overall, the TCCON comparison demonstrates a high quality of the TROPOMI CH₄ retrievals.

As expected, the coverage and data volume of GOSAT and GOSAT-2 is much lower than for TROPOMI. Differences in coverage are found between different retrievals and especially between full physics and proxy retrievals. For the European domain, the coverage provided by the full physics algorithms is very low, in particular in winter, and the proxy retrievals appear better suited for regional flux inversions in terms of coverage. For GOSAT-2, better coverage is obtained compared to GOSAT with the NIES GOSAT-2 full physics dataset achieves coverage that approaches that from a proxy dataset.

On a global scale, the different GOSAT and GOSAT-2 datasets compare well. On a European scale, differences are more pronounced and the correlation between datasets can be low so that the choice of dataset can be expected to have an impact on regional flux inversions.

The assessment of GOSAT and GOSAT-2 data against ground-based TCCON data shows that biases tend to be low for all retrievals with values below 20 ppb and typical values of 5-10 ppb. The lowest absolute biases are observed for FOCAL and UoL-FP (FP) for GOSAT and for NIES and FOCAL for GOSAT-2. In terms of regional accuracy, best performance is found for UoL-FP proxy and FOCAL (FP) for GOSAT and for NIES for GOSAT-2.



TABLE OF CONTENTS

Document History.....	2
Summary	3
1. Introduction	5
2. Datasets	6
2.1. TROPOMI L2 XCH ₄	6
2.1.1. Operational – reprocessed data product RPRO version 02.04.00	6
2.1.2. SRON RemoTeC-S5P XCH ₄ scientific product version 19.446	7
2.1.3. University of Bremen WFM-DOAS data product version 1.8.....	8
2.2. GOSAT L2 XCH ₄	9
2.3. GOSAT-2 L2 XCH ₄	12
2.4. Total Carbon Column Observing Network (TCCON)	13
3. Analysis/Comparison of TROPOMI XCH ₄ data products	13
3.1. Methodology	13
3.2. Results and Discussion	14
3.2.1. Global Maps of monthly mean XCH ₄	14
3.2.2. Maps of monthly mean XCH ₄ – Europe.....	19
3.2.3 Time series	26
3.2.4. Single Orbits – Plume Studies.....	28
4. Analysis/Comparison of GOSAT and GOSAT-2 XCH ₄ data products	31
4.1. Methodology	31
4.2. Results and Discussion	31
4.2.1. Global Maps of seasonal mean XCH ₄ from GOSAT	31
4.2.2. Maps of seasonal mean XCH ₄ from GOSAT – Europe.....	37
4.2.3. Global Maps of seasonal mean XCH ₄ from GOSAT-2.....	43
4.2.4. Maps of seasonal mean XCH ₄ from GOSAT-2 – Europe	48
5. Comparison with TCCON XCH ₄	54
5.1. Methodology	54
5.2. Results and Discussion	54
5.2.1 TROPOMI XCH ₄ Comparison	54
5.2.2. GOSAT XCH ₄ Comparison	64
5.2.3. GOSAT-2 XCH ₄ Comparison.....	70
6. Conclusions	76
Acknowledgements	78
References	78



1. Introduction

Methane (CH₄) total atmospheric columns are measured by several satellite missions (GOSAT/-2, TROPOMI). GOSAT provides a continuous data record since 2009, which is now complemented by GOSAT-2. GOSAT/-2 has a coarse sampling pattern where individual soundings with a diameter of 10 km are spaced out by 100-200 km. Thus, GOSAT/-2 data is useful for regional scale flux inversions but is not well suited for more localised anthropogenic emission sources.

The more recently launched (2017) TROPOspheric Monitoring Instrument (TROPOMI) on board the Sentinel-5 Precursor satellite provides much superior coverage. It provides measurements with a spatial resolution of 7km × 7km/5km and daily global coverage. Besides the more conventional surface flux inversions (e.g. Lunt et al., 2021, Tsuruta et al., 2023), this has allowed the application of TROPOMI CH₄ data to investigate localised CH₄ sources (Schneising et al., 2020, Maasackers et al, 2022).

This is the second report on the assessment of satellite CH₄ data. In the first report, we evaluated the different TROPOMI CH₄ datasets that are generated with different retrievals: the operational TROPOMI product, the SRON data product and the IUP Bremen WFDM data products. In this report, we have evaluated seven GOSAT and five GOSAT-2 CH₄ datasets. For GOSAT, this includes the FOCAL, NIES, RemoTeC, UoL-FP retrievals using full-physics and proxy methods. For GOSAT-2, the UoL-FP retrieval is not available.

The evaluation includes an inter-comparison of the data products and an assessment against ground-based reference measurements from the TCCON network for a global and European domain.

This second report is an update of the first report and we included the first report as part of this report to allow intercomparisons between TROPOMI and GOSAT.



2. Datasets

2.1. TROPOMI L2 XCH₄

2.1.1. Operational – reprocessed data product RPRO version 02.04.00

Retrieval:

The S5P operational CH₄ retrieval algorithm is based on RemoTeC. The methane total column-averaged dry-air mole fraction (XCH₄) is retrieved from TROPOMI measurements of sun-light backscattered by Earth's surface and atmosphere in the NIR and SWIR. The S5P RemoTeC algorithm uses the full-physics approach that simultaneously retrieves the amount of atmospheric CH₄ and the physical scattering properties of the atmosphere. (Lorente et al., 2021)

Structure and version of the data set:

The data product (<http://doi.org/10.5270/S5P-3lcdqiv>) is stored as NetCDF4 file containing both the data and the metadata for the product. It is stored as a single file per orbit. In this analysis data version 02.04.00 is used.

Product Identifier: L2__CH4__

Example filename:

S5P_RPRO_L2__CH4__20180501T151424_20180501T165554_02841_03_020400_20221107T155403.nc

Variables used in this analysis:

Name/Data	Symbol	Units	Description	Data type	Dimension
longitude, longitude_bounds	lon	degree	SWIR pixel longitude (center & corners)	float	1,4
latitude, latitude_bounds	lat	degree	SWIR pixel latitude (center & corners)	float	1,4
methane_mixing_ratio_ bias_corrected	XCH ₄	ppb	bias corrected XCH ₄	float	1
qa_value	QA value for CH ₄			int	1

Table 1: Selected contents of the output product, as used in this analysis (S5P ATBD, 2022).

Applied filter and bias correction:

Following the recommendations for data usage (S5P MPC Product Readme Methane V02.05.00):

- The TROPOMI XCH₄ bias corrected data (methane_mixing_ratio_bias_corrected) is used. The bias correction is based on the retrieved surface albedo to further improve the accuracy and the fitness for purpose of the TROPOMI CH₄ product (S5P ATBD, 2022).
- A quality assurance value qa_value > 0.5 has been chosen. It includes, since version 2.3.1, pixels both over land and over ocean. Filtering on qa_value > 0.5 does not remove all pixels considered bad. Some pixels with too low methane concentrations are still present.

Known Data Quality Issues (S5P MPC Product Readme Methane V02.05.00):

- Single TROPOMI overpasses show stripes of erroneous CH₄ values in the flight direction.



- Uncertainties estimation: Uncertainties for the XCH₄ are only based on the single sounding precision due to measurement noise. For applications requiring an overall uncertainty estimate, it is proposed to multiply the provided error by a factor 2, which reflects the scatter of single sounding errors in the TCCON validation.

2.1.2. SRON RemoTeC-S5P XCH₄ scientific product version 19.446

Retrieval:

The SRON scientific product is based on the RemoTeC-S5P XCH₄ retrieval algorithm. Differences between the operational and SRON product (SRON Product User Guide, 2022) are:

- Altitude DEM: SRTM 15" (SRON), GMTED2010 S5P (Operational)
- Meteorology: ECMWF reanalysis (SRON), ECMWF forecast (Operational)

Note that the impact of the difference in meteorology is very small. The impact of the change in the DEM is significant and is mainly observed around Greenland.

Structure and version of the data set:

The data is provided in netCDF format and stored in a single file per orbit. It can be freely downloaded via the ftp site <ftp://ftp.sron.nl/open-access-data-2/TROPOMI/tropomi/>

Example Filename: s5p_l2_ch4_0446_<orbit number>.nc

Within this analysis the latest available data version 19_446 was used.

Applied filter and bias correction (SRON Product User Guide, 2022):

- In accordance with the operational data product, the quality assurance value qa_value > 0.5 was chosen.
- Filter setting used for the SRON scientific product are the same as applied for the operational data product
- TROPOMI CH₄ bias corrected data has been used



Variables used in this analysis:

Name/Data	Symbol	Units	Description	Data Type	Dimension
group: target_product					
xch4_corrected	XCH4	ppb	bias corrected XCH4	float	1
group: diagnostics					
qa_value	QA value for CH4			float	1
group: instrument					
longitude_center	lon	degree	SWIR pixel longitude (center)	float	1
latitude_center	lat	degree	SWIR pixel latitude (center)	float	1
longitude_corners		degree	SWIR pixel longitude (corners)	float	4
latitude_corners		degree	SWIR pixel longitude (corners)	float	4

Table 2: Selected contents of the output product, as used in this analysis.

2.1.3. University of Bremen WFM-DOAS data product version 1.8**Retrieval:**

The Weighting Function Modified Differential Optical Absorption Spectroscopy (WFMD) retrieval algorithm simultaneously retrieves the atmospheric column-averaged dry-air mole fractions XCH₄ from TROPOMI's radiance measurements in the SWIR spectral range. It is a linear least-squares method based on scaling (or shifting) pre-selected atmospheric vertical profiles. The vertical columns of the desired gases are determined from the measured sun-normalised radiance by fitting a linearised radiative transfer model to it (Schneising et al., 2019, 2023).

Structure and version of the data set:

The data is provided in netCDF format and stored in one file per day. It can be downloaded from: https://www.iup.uni-bremen.de/carbon_ghg/products/tropomi_wfmd/. We have used data version 1.8. This version includes

- Implementation of a dedicated de-stripping filter, which optimally preserves the original spatial trace gas features
- optimised quality filter reducing the number of outliers
- improved digital elevation model, this reduces the pseudo-noise component, resulting in an improved random error

Example Filename: ESACCI-GHG-L2-CH4-CO-TROPOMI-WFMD-20180501-fv3.nc



Applied filter and corrections:

- Quality flag = 0 (“good”) was applied.
- Post-processing: machine-learning-based quality filter. In v1.8, the cloud filtering over the Arctic ocean is considerably improved.

Variables used in this analysis:

Name/Data	Symbol	Unit	Description	Data Type	Dimension
longitude	lon	degree north	center longitude of the measurement, -90. to 90.	float	1
latitude	lat	degree east	center latitude of the measurement -180. to 180.	float	1
longitude_corners	lon	degree north	corner longitudes of the measurement, -90. to 90.	float	4
latitude_corners	lat	degree east	corner latitudes of the measurement, -180. to 180.	float	4
xch4	XCH4	ppb	XCH ₄	float	1
xch4_quality_flag	QA value for CH ₄		0 - “good quality” 1 - “potentially bad quality”	int	1

Table 3: Selected contents of the output product, as used in this analysis.

2.2. GOSAT L2 XCH₄

The GOSAT L2 XCH₄ datasets for the assessment have been taken from the Ensemble Median Algorithm (EMMA) produced for the Copernicus Climate Change Service. The purpose of the Ensemble Median Algorithm (EMMA) products is to generate a merged dataset for climate applications and is described in Reuter et al. (2020). EMMA uses as input individual Level 2 datasets generated by the different algorithms available for GOSAT (see Table 4: GOSAT XCH₄ retrieval algorithms). This includes full-physics (FP) and proxy retrievals.

EMMA already applies a level of harmonisation of the datasets:

- Only cloud-filtered and quality-filtered data is used
- All datasets have been brought onto a common a priori. This has been achieved by removing the individual a priori profile and replacing it with the simple climatology SLIM (Noël et al., 2022) according to the method described in Wunch et al. (2011) or Rodgers (2000).



Retrieval	Method	Reference
FOCAL-FP v3.0	Full physics	Noël et al. (2022)
FOCAL-PR v3.0	Proxy	Noël et al. (2022)
NIES v02.9xbc	Full physics	Yoshida et al., 2013
RemoTeC-FP v2.3.8	Full physics	Detmers et al. (2017a)
RemoTeC-PR v2.3.9	Proxy	Detmers et al. (2017b)
UoL-FP v7.3	Full physics	Boesch and Di Noia (2024)
UoL-PR v9.0	Proxy	Parker et al. (2020)

Table 4: GOSAT XCH₄ retrieval algorithms

Retrievals:

NIES: The retrieval algorithm for the SWIR L2 product developed at NIES (Yoshida et al., 2013) is a full physics-based algorithm that explicitly considers the scattering processes by particles in the atmosphere in the radiative transfer calculations. To speed-up the radiative transfer calculation, the fast radiative transfer model proposed by Duan et al. (2005) is used which calculates the single-scattering radiance accurately and the multiple-scattering radiance approximately based on the equivalence theorem with a double-k distribution approach. The retrieval performs a simultaneous 4-band retrieval to infer CO₂ and CH₄ profiles on 15 vertical layers together with aerosol and surface parameters using the optimal estimation method. The aerosol vertical profile is retrieved on 6 layers. Also retrieved is the logarithm of the mass mixing ratio of fine-mode aerosols (carbonaceous and sulfate) and coarse-mode aerosols (soil dust and sea salt) with a priori values taken from the SPRINTARS model. Aerosol optical properties are computed based on information from the SPRINTARS model. Post-screening of the retrieval is based on the degrees of freedom, fit quality (mean-squared values of the residual spectra), AOD at 1.6 microns, surface pressure deviation from a priori, and the so-called blended albedo. The NIES product has been bias-corrected according to Inoue et al. (2016).

FOCAL: The FOCAL (Fast atmospheric trace gases retrieval) method is based on a full-physics retrieval in which scattering is approximated by a single layer so that an analytic solution can be computed (Reuter et al., 2017a, b). Atmospheric trace gases profiles on 5 layers, scattering parameter and surface parameter are estimated simultaneously using the optimal estimation method from a multi-window fit. First, a basic post-processing step is carried out based on filtering for good convergence, maximum residual-to-signal ratio, and maximum SZA of 75°. This is followed by quality filtering using a method based on minimisation of the local variance. Here, the variance of the difference between the retrieved quantity and its median of binned data is computed and then variables from a given list of candidate variables are selected based on their ability in reducing the local variance when removing data according to thresholds. Finally, a bias correction is applied derived using random forest regression where the SLIM climatology is used as reference data. The FOCAL proxy product is derived from the normal FOCAL XCO₂ and XCH₄ products by ratioing and normalisation with the SLIM CO₂ climatology.



RemoteTeC: Remote Sensing of Greenhouse Gases for Carbon Cycle Modeling (RemoTeC) is a full multiple scattering retrieval that employs the Phillips-Tikhonov regularization scheme to estimate atmospheric, and surface parameters from simulations fit to 4 windows (Schepers et al., 2012). To avoid time consuming line-by-line radiative transfer calculations the linear-k method developed by Hasekamp and Butz (2008) is used. CO₂ and CH₄ profiles are retrieved on 12 vertical layers. Aerosols are parameterised using a Gaussian shaped aerosol profile where height and width is retrieved together with the total aerosol column and an aerosol size parameter α (power of an assumed power law size distribution function). The XCH₄ L2 data is bias-corrected through regression analysis against TCCON data using the parameters solar zenith angle and aerosol filter parameter (an empirical parameter that combined different aerosol parameters). The full physics data is quality-filtered using a number of parameters including fit quality, aerosol parameters, and clear-sky ratio of CO₂ and H₂O. The proxy variant uses a simplified retrieval where the scattering radiative transfer is replaced with an absorption-only (non-scattering) calculation and no aerosol parameters are included. The retrieved XCH₄/XCO₂ ratio is normalized using Carbontracker model data. Quality-filtering of the proxy data is less stringent and a simple bias-correction is applied.

UoL-FP: The University of Leicester Full Physics algorithm (UoL-FP) is a full multiple scattering retrieval algorithm that used the optimal estimation method to infer CO₂ and CH₄ profiles together with aerosol and surface parameters (Cogan et al., 2012). The forward model of the algorithm uses the Low-Stream-Interpolation method to accelerate the time-consuming radiative transfer calculations (O'Dell, 2010). CO₂ and CH₄ profiles are inverted on 20 vertical levels. Aerosols are represented by a large and small mode aerosol profile with aerosol optical properties derived from a CAMS-based climatology. The XCH₄ data is bias-corrected by regression analyses against TCCON data for aerosol and surface parameters. The quality-filtering is primarily based on fit-quality and a posteriori errors. Similar to RemoTeC, the proxy variant of UoL-FP uses a simplified, fast forward model and no aerosol parameters are included in the retrieval. The normalisation of the retrieved XCH₄/XCO₂ ratio uses the median of an ensemble of models (CAMS, NOAA CarbonTracker, Geos-Chem) (Parker et al, 2020). Quality-filtering based on fit quality is applied and a global offset is corrected that has been derived from comparisons to TCCON.

Structure and version of the data set:

- The RemoTeC and UoL-FP datasets are provided in netCDF format and available from the Copernicus Atmosphere Data store (<https://ads-beta.atmosphere.copernicus.eu/>)
- The NIES dataset is provided in hdf5 format and available from the GOSAT Data Archive Service (GDAS) https://data2.gosat.nies.go.jp/index_en.html
- THE FOCAL dataset is provided in netCDF format and available from https://www.iup.uni-bremen.de/~ghguser/gosat_focal.php
- The EMMA dataset v4.5 is provided in netCDF format and available from the Copernicus Atmosphere Data store (<https://ads-beta.atmosphere.copernicus.eu/>)



Applied filter and corrections:

- Only bias-corrected and quality-filtered data has been used
- See above retrieval description and references for more information on the bias-correction and quality filtering for individual retrievals

2.3. GOSAT-2 L2 XCH₄

Similar to GOSAT L2 XCH₄, GOSAT-2 L2 XCH₄ data has also been taken from the EMMA v4.5 dataset. The included algorithms are similar to those for GOSAT, except that no UoL-FP dataset is available for GOSAT-2 (See Table 5). The same EMMA harmonisation procedure has been applied for GOSAT-2 as for GOSAT.

Retrievals

In the case of the NIES GOSAT-2 retrieval, the used algorithm is similar to the GOSAT retrieval. One change is that aerosols are now also represented on 15 vertical layers and no longer on 6 layers only. In contrast to the GOSAT dataset, no bias correction has been applied in the NIES GOSAT-2 v2.00 product. However, a bias correction has been developed subsequently and it can be applied by the user. This bias correction depends on 3 parameters (surface pressure difference, AOT, ILS stretch) and is described in Yoshida et al., (2023).

For FOCAL, the retrieval for GOSAT and GOSAT-2 is identical and the same methods are used for quality-flagging and bias correction but the included parameters and thresholds have been tailored to GOSAT-2 and thus will differ to those of the GOSAT retrieval.

The RemoTeC retrieval applied to GOSAT-2 is the same as for GOSAT, but the bias correction for GOSAT-2 uses a different set of parameters (surface albedo for land, the ratio of retrieved to a priori O₂ column for ocean). Similar quality-filtering is applied to GOSAT-2 as for GOSAT.

Retrieval	Method	Reference
FOCAL-FP v3.0	Full physics	Noël et al. (2022)
FOCAL-PR v3.0	Proxy	Noël et al. (2022)
NIES v02.00	Full physics	Yoshida and Oshio, 2020
RemoTeC-FP v2.0.0	Full physics	Krisna et al. (2021)
RemoTeC-PR v2.0.0	Proxy	Krisna et al. (2021)

Table 5: GOSAT-2 XCH₄ retrieval algorithms

Structure and version of the data set:

- The RemoTeC GOSAT-2 datasets is provided in netCDF format and available from the Copernicus Atmosphere Data store (<https://ads-beta.atmosphere.copernicus.eu/>)
- The NIES GOSAT-2 dataset is provided in hdf5 format and available from the GOSAT Data Archive Service (GDAS) https://data2.gosat.nies.go.jp/index_en.html



- THE FOCAL GOSAT-2 dataset is provided in netCDF format and available from https://www.iup.uni-bremen.de/~ghguser/gosat_focal.php
- The EMMA dataset v4.5 is provided in netCDF format and available from the Copernicus Atmosphere Data store (<https://ads-beta.atmosphere.copernicus.eu/>)

Applied filter and corrections:

- Only quality-filtered data has been used. The NIES data is not bias corrected. All other GOSAT-2 datasets have a bias correction applied
- See above retrieval description and references for more information on the bias-correction and quality filtering for individual retrievals

2.4. Total Carbon Column Observing Network (TCCON)

The Total Carbon Column Observing Network (TCCON) is a network of ground-based Fourier transform spectrometers. The first instrument was installed in 2004 at Park Falls, USA. The network has expanded to more than 25 operational stations worldwide. It measures direct solar spectra in the NIR to SWIR and provides atmospheric column-averaged dry-air mole fractions of CO₂, CH₄, CO, N₂O, H₂O, HDO, and HF (Wunch et al., 2015). The TCCON error assessment for the GGG2020 release estimates a total error of 0.4% (7 ppb) for CH₄ (Laughner et al., 2023).

Structure and version of the data set

The data is provided in netCDF format and can be downloaded from <http://tccodata.org/>. It contains the retrieved values, and ancillary data like surface pressure, temperature, averaging kernels and a priori profiles. (<https://tcon-wiki.caltech.edu/Main/DataDescriptionGGG2020>).

For this analysis, only European sites were selected, as summarised in Table 6: European TCCON sites used in the comparison; <https://tccodata.org/> (last access: 08.11.2023 for Sodankylä site, 01.08.2023 other sites) The current data version is GGG2020.

Site	Start Date	End Date	Version	Reference
Bremen	2009-01-06	2021-06-24	GGG2020.R0	Nothold et al., 2022
Garmisch	2007-07-18	2023-05-04	GGG2020.R0	Sussmann et al., 2023
Harwell	2021-05-30	2023-09-30	GGG2020.R0	Weidmann et al., 2023
Karlsruhe	2014-01-15	2023-06-26	GGG2020.R1	Hase et al., 2023
Orléans	2009-09-06	2022-10-12	GGG2020.R0	Warneke et al., 2022
Paris	2014-09-23	2022-06-29	GGG2020.R0	Té et al., 2022
Sodankylä	2009-05-16	2023-05-30	GGG2020.R0	Kivi et al., 2022

Table 6: European TCCON sites used in the comparison; <https://tccodata.org/> (last access: 08.11.2023 for Sodankylä site, 01.08.2023 other sites)

3. Analysis/Comparison of TROPOMI XCH₄ data products

3.1. Methodology

Three different TROPOMI XCH₄ data products, as introduced in section 2, were compared. For this comparison, the data has been converted to monthly means and gridded on a 0.5° × 0.5° grid. The resulting global and European comparison maps together with the standard deviation, as a measure of



the variation of the daily means, and the number of measurements available per grid box are presented in Section 3.2. Additionally, we derived the number of days with sufficient measurements per grid box and months. The limit was chosen to be 10 data points. Direct comparison of the WFMD and the SRON scientific product with the operational data set are given as scatterplots. Note that potential differences in a priori CH_4 profiles used in the different retrievals have not been corrected for this comparison.

3.2. Results and Discussion

The following sections show example maps for winter and summer months, February 2020 and August 2020 respectively, on a global scale and for Europe. The complete set of Figures for the full TROPOMI record data record from May 2018 to May 2022 is available from <https://nc.uni-bremen.de/index.php/s/AZNgkQtrHrZSbgf>.

3.2.1. Global Maps of monthly mean XCH_4

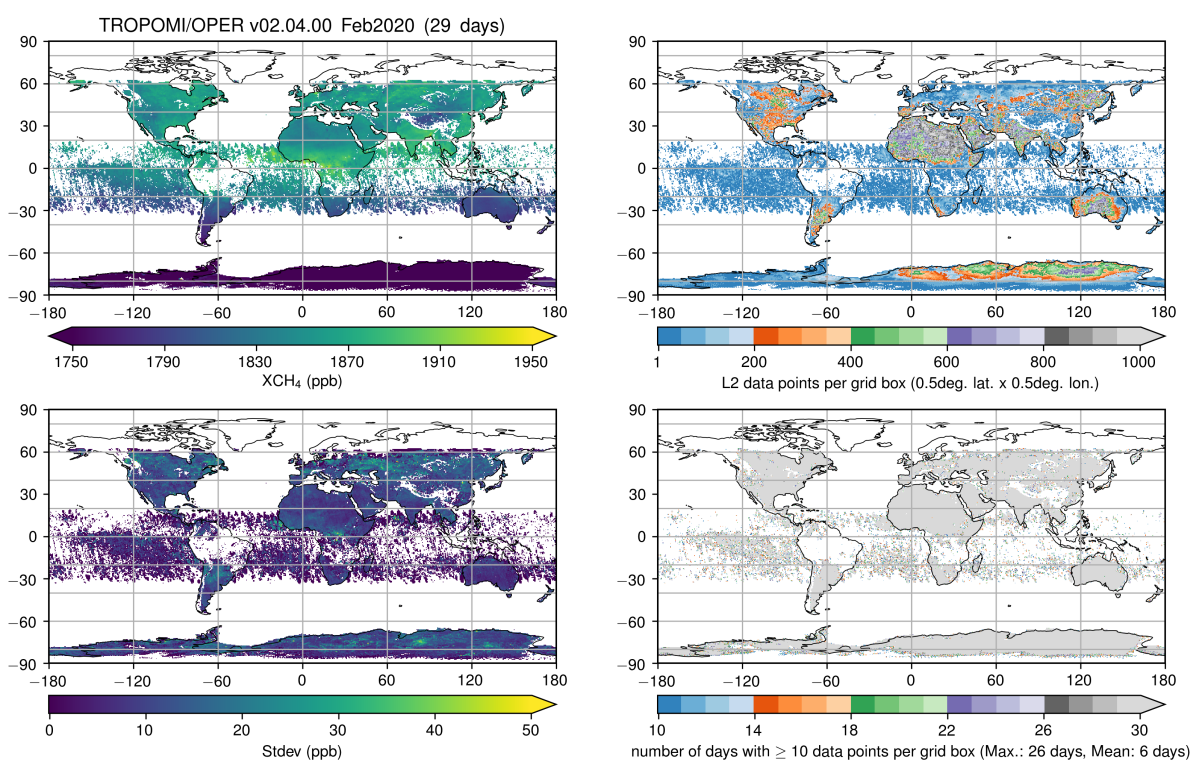


Figure 1: *Left:* Monthly averages of the operational (reprocessed) data product RPRO version 02.04.00 (*top panel*) and corresponding standard deviation for February 2020 (*bottom panel*). *Right:* Number of measurements contained in monthly mean as shown in the left panel (*top panel*) and number of days with more than 10 measurements per grid cell (*bottom panel*).

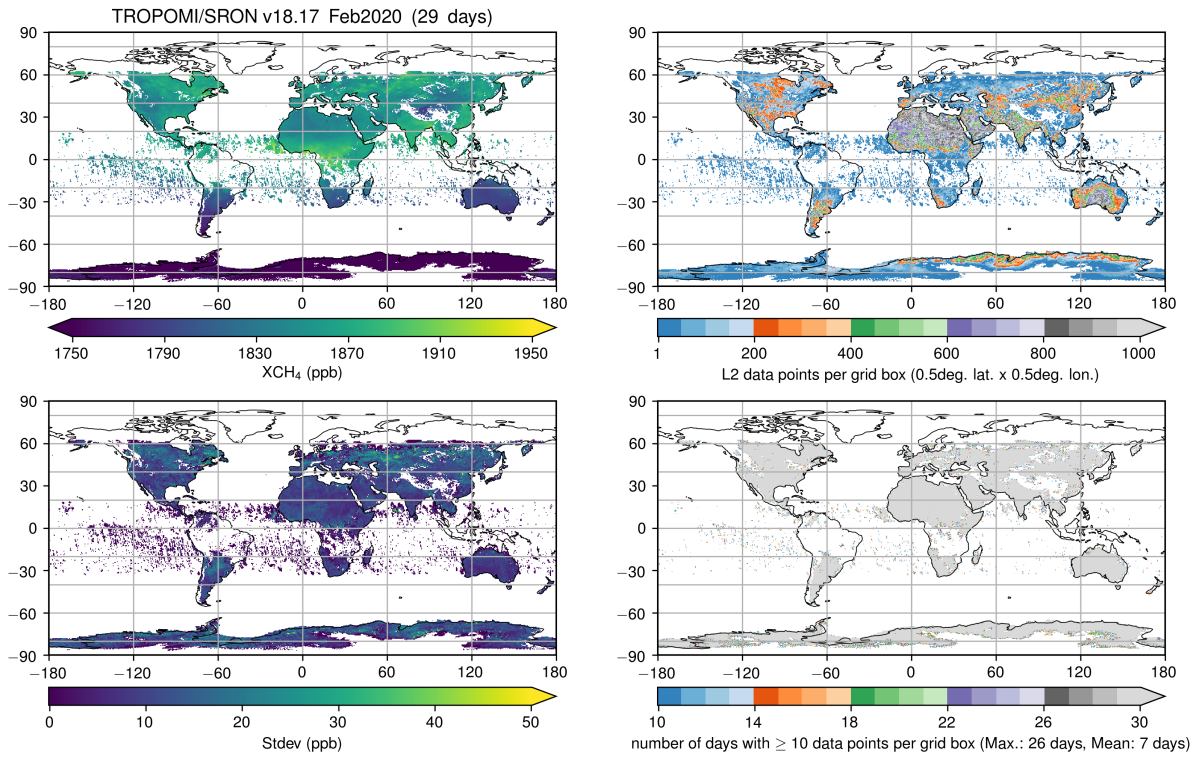


Figure 2: As Figure 1 but for SRON RemoTeC-S5P XCH₄ scientific product version 19.446

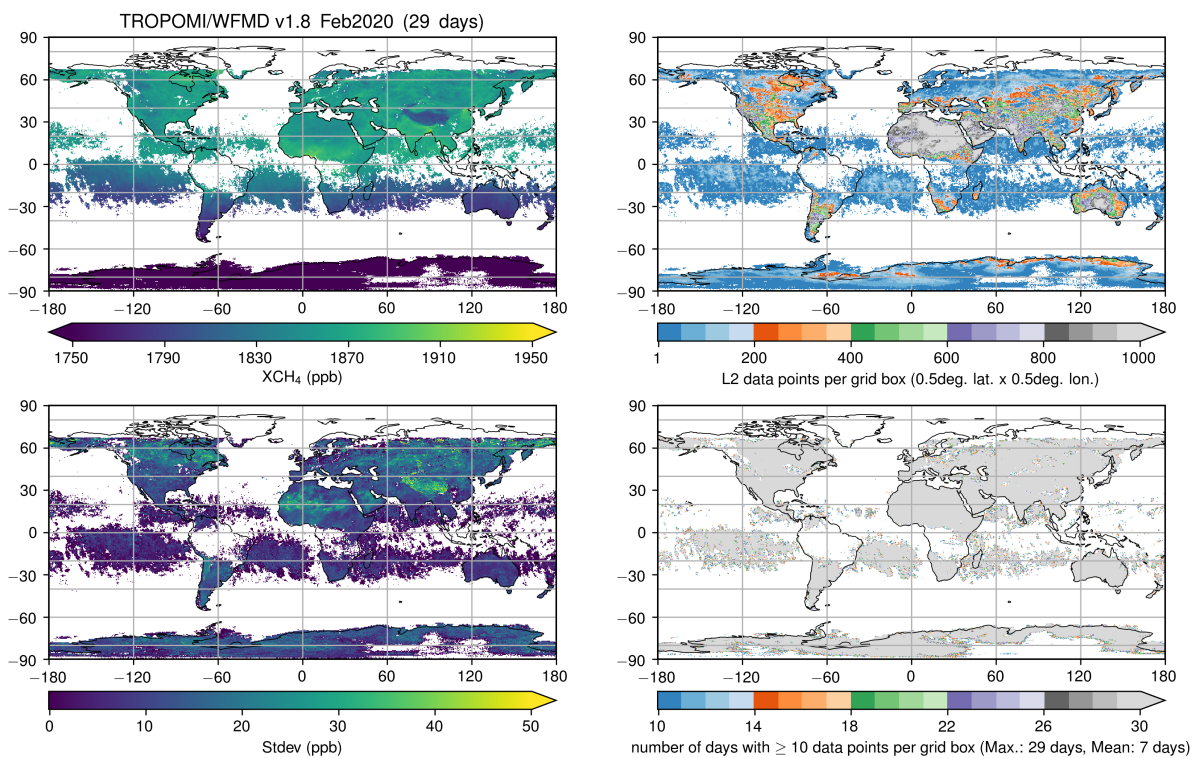


Figure 3: As Figure 1 but for the University of Bremen WFM-DOAS data product version 1.8



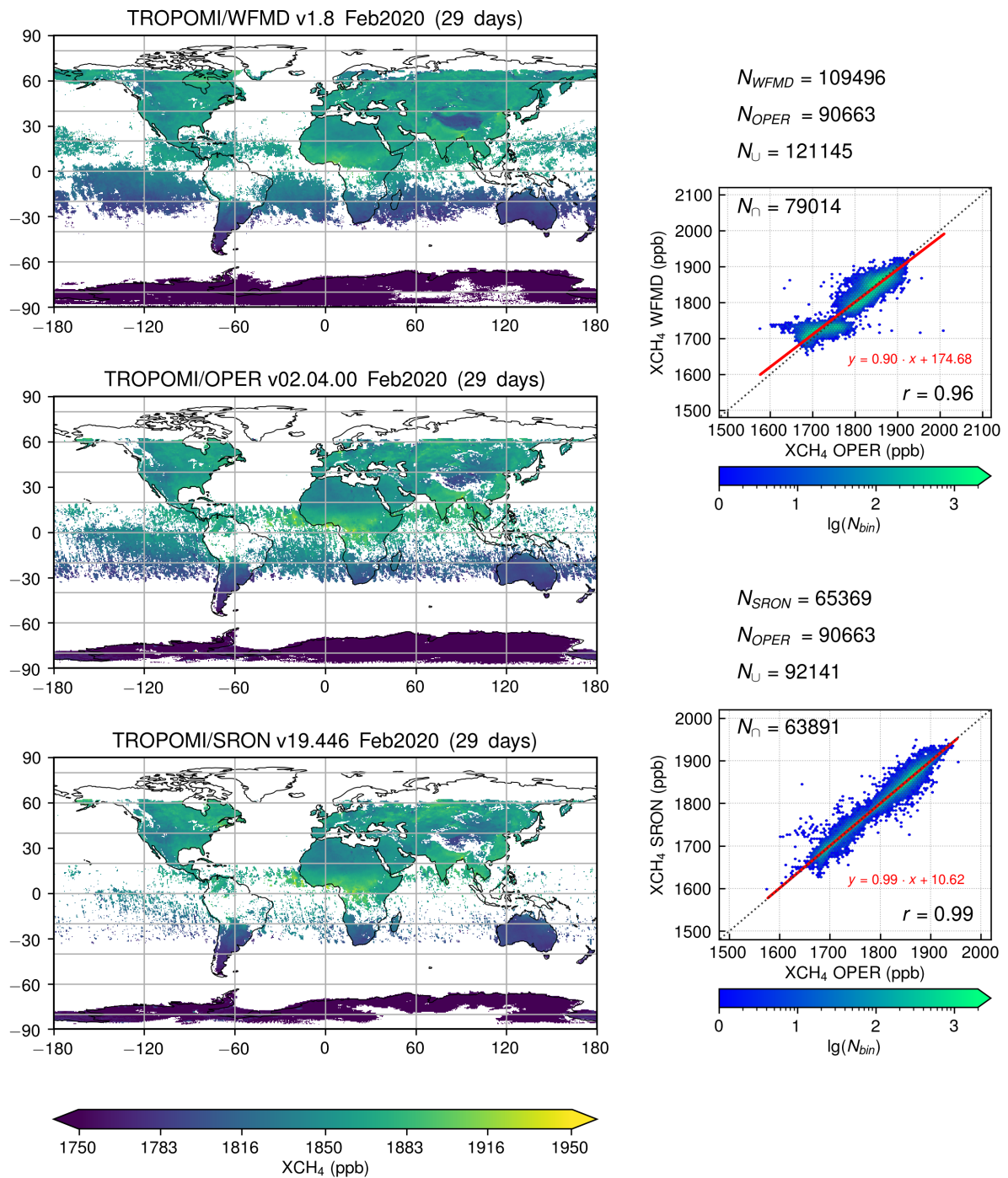


Figure 4: Comparison of TROPOMI monthly mean XCH₄ for three data products as shown in Figure 1 complemented with scatterplots. N_o gives the number of data points and r the correlation coefficient. Also given is a linear fit.

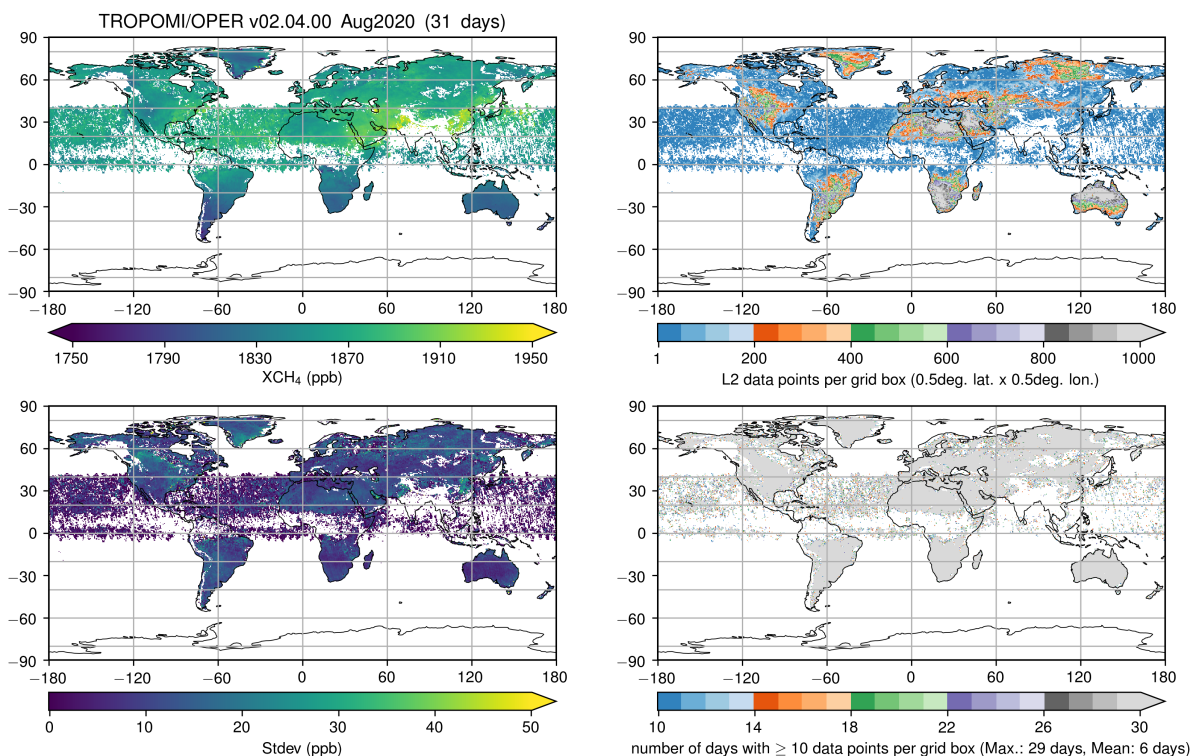


Figure 5: Left: Monthly averages of the operational (reprocessed) data product RPRO version 02.04.00 and corresponding standard deviation for August 2020. Right: Number of measurements contained in monthly mean as shown in the left panel (top) and number of days with more than 10 measurements per grid cell (bottom).

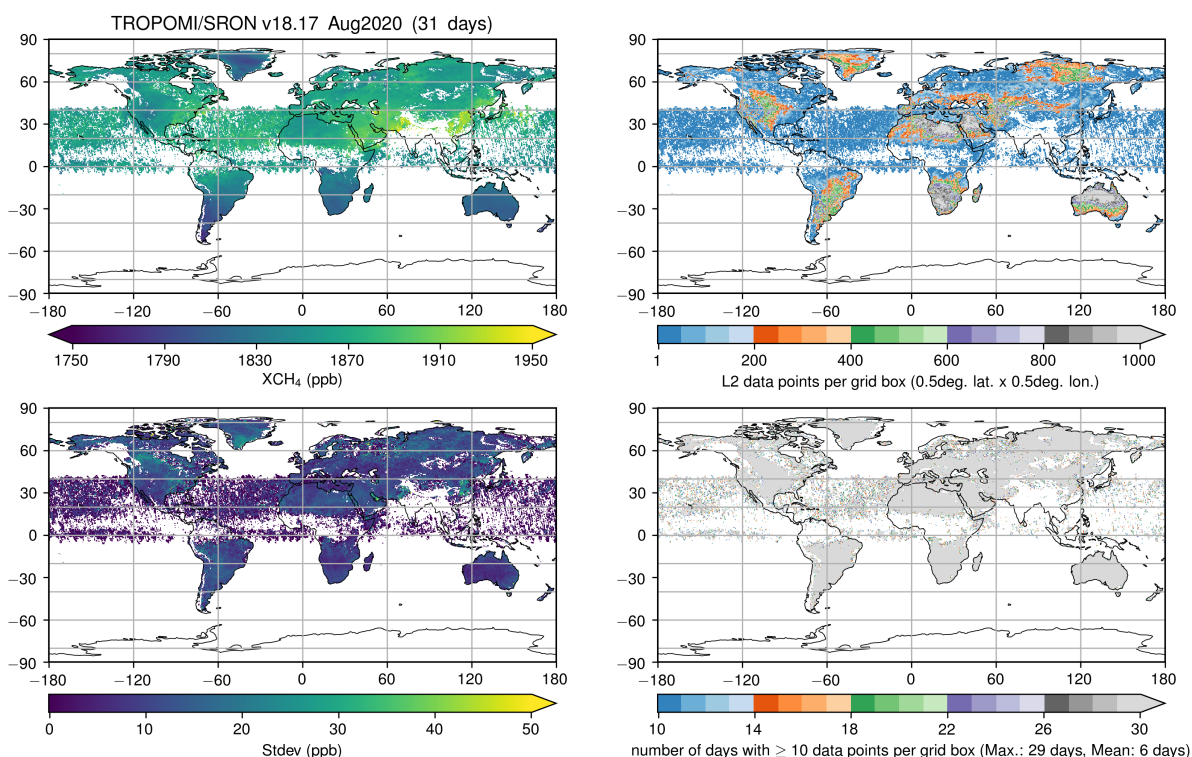


Figure 6: As Figure 5 but for SRON RemoTeC-S5P XCH₄ scientific product version 19.446



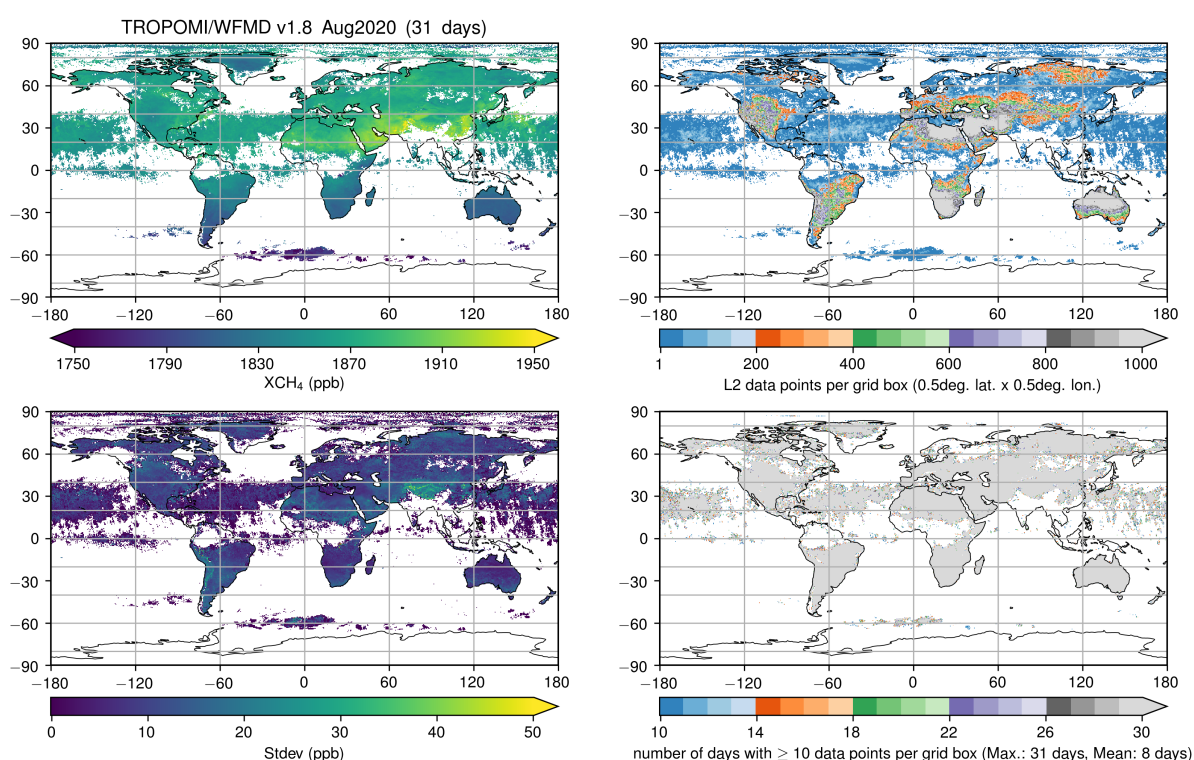


Figure 7: As Figure 5 but the University of Bremen WFM-DOAS data product version 1.8.

Overall, the global maps of TROPOMI XCH₄ are in good agreement between the three data products, the operational (reprocessed) data product RPRO version 02.04.00, the SRON RemoTeC-S5P XCH₄ scientific product version 19.446 and the University of Bremen WFM-DOAS data product version 1.8. The WFMD data product typically provides more data points and better coverage. This is well visible at high latitudes or over water. As expected, the operational product and the SRON product show high agreement as they are based on the same algorithm. As shown by the scatter plots, slightly larger differences are observed between the WFMD dataset and the operational dataset and the correlation coefficient is typically a bit reduced. The WFMD dataset shows a larger standard deviation over some regions which is likely the result of the more relaxed quality filter and the subsequent higher data throughput.

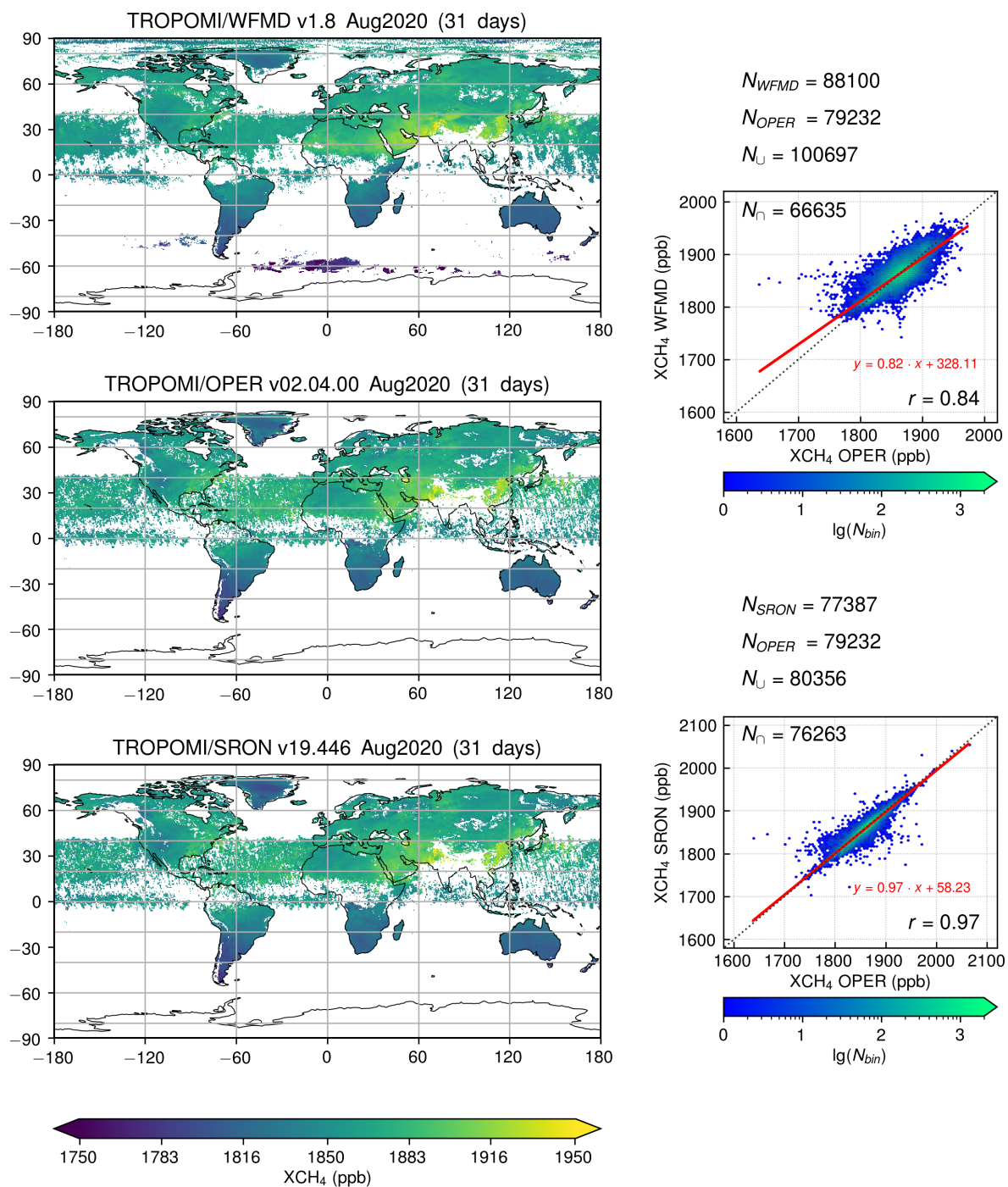


Figure 8: Comparison of TROPOMI monthly mean XCH₄ for three data products as shown in Figure 5 complemented with scatterplots. N_0 gives the number of data points and r the correlation coefficient. Also given is a linear fit.

3.2.2. Maps of monthly mean XCH₄ – Europe

We have repeated the global analysis from Section 3.2.1 but for the European domain. This was chosen to cover the longitudes 20°W to 50°E and the latitudes 30°N to 75°N. Note the changed colour scale in comparison to Section 3.2.1.

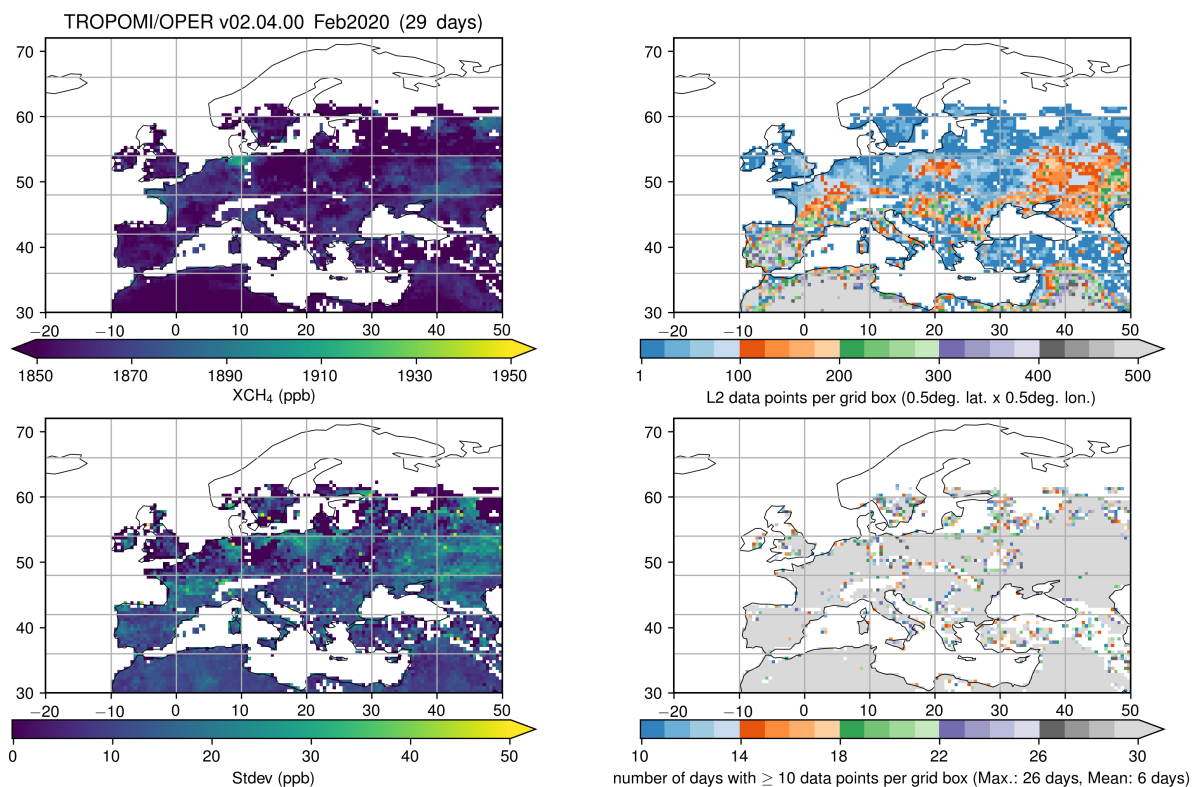


Figure 9: Left: Monthly averages of the operational (reprocessed) data product RPRO version 02.04.00 and corresponding standard deviation for February 2020. Right: Number of measurements contained in monthly mean as shown in the left panel (top) and number of days with more than 10 measurements per grid cell (bottom).

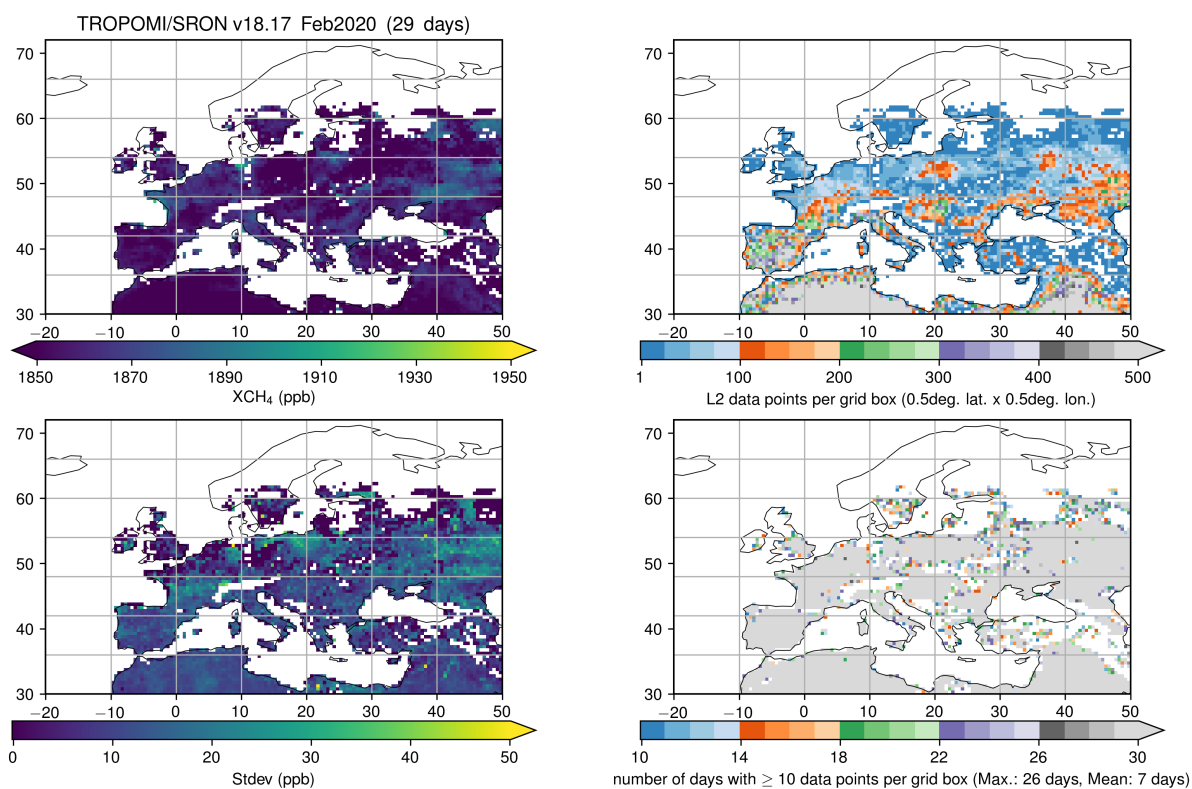


Figure 10: As Figure 9 but for the SRON RemoTeC-S5P XCH₄ scientific product version 19.446



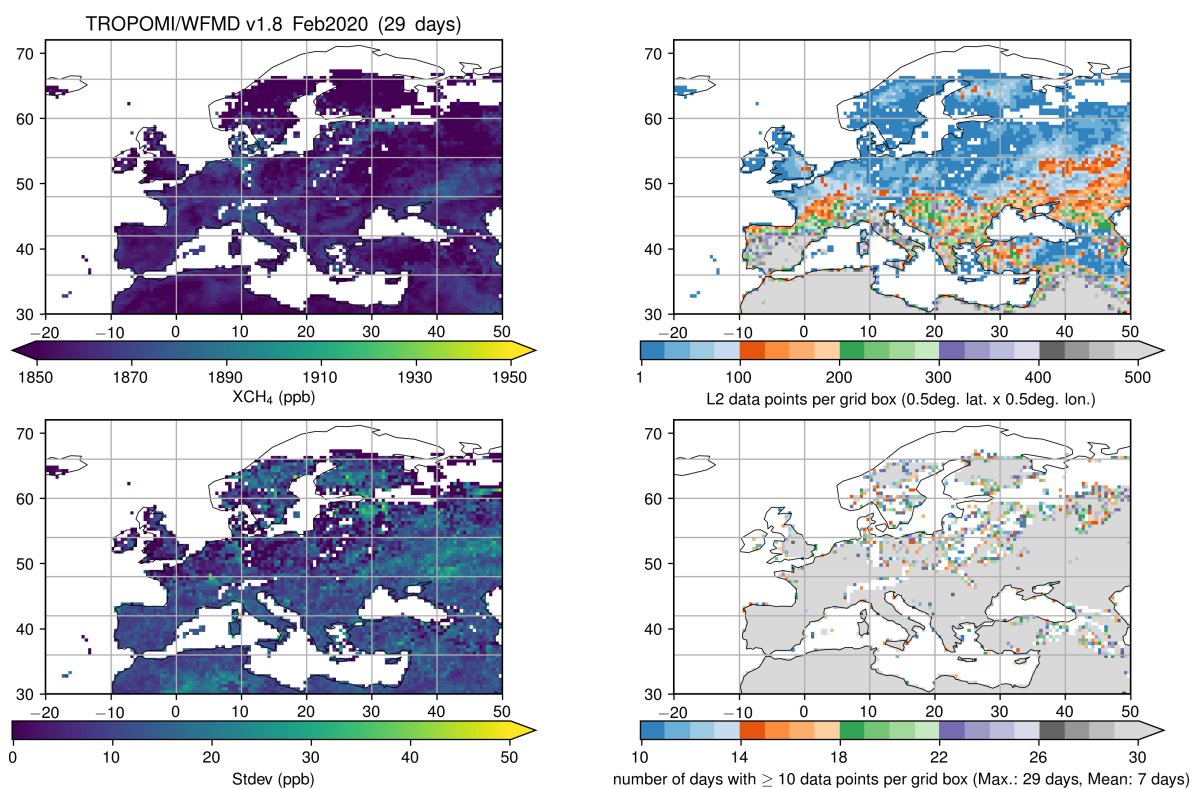


Figure 11: As Figure 9 but for the Bremen WFM-DOAS data product version 1.8

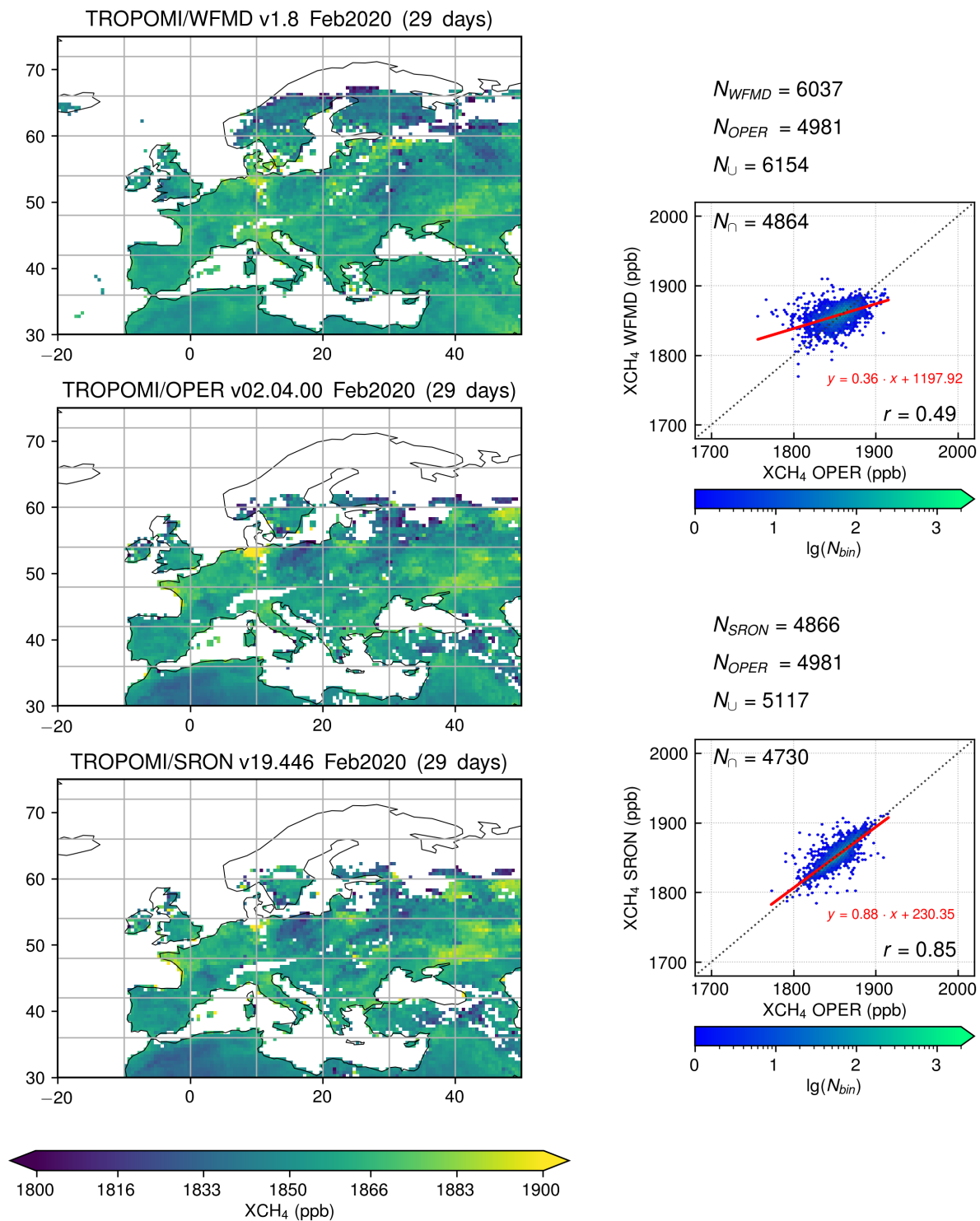


Figure 12: Comparison of TROPOMI monthly mean XCH_4 for three data products as shown in Figure 9 complemented with scatterplots. N_{\cap} gives the number of data points and r the correlation coefficient. Also given is a linear fit.

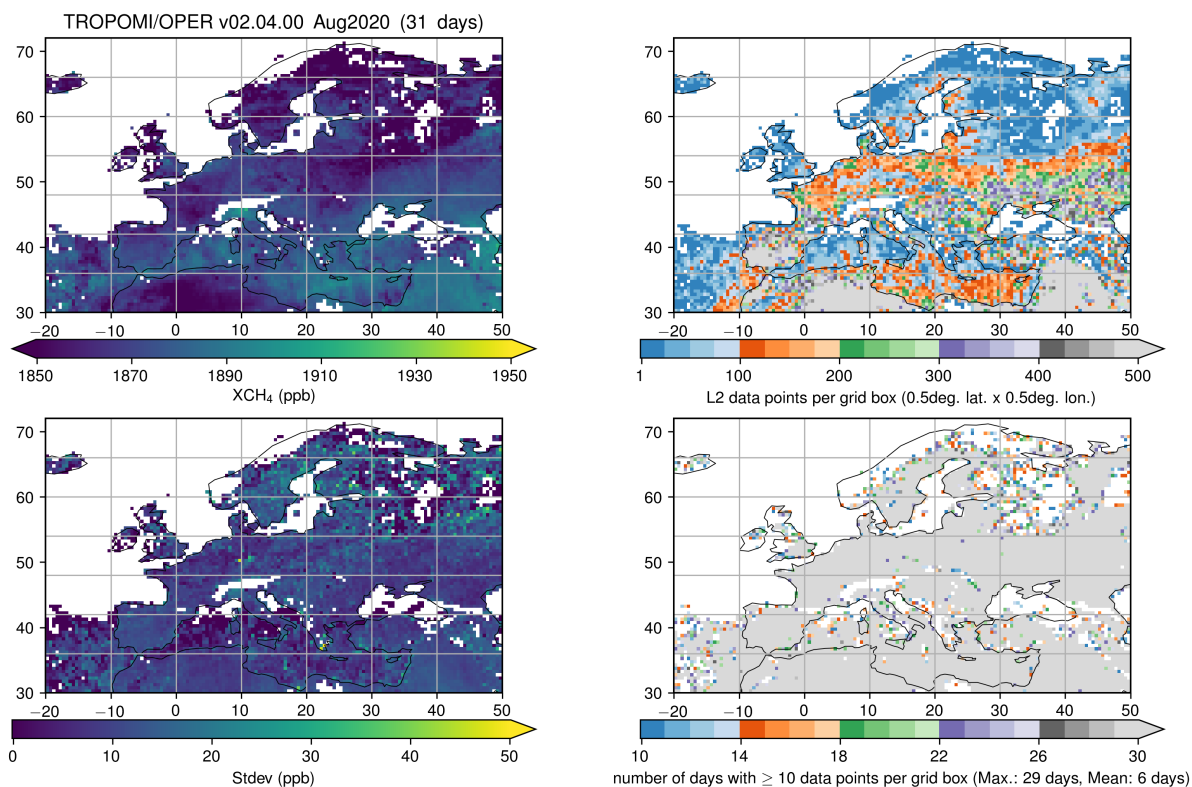


Figure 13: Left: Monthly averages of the operational (reprocessed) data product RPRO version 02.04.00 and corresponding standard deviation for August 2020. Right: Number of measurements contained in monthly mean as shown in the left panel (top) and number of days with more than 10 measurements per grid cell (bottom).

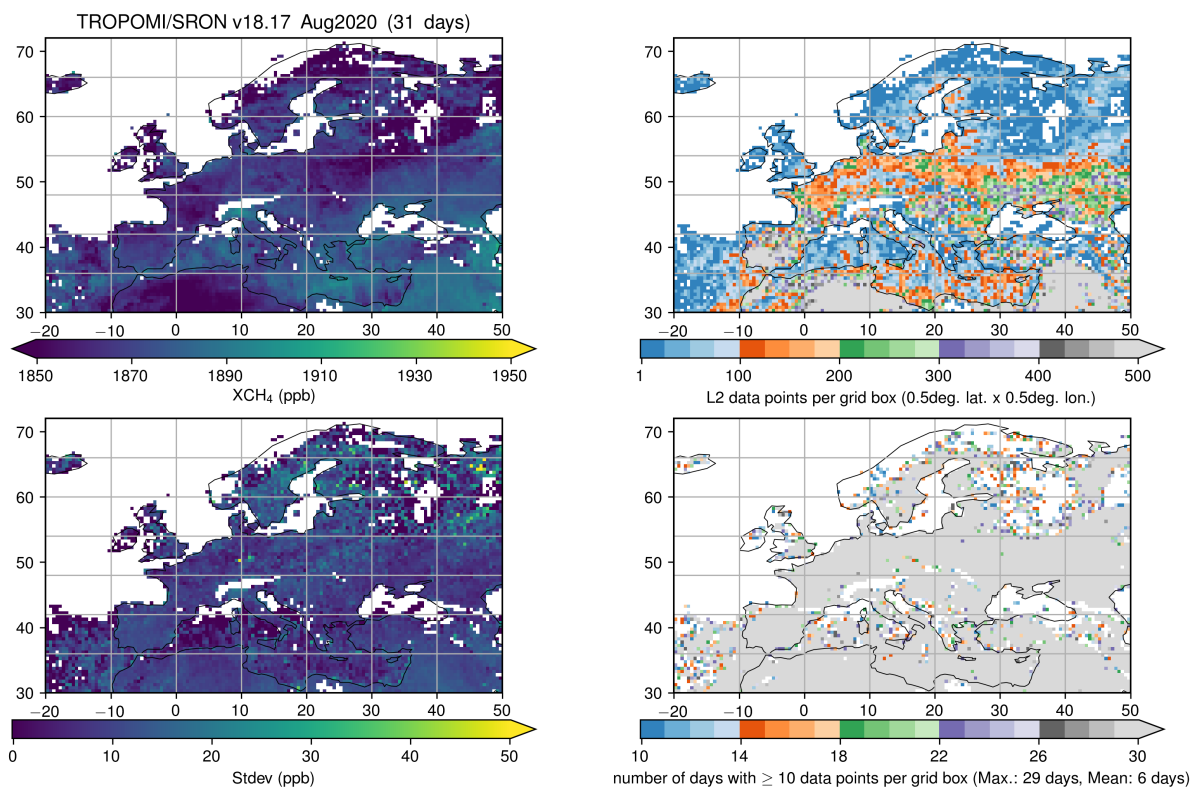


Figure 14: As for Figure 13 but for the SRON RemoTeC-S5P XCH₄ scientific product version 19.446



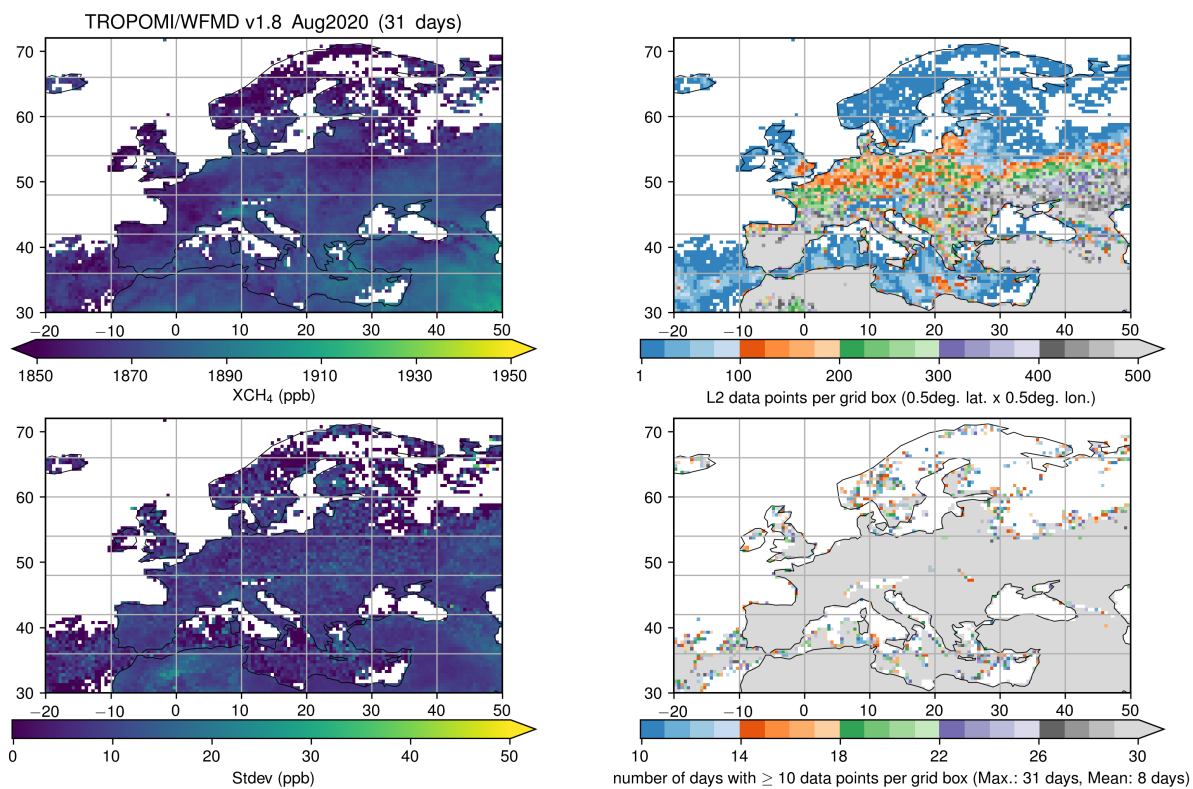


Figure 15: As for Figure 13 but for the University of Bremen WFM-DOAS data product version 1.8

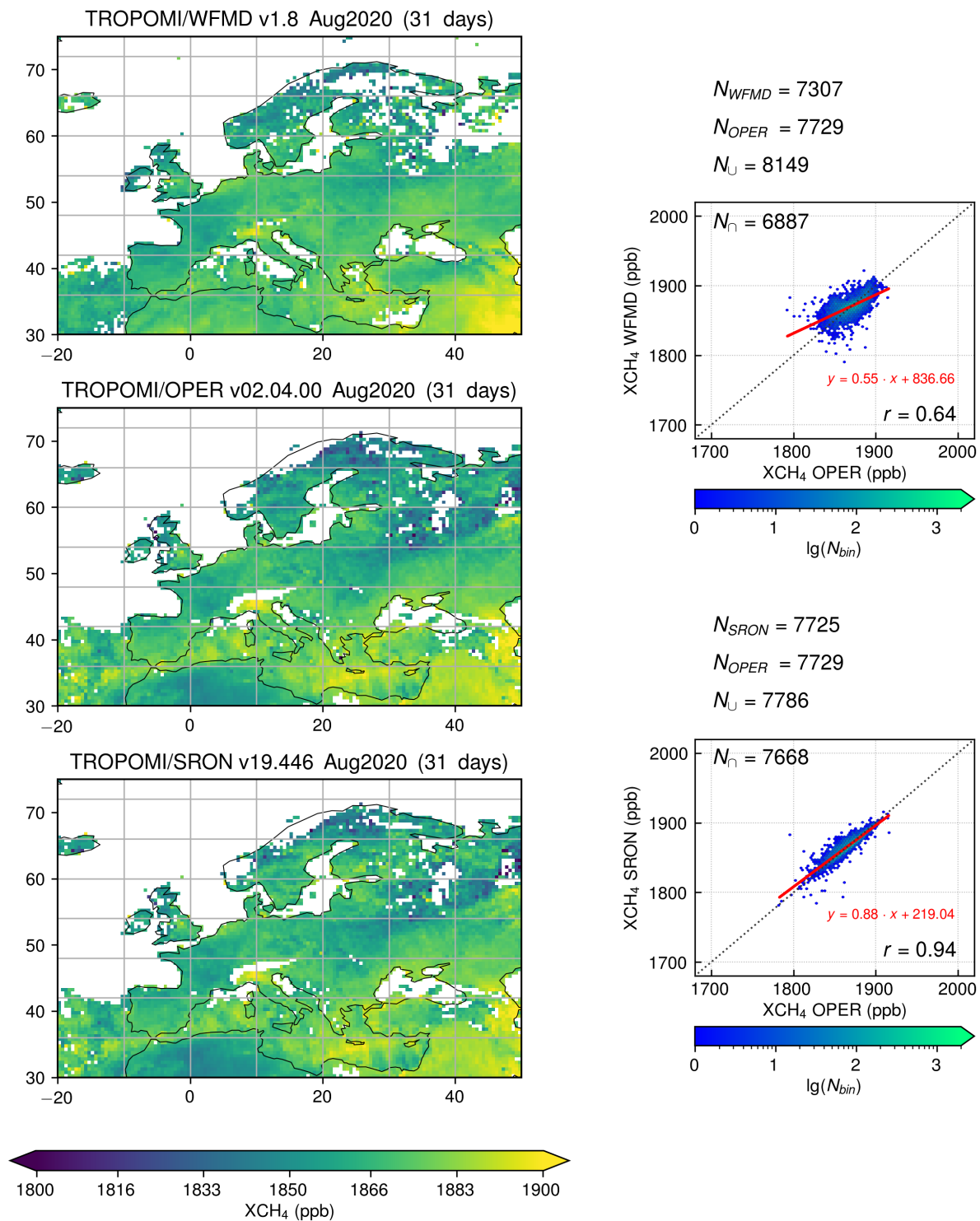


Figure 16: Comparison of TROPOMI monthly mean XCH₄ for three data products as shown in Figure 13 complemented with scatterplots. N_{\cap} gives the number of data points and r the correlation coefficient. Also given is a linear fit.

The European comparison shows very similar features as for the global comparison. The WFMD dataset shows typically higher data volume and better coverage. This is very pronounced in winter while in summer the WFMD dataset surprisingly shows somewhat lower number of days with data over high latitudes. This is likely caused by the chosen threshold of 10 soundings and it appears that in the case of WFMD, this threshold is missed while it is just passed in the SRON and operational products. Again, we find the expected excellent agreement between the operational and the SRON product. Differences to the WFMD product are now more enhanced on this smaller scale and we obtain a modest correlation with coefficients of 0.49 and 0.64. It is possible that differences in a priori CH_4 profiles between the retrievals contribute to the lower correlation in winter. This indicates that the choice of data product will be important and we can expect different results when they are used in surface flux inversions.

3.2.3 Time series

Figure 17 shows time series of the globally and monthly averaged XCH_4 , for the time period from May 2018 till May 2022. All datasets show the seasonal cycle and the annual increase in global methane. As already observed earlier, the operational and the SRON product agree very well. However, the WFMD product shows higher values in northern hemispheric winter and thus a lower seasonal amplitude. This is likely a consequence of the different coverage of the different datasets.

The number of contributing measurements is in general higher for the Bremen WFMD data product. The operational and the SRON scientific product show much larger variations throughout a year in the number of data points. Both datasets consist nearly of the same number of data points with a few exceptions in winter 2019 and 2020.

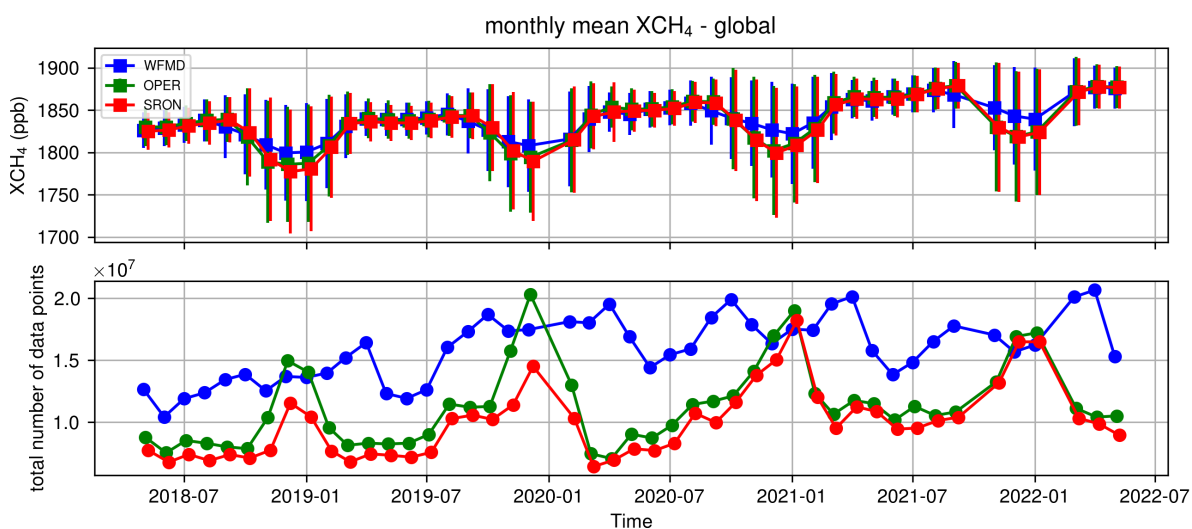


Figure 17: *Upper panel:* Time series of TROPOMI monthly mean XCH_4 for the 3 data products on a global scale. *Lower panel:* corresponding number of measurements. The error bars give the standard-deviation of the monthly data.

The time series for the European domain is given in Figure 18. All 3 datasets show similar trend with a tendency by the WFMD dataset to show higher values throughout most the time period. The datasets agree better in winter. The observed differences are likely again the result of differences in spatial

coverage. For the European domain, we find that WFMD consistently has roughly 50% more data compared to the operational and SRON product.

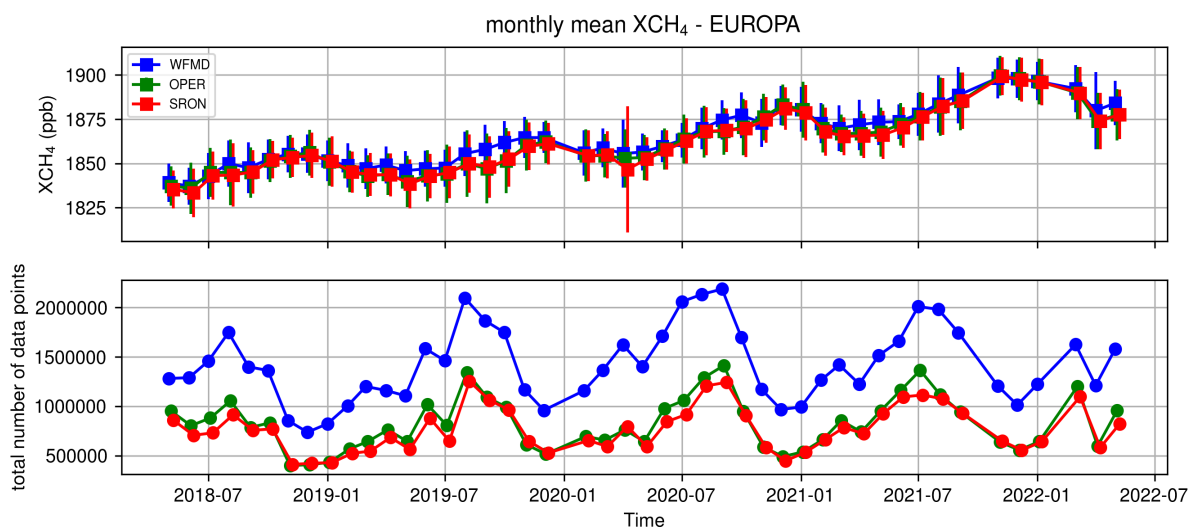


Figure 18: Upper panel: Time series of TROPOMI monthly mean XCH₄ representative for the European domain. Lower panel: corresponding number of measurements. The error bars give the standard-deviation of the monthly data.

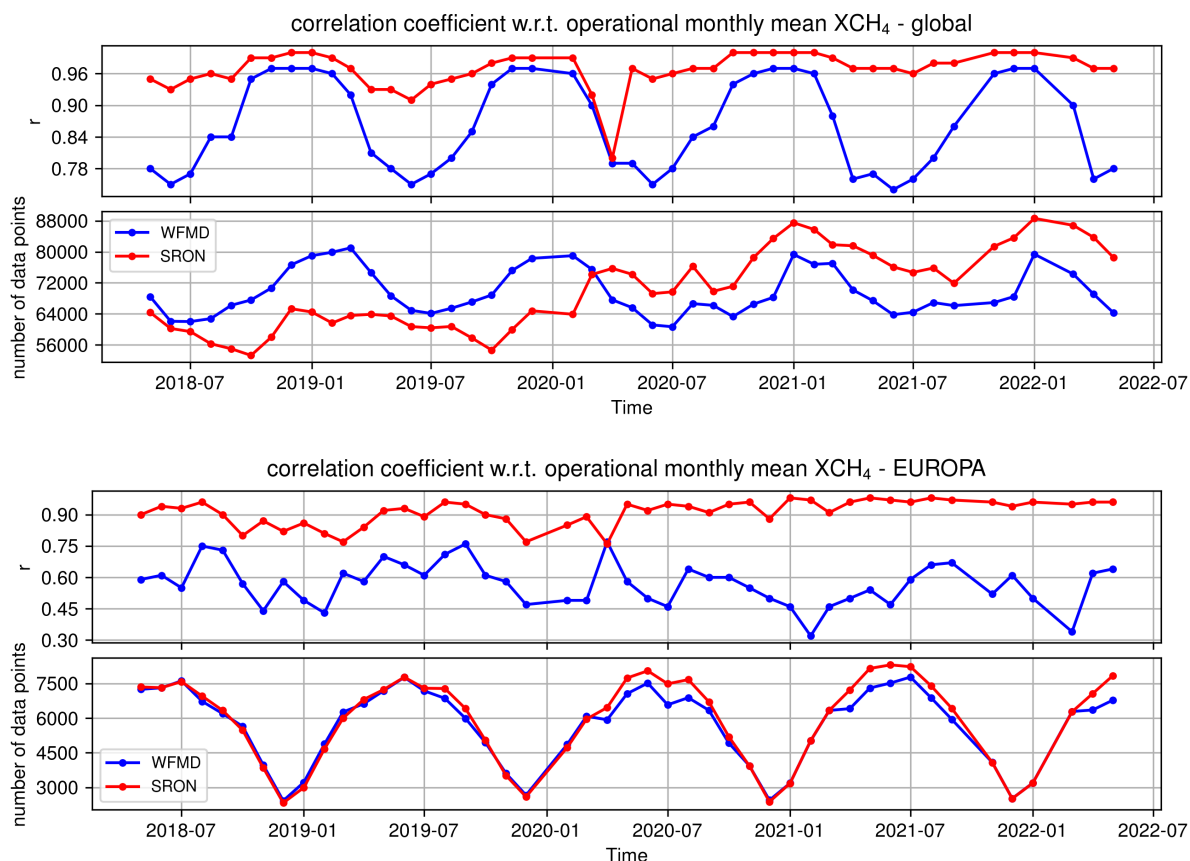


Figure 19: Time Series of the correlation coefficient r for the comparison WFMD - operational (blue lines) and SRON – operational (red lines) as shown in Figure 4: Comparison of TROPOMI monthly mean XCH₄ for three data products as shown in Figure 1 complemented with , Figure 8Top: global; Bottom: Europe.



Figure 19 shows the correlation coefficient between the SRON and the WFMD product with the operational product globally and for Europe. As already mentioned, we expect a high correlation between the SRON product and the operational product and this is also observed on both domains but with an outlier in spring 2020. The correlation between WFMD and the operational product is lower. For the global domain, we observe a summer – winter difference with much higher correlations for winter than for summer. This pattern is not visible for the European domain where the correlation coefficient scatters around a value of 0.5. The number of common datapoints with the operational product is initially higher for WFMD but this changes in the second half of the time series. Over the European domain, the common datapoints is similar between the SRON and WFMD product.

3.2.4. Single Orbits – Plume Studies

Figure 20 displays examples for single overpass measurements over regions with strong local hotspot emissions. This includes the Upper Silesian Coal Basin in Poland and the Permian, USA and Turkmenistan. The figures compare results for the Bremen WFMD XCH₄ data product and the operational (RPRO v02.04.00) dataset.

In general, an emission plume is visible in all cases with both datasets. The WFMD product tends to have higher coverage (except in overpass over the Silesian Coal Basin on 6 June 2018) which is important for the plume detection. In the operational product, an across-track striping feature is visible. Possible stripes of erroneous CH₄ value in flight direction is mentioned in the S5P MPC Product Readme document. This has been removed in the WFMD dataset. The scatter plot shows good agreement between both datasets with typical correlation coefficients of around 0.8. However, in some cases, clear offsets are observed (e.g. in the upper example shown in Figure 20). To what extent this will impact the emission estimation still needs to be studied.



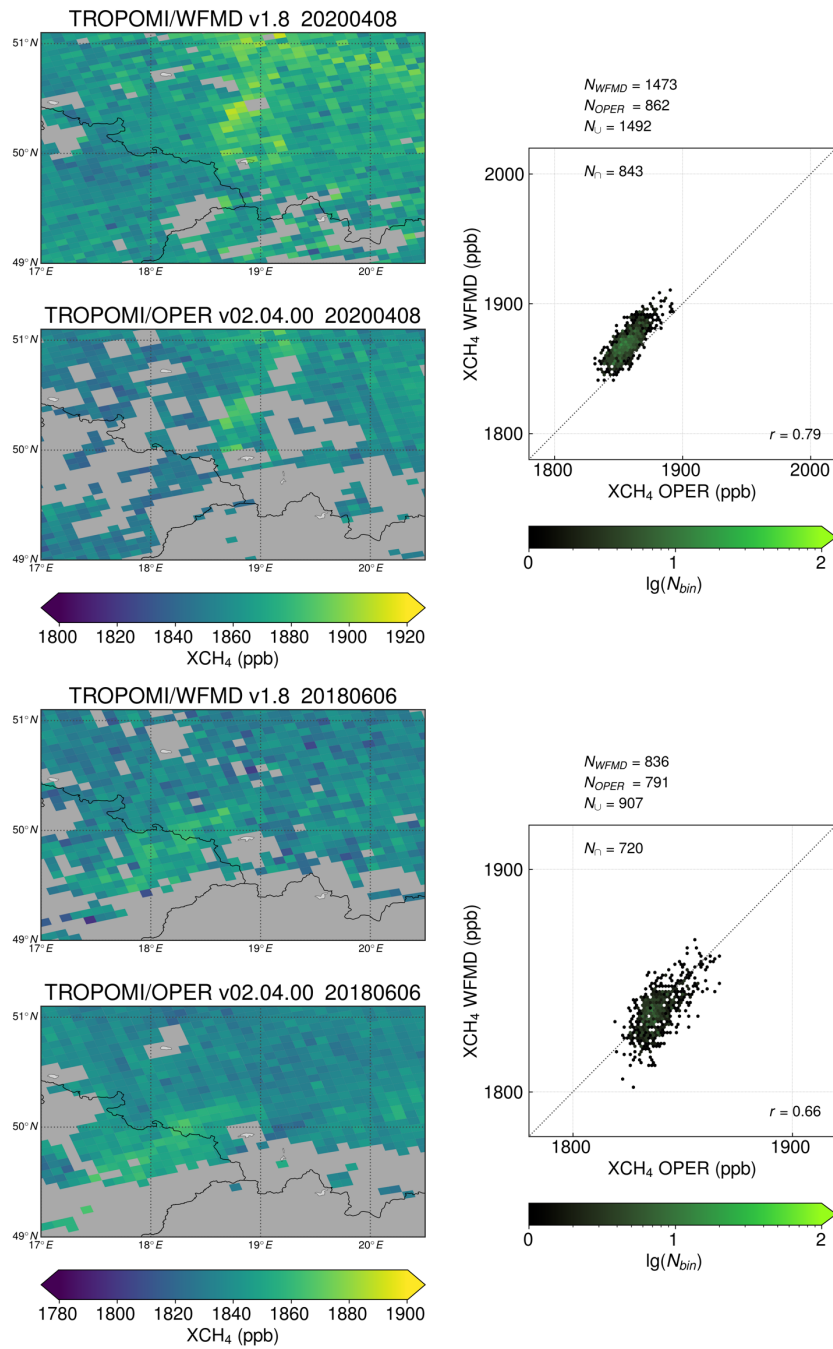


Figure 20: Single overpass, Upper Silesian Coal Basin in Poland

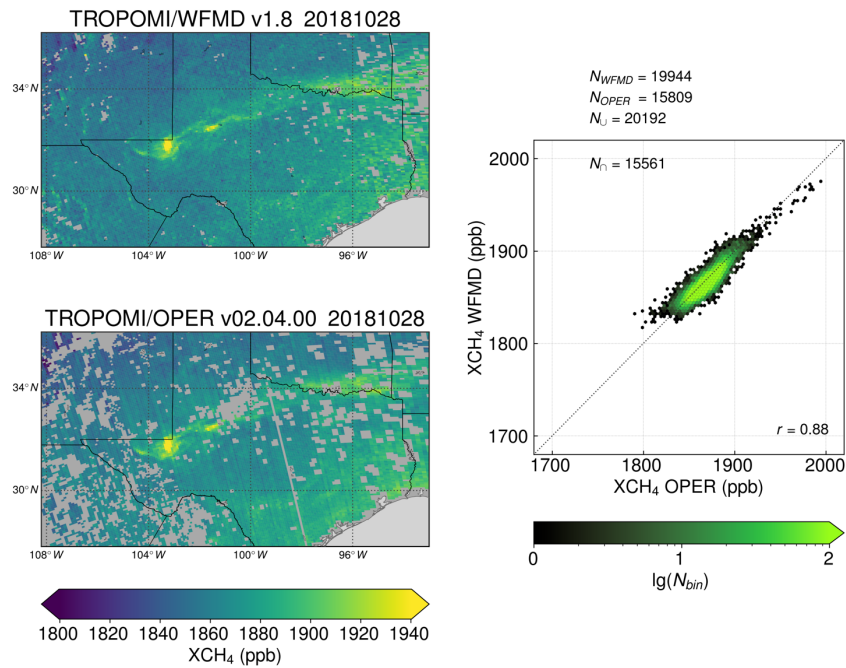


Figure 21: Single orbit data. Permian, USA with enhancements due to emissions from the oil and gas industry.

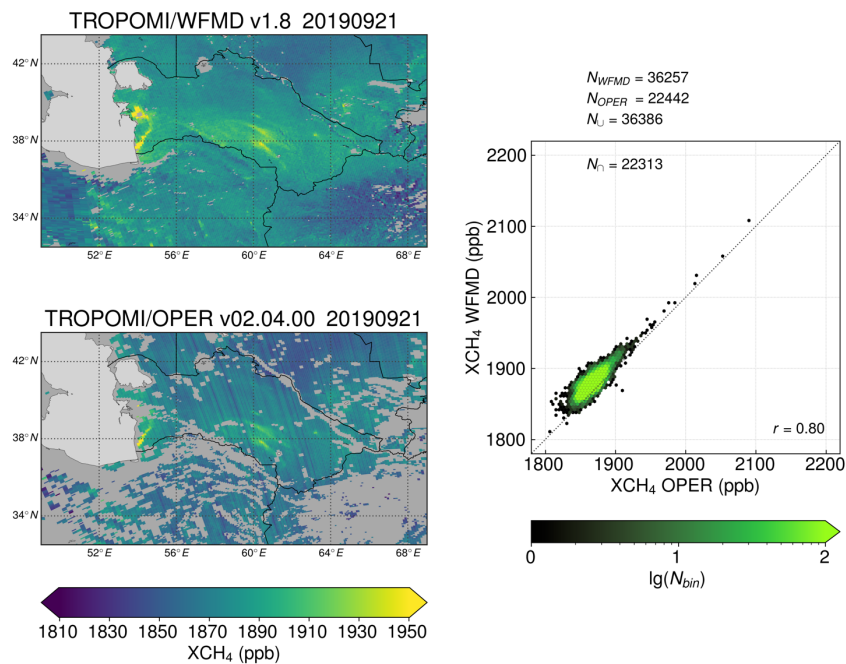


Figure 22: Single orbit data. Turkmenistan with enhancements due to emissions from the oil and gas industry.

4. Analysis/Comparison of GOSAT and GOSAT-2 XCH₄ data products

4.1. Methodology

Seven different GOSAT and five different GOSAT XCH₄ data products have been used for the comparison. As for TROPOMI, the data has been converted to monthly means and gridded on a 2° × 2° grid. However, due to the sparseness of the GOSAT and GOSAT-2 data, the maps are given as seasonal averages. The resulting global and European comparison maps and the number of measurements available per grid box are given in Section 4.2. Direct comparisons between the data sets are again given as scatterplots. In contrast to the TROPOMI comparisons, all datasets have been converted to a common CH₄ a priori profile.

4.2. Results and Discussion

The following sections show example maps for winter 2020 and summer 2020 respectively, on a global scale and for Europe. All Figures for the year 2020 are available from <https://nc.uni-bremen.de/index.php/s/3WFgkLfPBMyYarF>.

4.2.1. Global Maps of seasonal mean XCH₄ from GOSAT

The maps below clearly show the much lower coverage of GOSAT compared to TROPOMI with gaps between different orbits as a result of the observational pattern of GOSAT (most pronounced over the ocean). The coverage of the full physics (FP) products over land shows large data gaps in the Tropics due to strict cloud filtering. Over land, the NIES product tends to have highest coverage among the FP retrievals. GOSAT has a dedicated sunglint mode which enables ocean observations with sufficient signal-noise within a latitude band around the subsolar point. As can be seen, different cut-off thresholds have been applied with RemoTeC and UoL-FP being stricter, resulting in reduced latitudinal coverage over the ocean. The proxy products achieve much improved spatial coverage due to reduced sensitivity to thin clouds and aerosols, which provides coverage also over the Tropics. The RemoTeC proxy product has the lowest coverage over land as well as over the ocean of the proxy datasets. Similar to the global TROPOMI comparison, we find a high level of correlation between the different GOSAT retrievals with correlations coefficients above 0.84 (using FOCAL FP as reference) with better agreement found in winter than in summer.



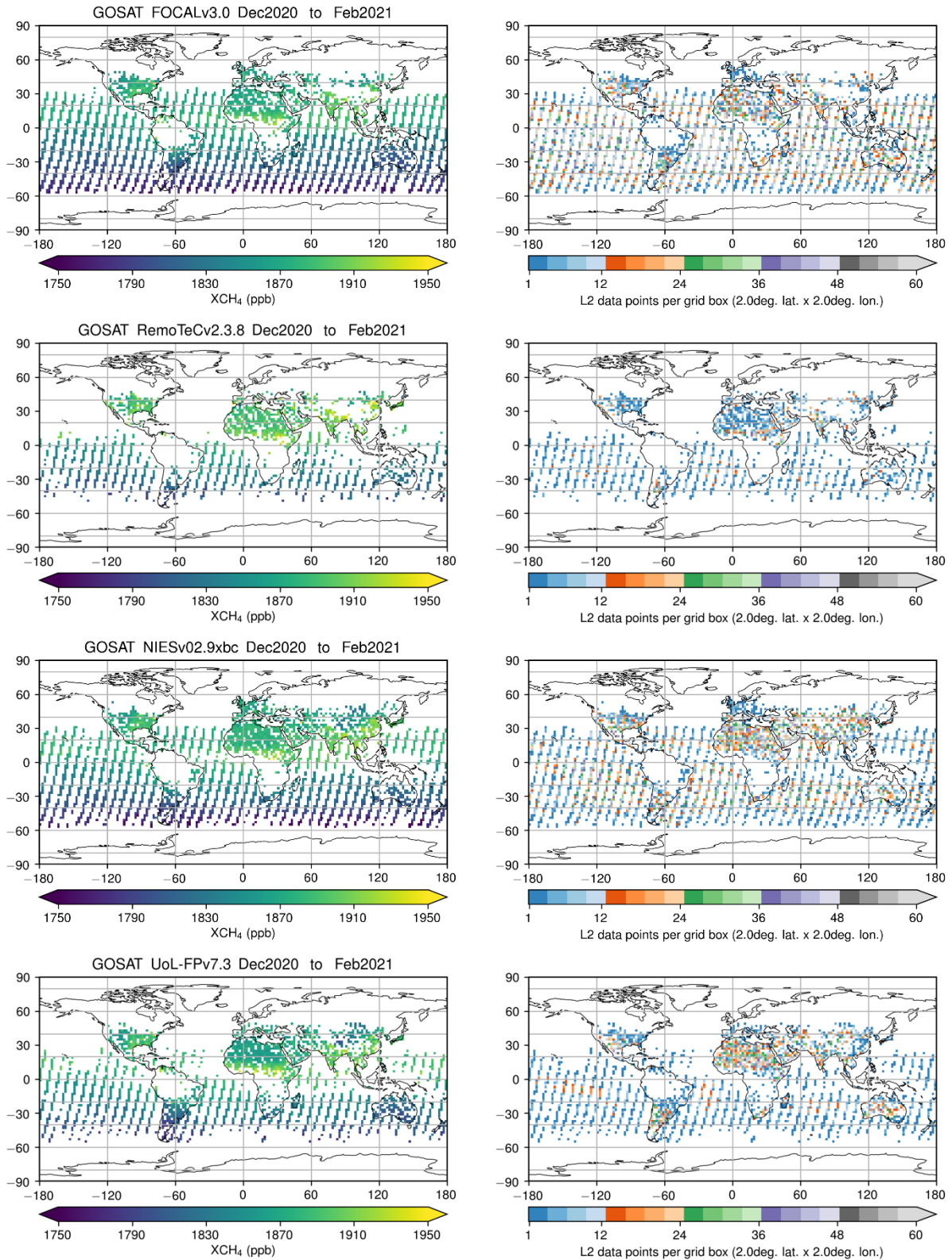


Figure 23: Seasonal averaged GOSAT products for winter 2020 (Dec. 2020 to Feb. 2021) for the following datasets: FOCAL, RemoTeC, NIES and UoL-FP full physics products and FOCAL, RemoTeC and UoL-FP proxy products (from top to bottom). The averaged XCH₄ is given in the left column and the number of datapoints per bin is given in the right column.

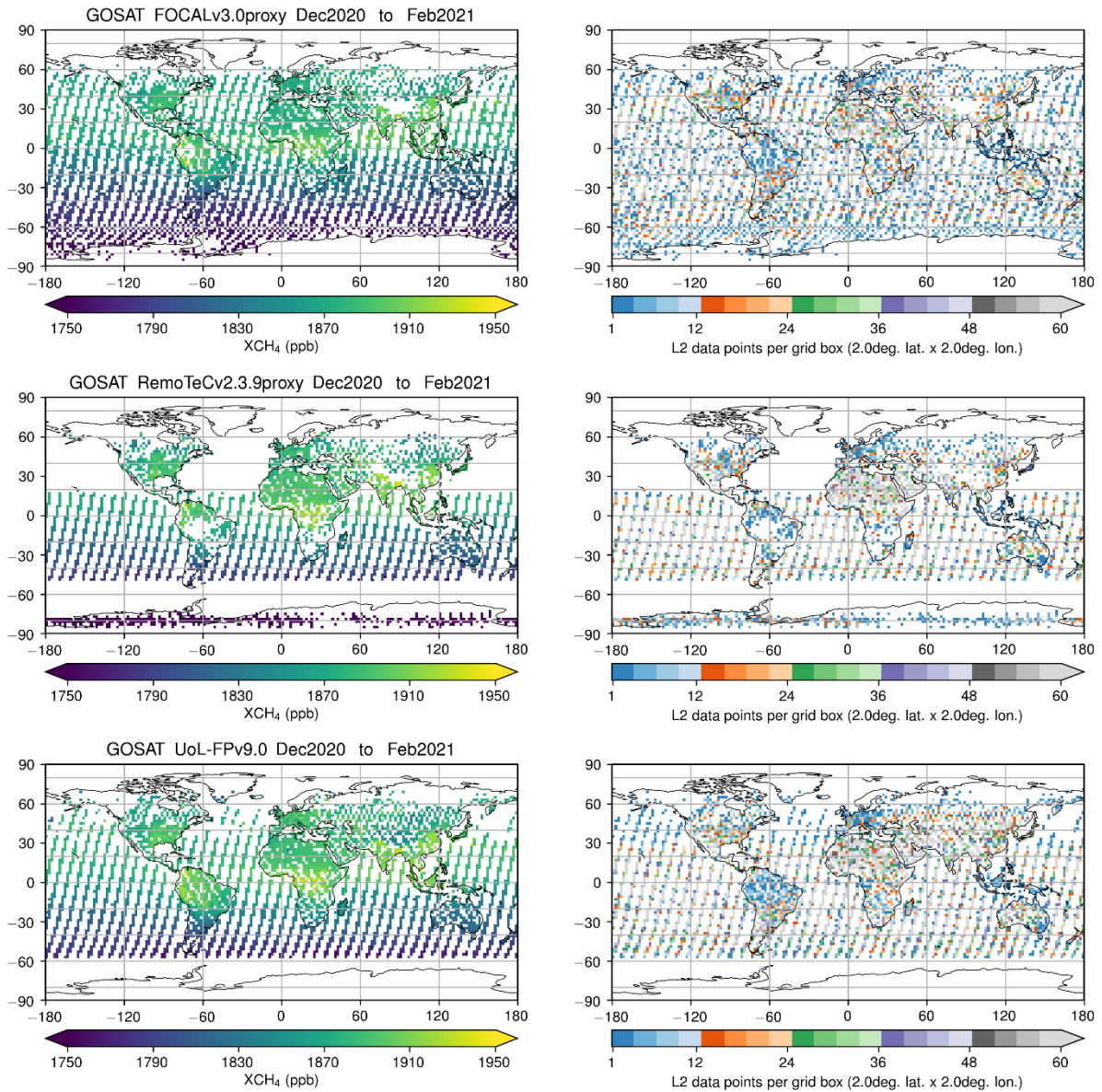


Figure 23: continued

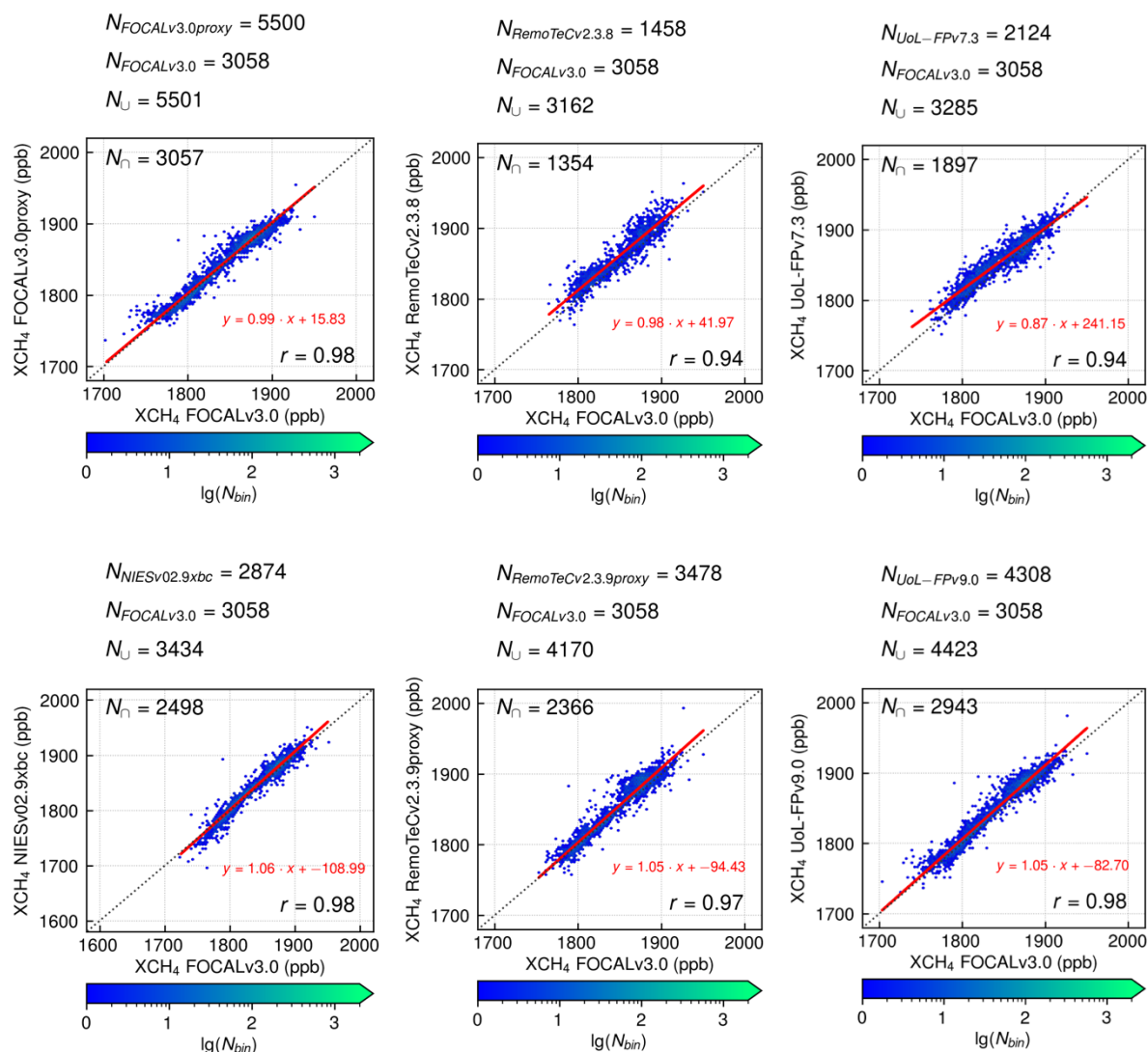


Figure 24: Scatterplots of GOSAT seasonal mean (winter) XCH₄. As reference (x-axis), we have chosen the FOCAL FP dataset.

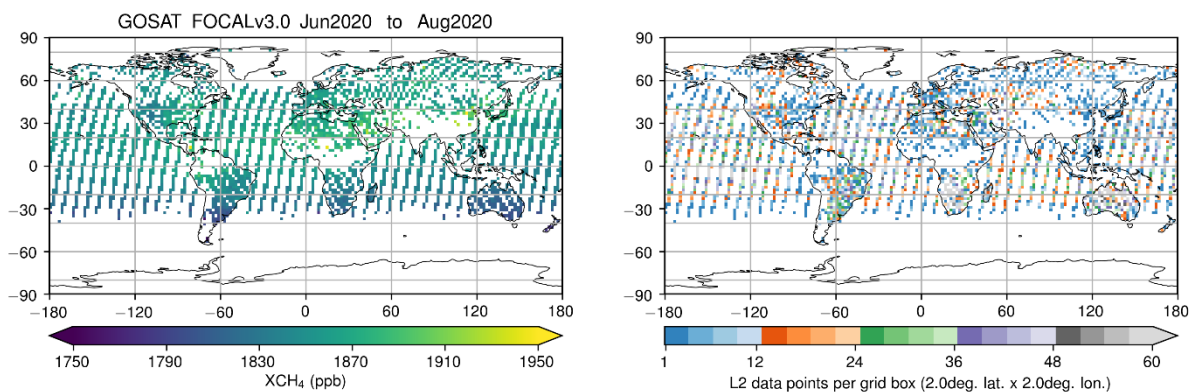


Figure 25: As Figure 23 but for summer 2020 (Jun. 2020 to Aug. 2020).

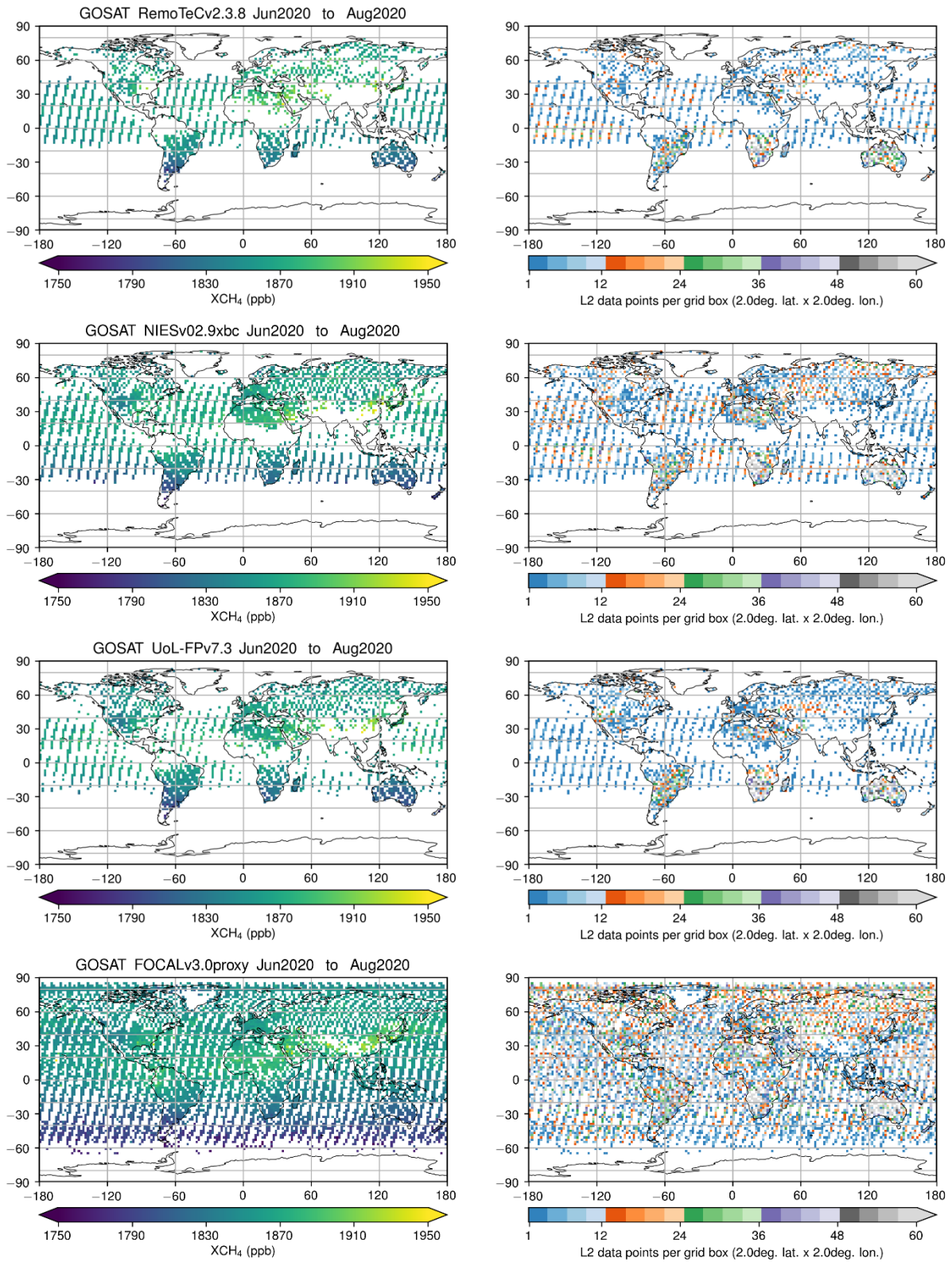


Figure 25: continued

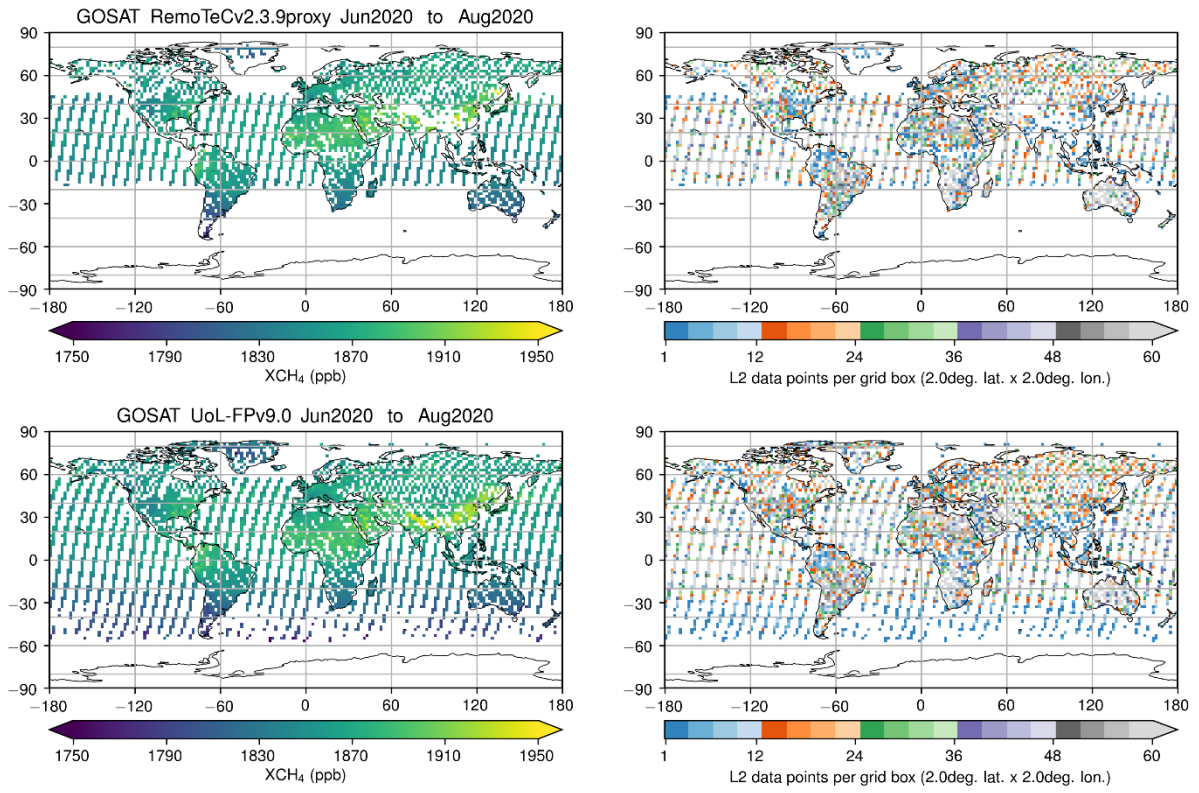


Figure 25: continued

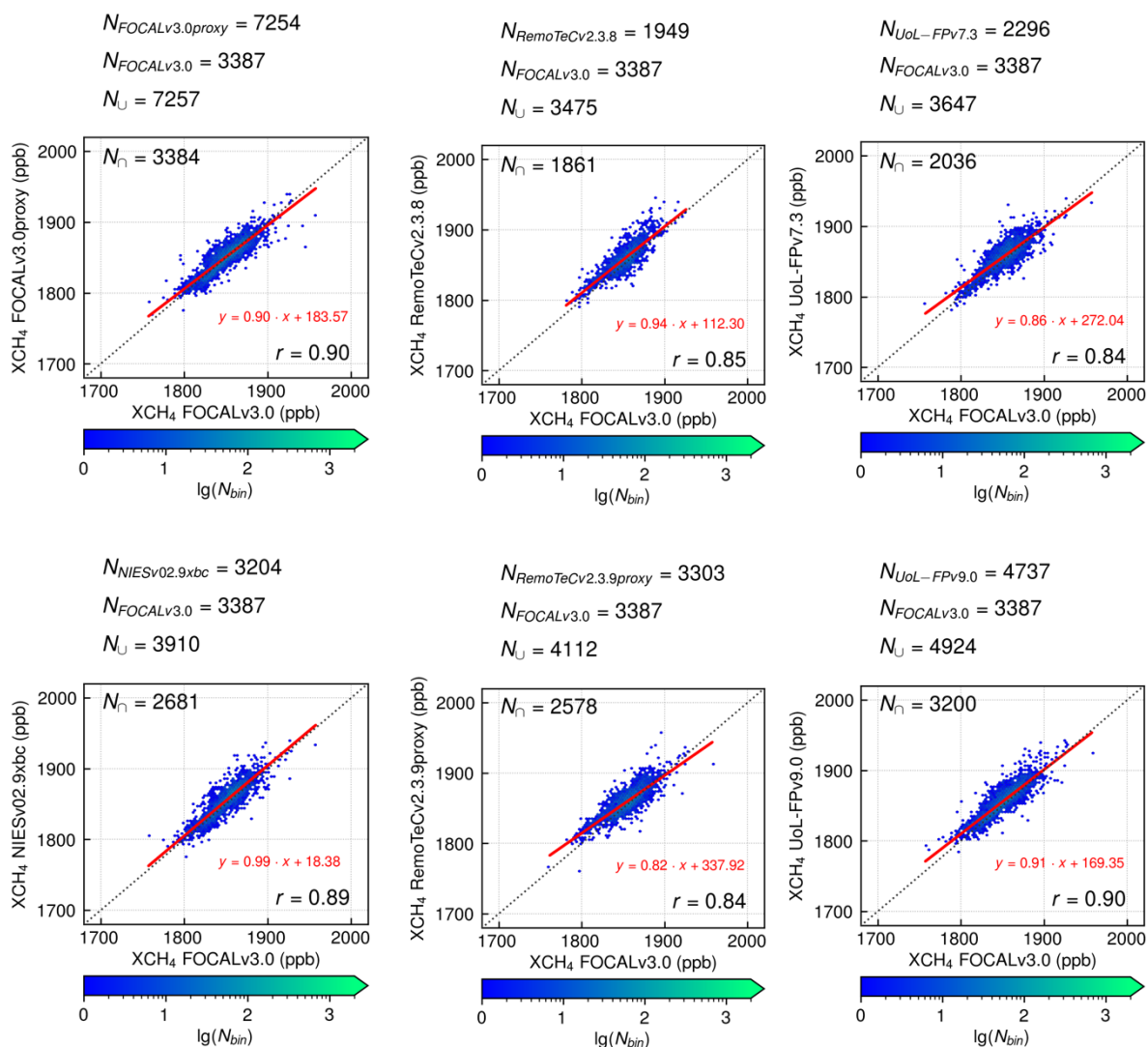


Figure 26: As Figure 24 but for summer 2020.

4.2.2. Maps of seasonal mean XCH₄ from GOSAT – Europe

The coarse and limited coverage of GOSAT is well visible in the European maps given below, in particular for winter with the NIES product having the highest coverage. Better coverage is obtained with the proxy retrievals where most of central Europe is observed in this seasonal winter map. Summer time coverage is better for all retrieval but is still low for the RemoTeC and UoL-FP FP retrievals. Again, the proxy approach achieves improved coverage of Europe and the FOCAL proxy product has also full coverage also over the ocean in summer (except for gaps due to the observational pattern of GOSAT). In terms of coverage, the GOSAT proxy products appear better suited for regional flux inversion due to the very low and seasonally-variable coverage of the FP products.

As has already been observed for TROPOMI, the correlation between the different datasets is significantly lower for the European domain compared to the global comparison. Correlations in winter can be particularly low due to the small number of datapoints. Differences between the datasets are now more pronounced than for the global comparison and we do observe noticeable differences between proxy datasets and the FOCAL FP dataset used as reference (most visible in winter).



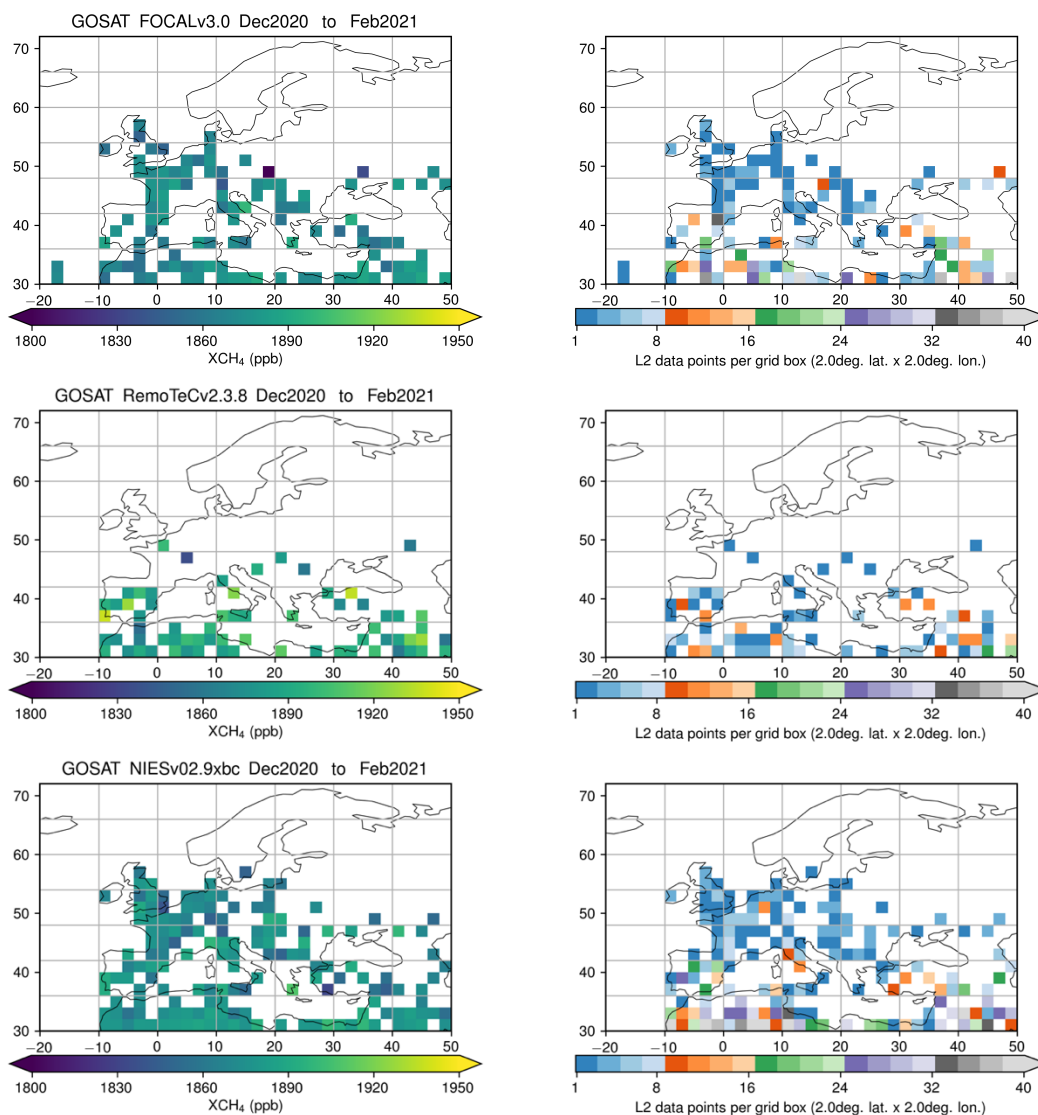


Figure 27: Seasonal averaged GOSAT products for Europe for winter 2020 (Dec. 2020 to Feb. 2021) for the following datasets: FOCAL, RemoTeC, NIES and UoL-FP full physics products and FOCAL, RemoTeC and UoL-FP proxy products (from top to bottom). The averaged XCH₄ is given in the left column and the number of datapoints per bin is given in the right column.

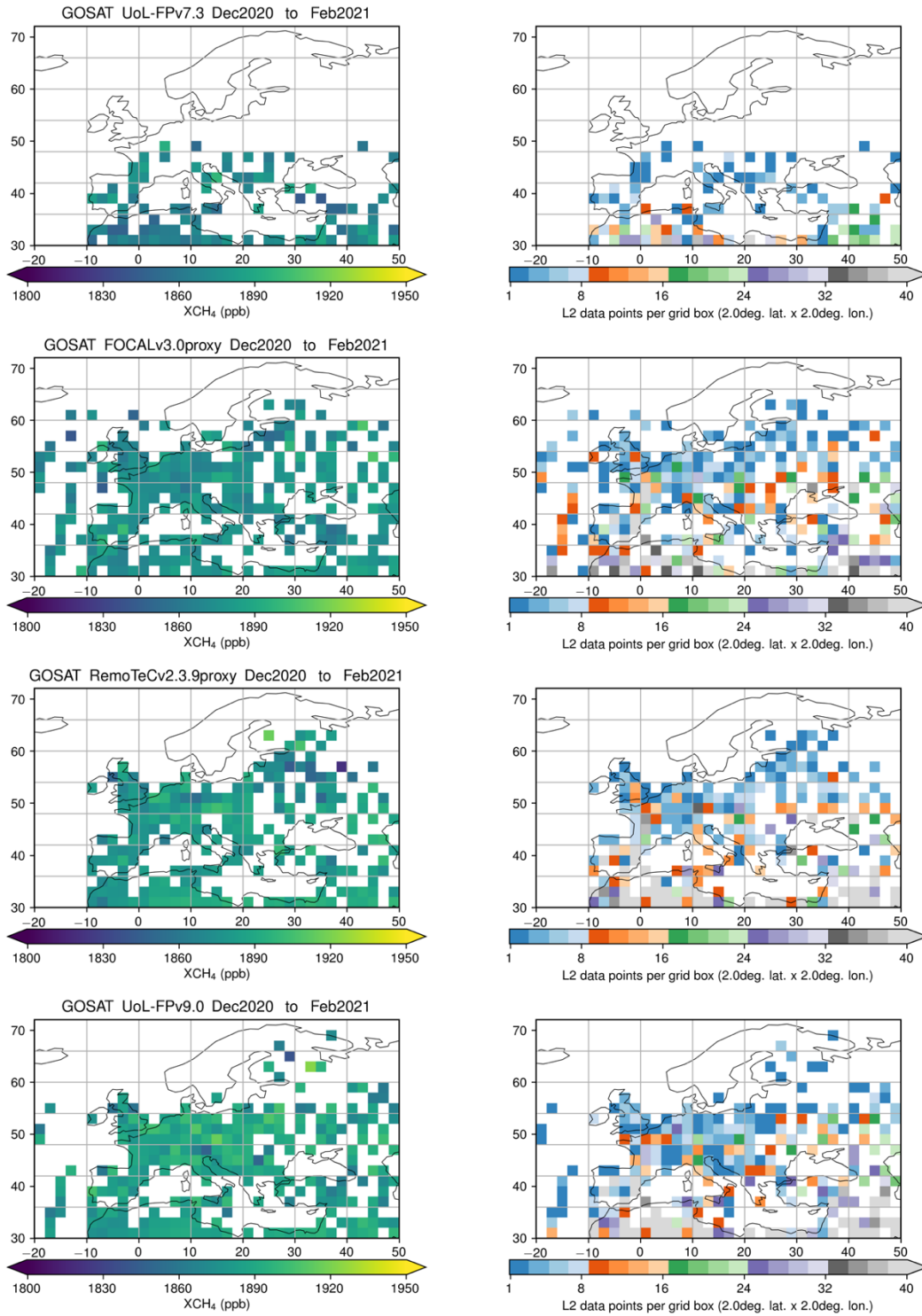


Figure 27: continued



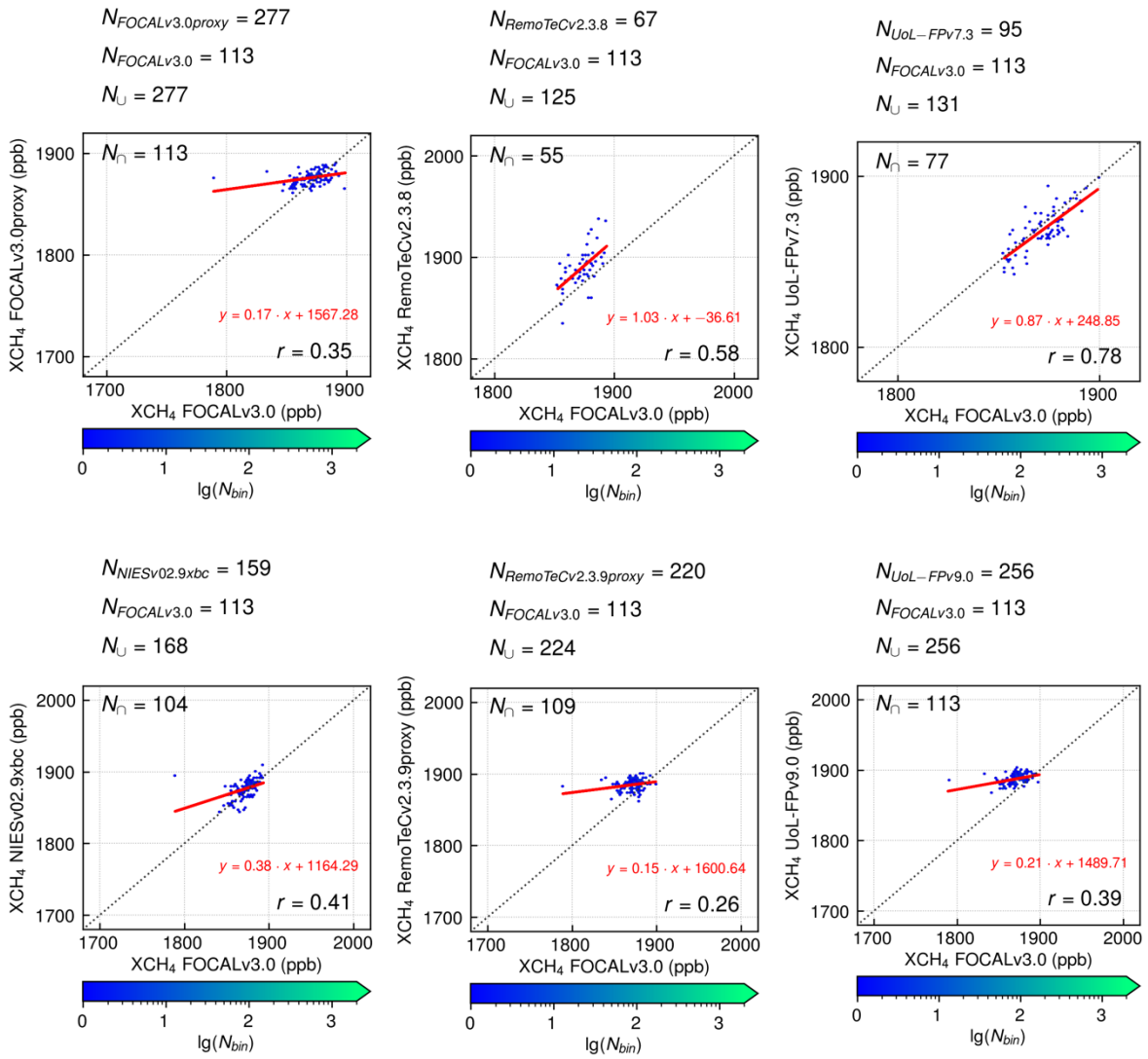


Figure 28: Scatterplots of GOSAT seasonal mean (winter) XCH₄ for Europe. As reference (x-axis), we have chosen the FOCAL FP dataset.

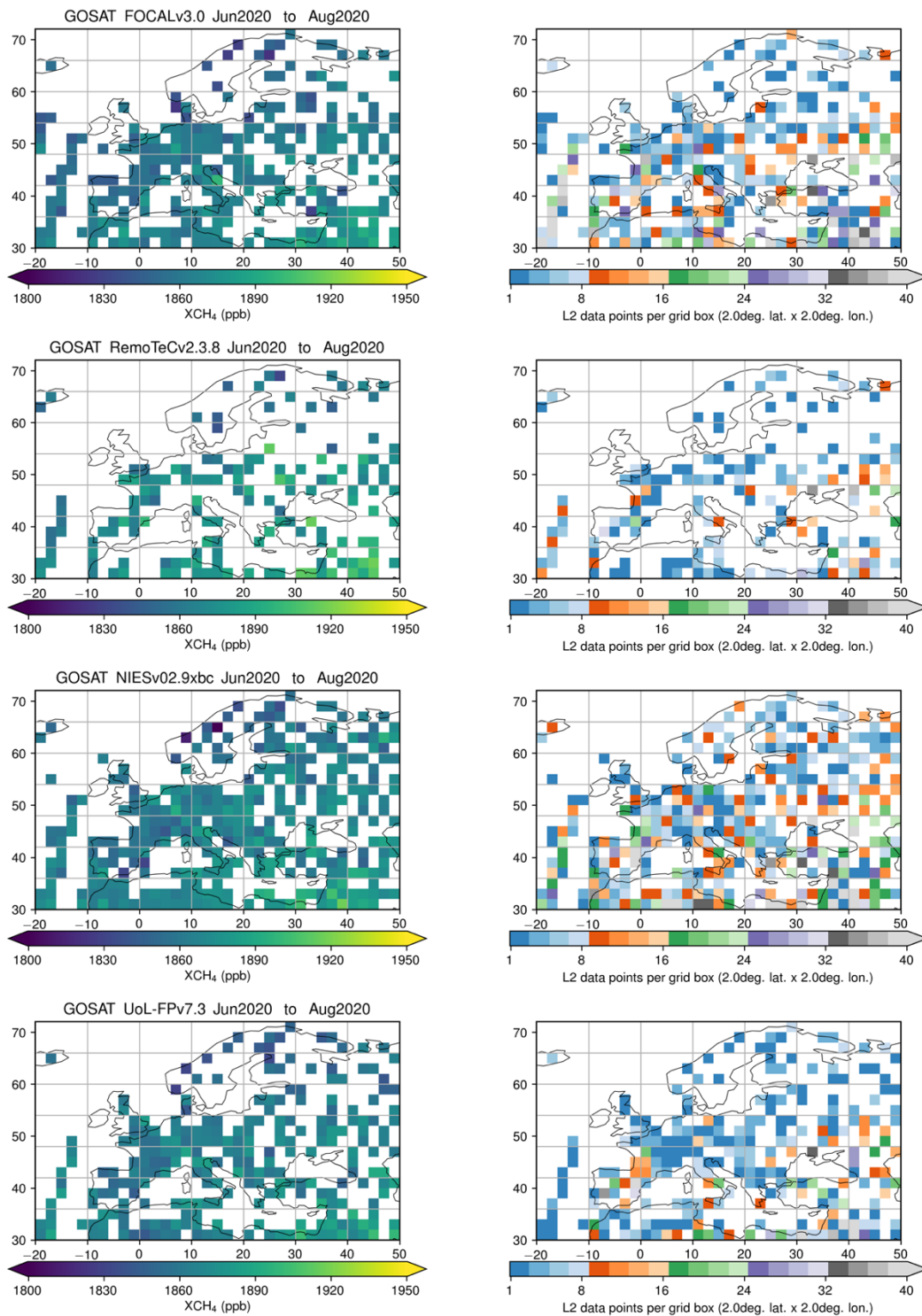


Figure 29: As Figure 27 but for summer 2020.



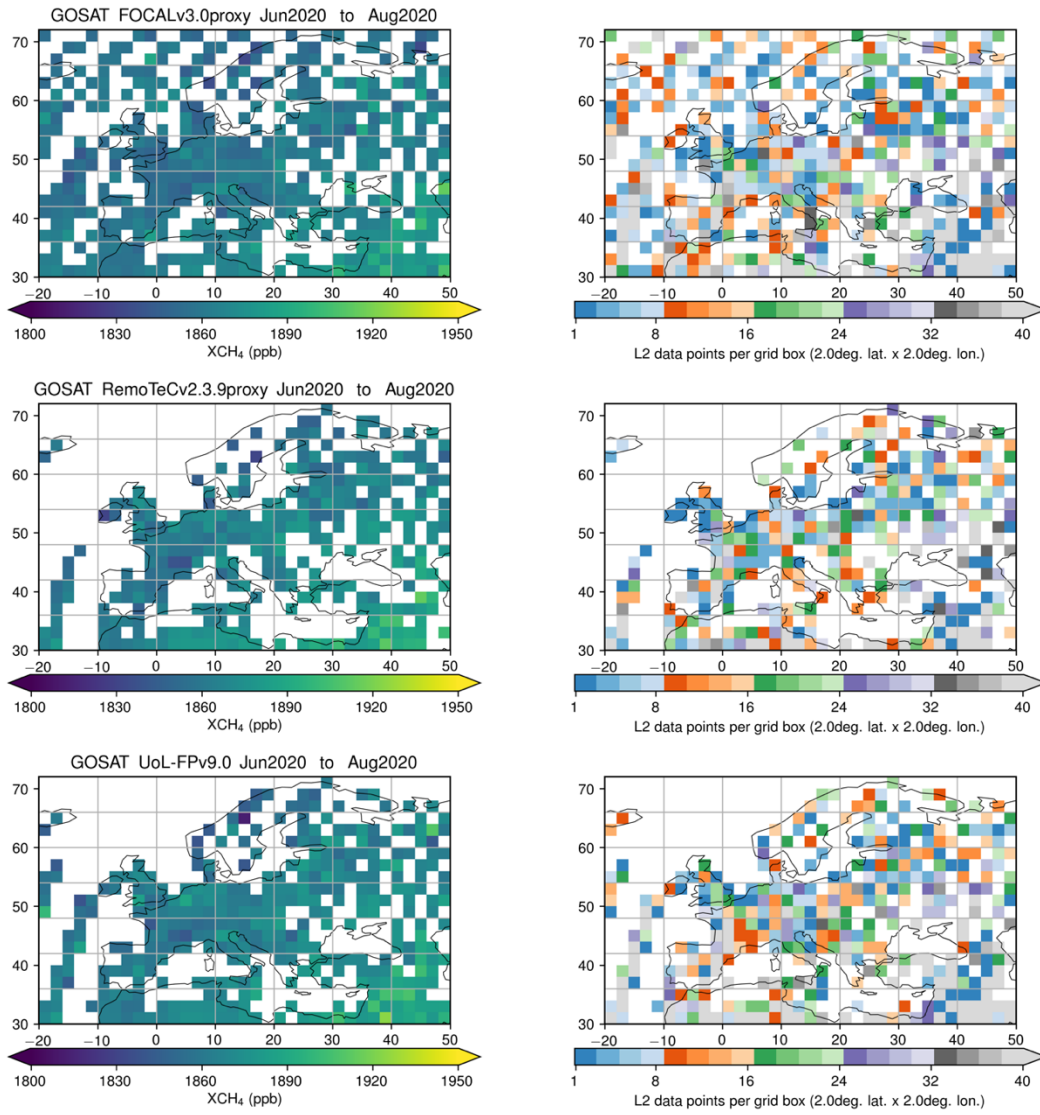


Figure 29: continued



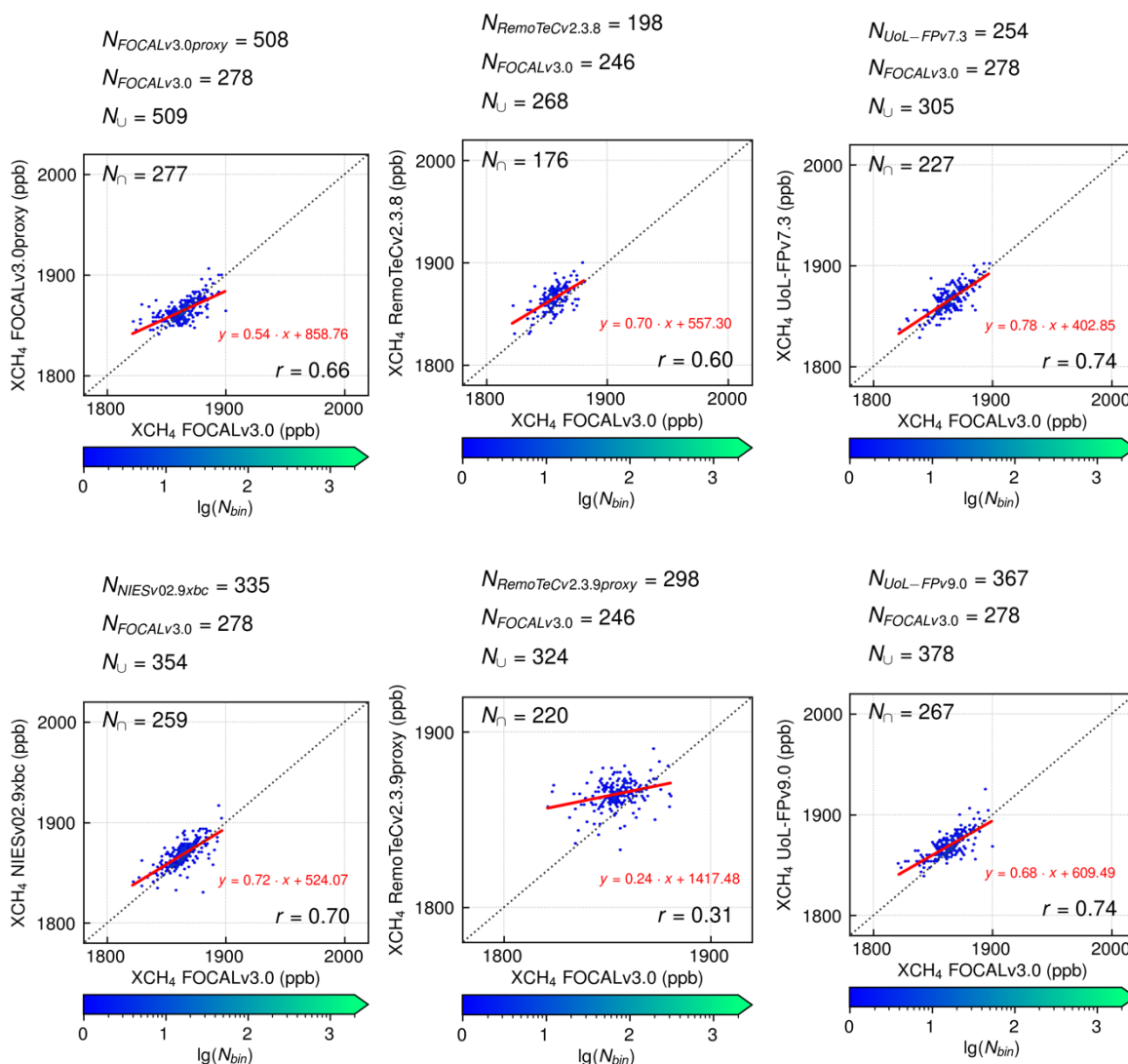


Figure 30: As Figure 28 but for summer 2020.

4.2.3. Global Maps of seasonal mean XCH₄ from GOSAT-2

The GOSAT-2 datasets show similar gaps in coverage as the GOSAT datasets but with improved and denser coverage. As for GOSAT, coverage can be improved with proxy approach. Among the FP products, the NIES GOSAT-2 retrieval achieves the best coverage with a coverage that comes close to the coverage obtained with proxy retrievals. On a global scale, we find again a high level of correlation, we find again a high level of correlation with a lower correlation coefficients and larger differences found in summer compared to winter.

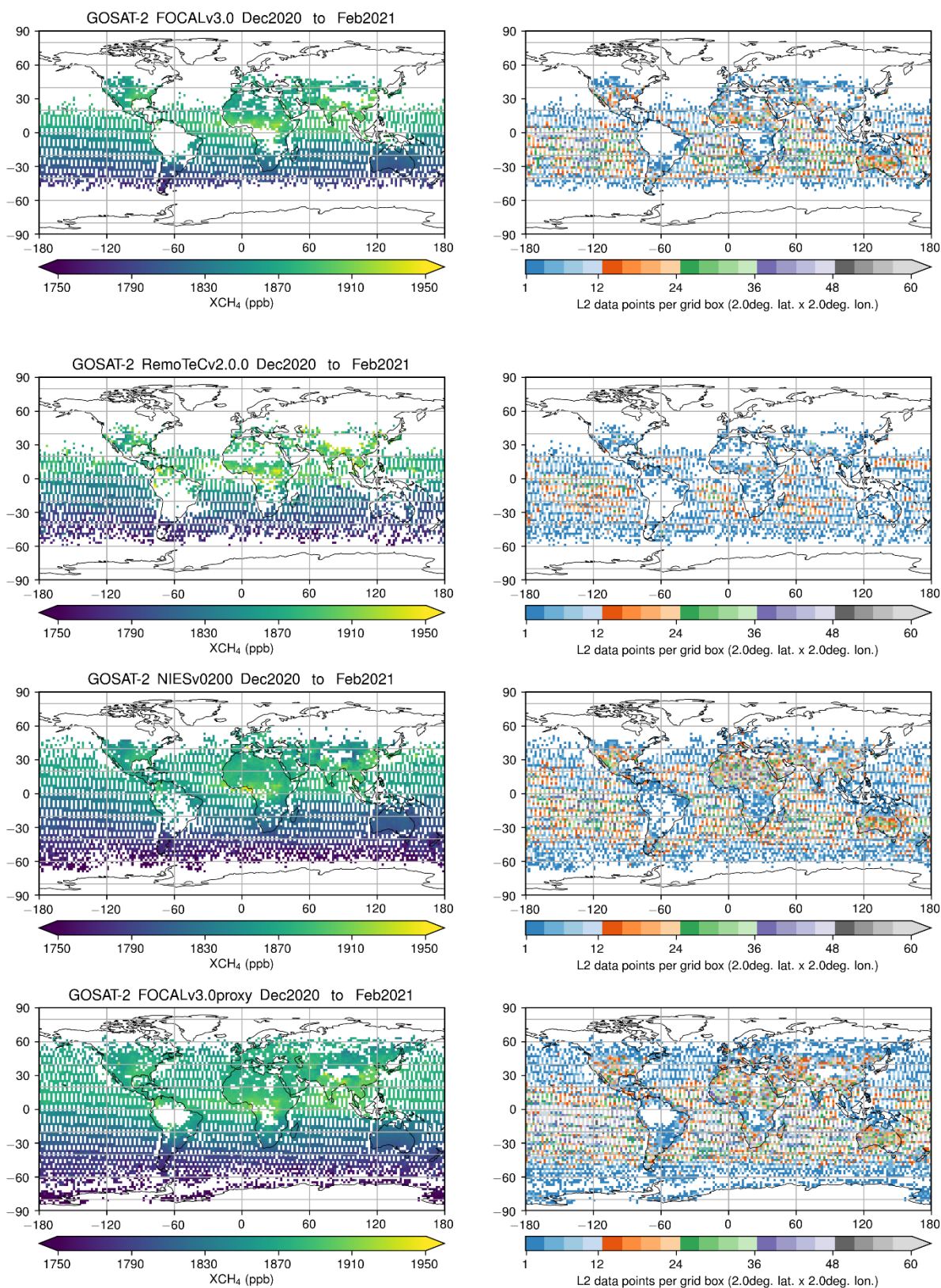


Figure 31: Seasonal averaged GOSAT-2 products for winter 2020 (Dec. 2020 to Feb. 2021) for the following datasets: FOCAL, RemoTeC, and NIES full physics products and FOCAL and RemoTeC proxy products (from top to bottom). The averaged XCH₄ is given in in the left column and the number of datapoints per bin is given in the right column.

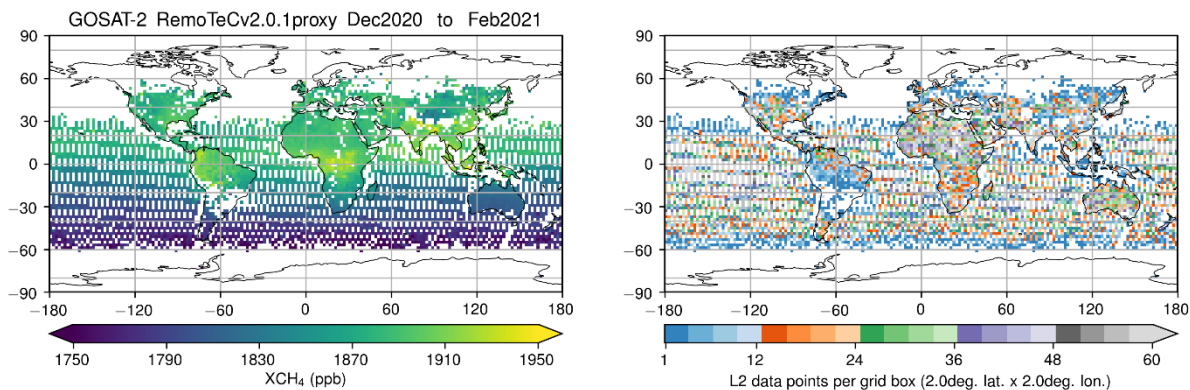


Figure 31: continued

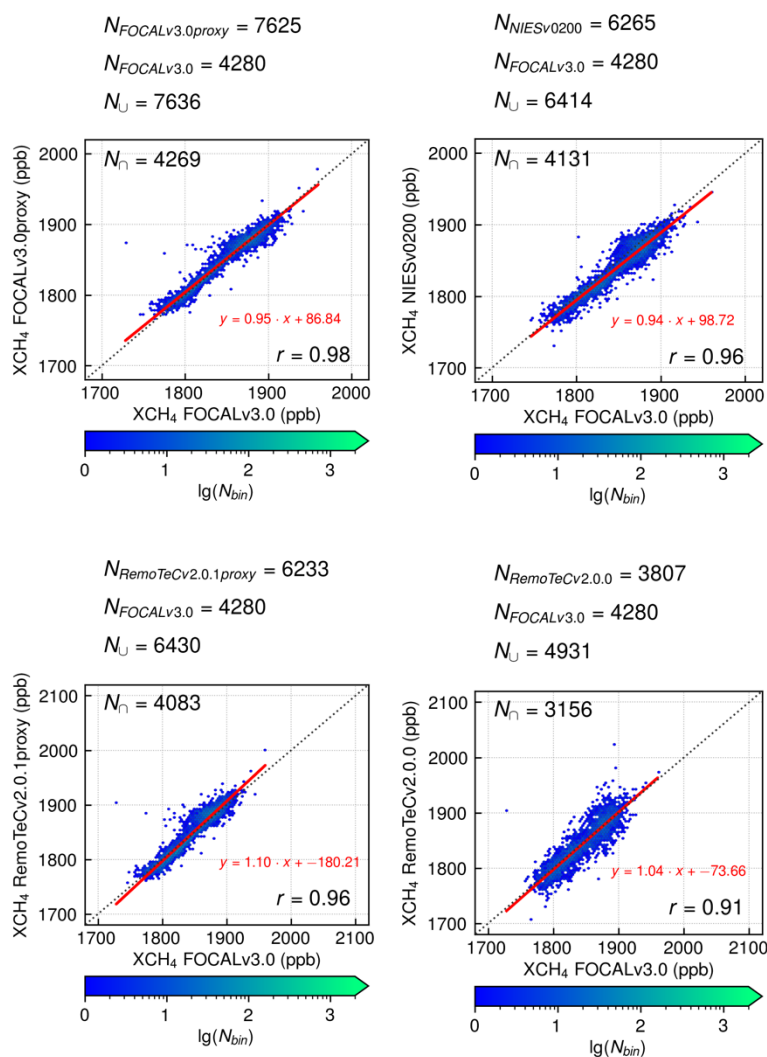


Figure 32: Scatterplots of GOSAT-2 seasonal mean (winter) XCH4. As reference (x-axis), we have chosen the FOCAL FP dataset.



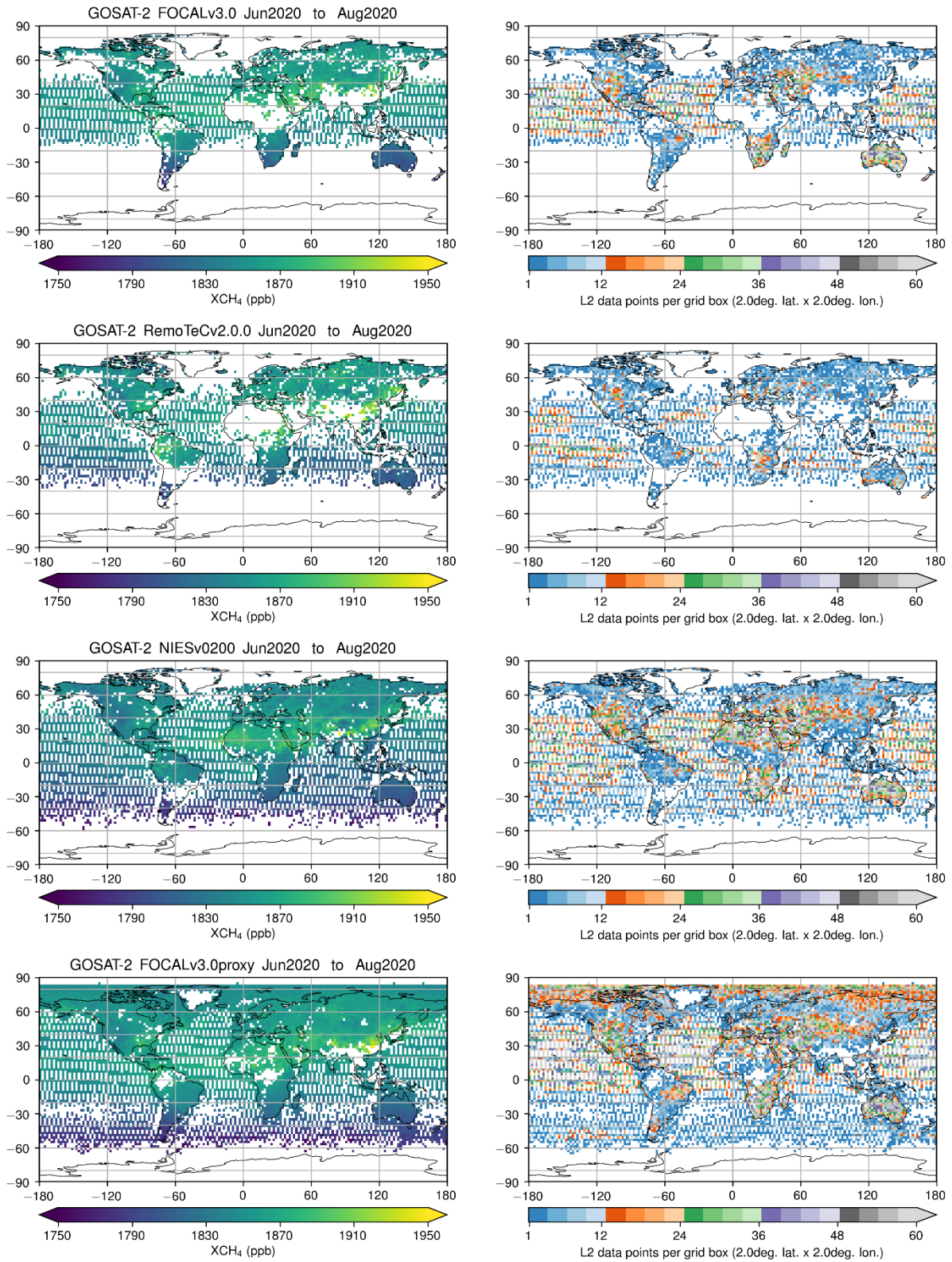


Figure 33: As Figure 31 but for Summer 2020.



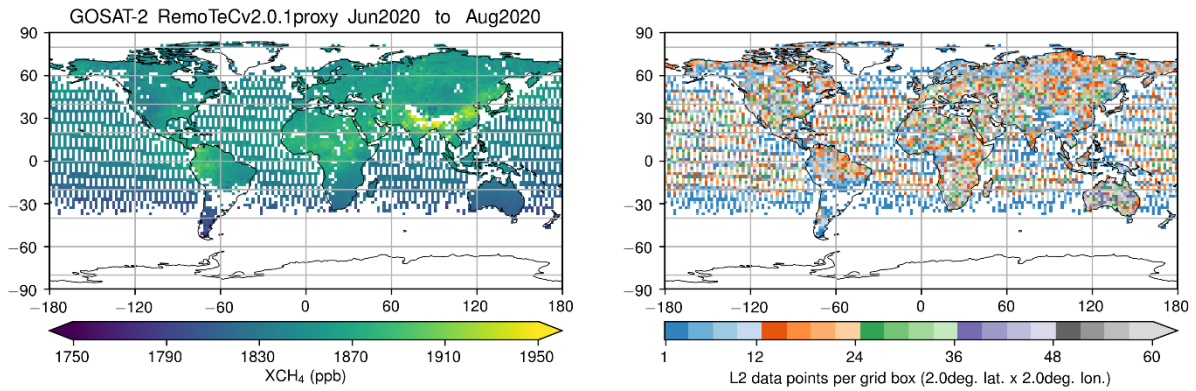


Figure 33: continued

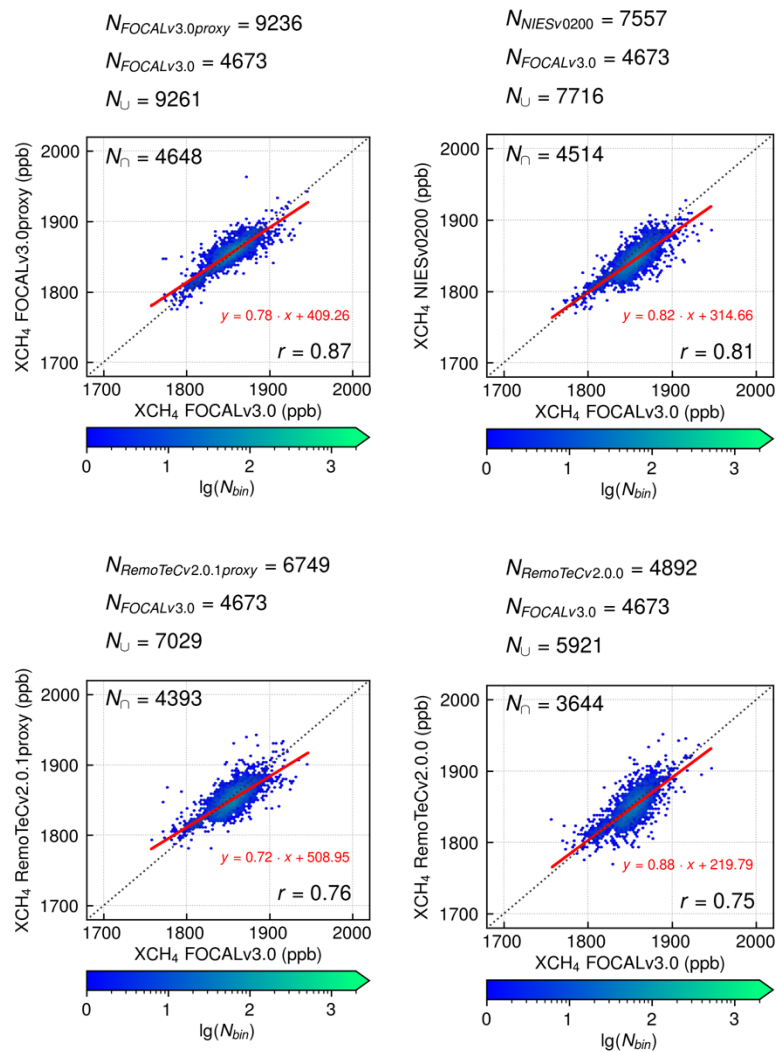


Figure 34: As Figure 32 but for summer 2020



4.2.4. Maps of seasonal mean XCH₄ from GOSAT-2 – Europe

As already observed for GOSAT, the coverage of the GOSAT-2 FP products for the European domain during winter is limited with the NIES product showing best coverage. Compared to GOSAT, the coverage of the FP products is improved for GOSAT-2. Using the proxy approach, much better coverage during winter is obtained up to a certain latitudinal cut-off. The better coverage of GOSAT-2 compared to GOSAT is well visible in summer where the FP datasets achieve good coverage over land. Using the proxy approach, FOCAL also obtains full coverage over the water bodies in summer.

As has already been observed for GOSAT; differences between the retrievals are more pronounced on a European scale compared to the global scale. For winter, correlation coefficients can be very low and the proxy products show clear differences to the FOCAL FP product. Better consistency between the datasets is found in summer where also more datapoints improve the statistics of the comparison.

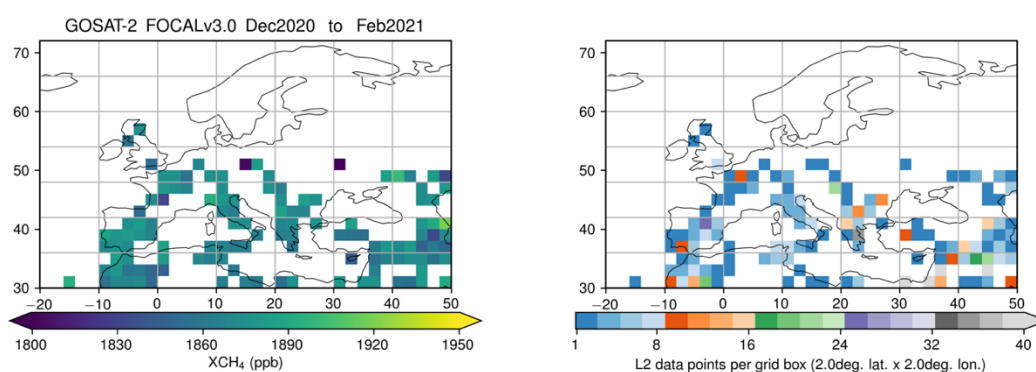


Figure 35: Seasonal averaged GOSAT-2 products for Europe for winter 2020 (Dec. 2020 to Feb. 2021) for the following datasets: FOCAL, RemoTeC and NIES full physics products and FOCAL and RemoTeC proxy products (from top to bottom). The averaged XCH₄ is given in the left column and the number of datapoints per bin is given in the right column.

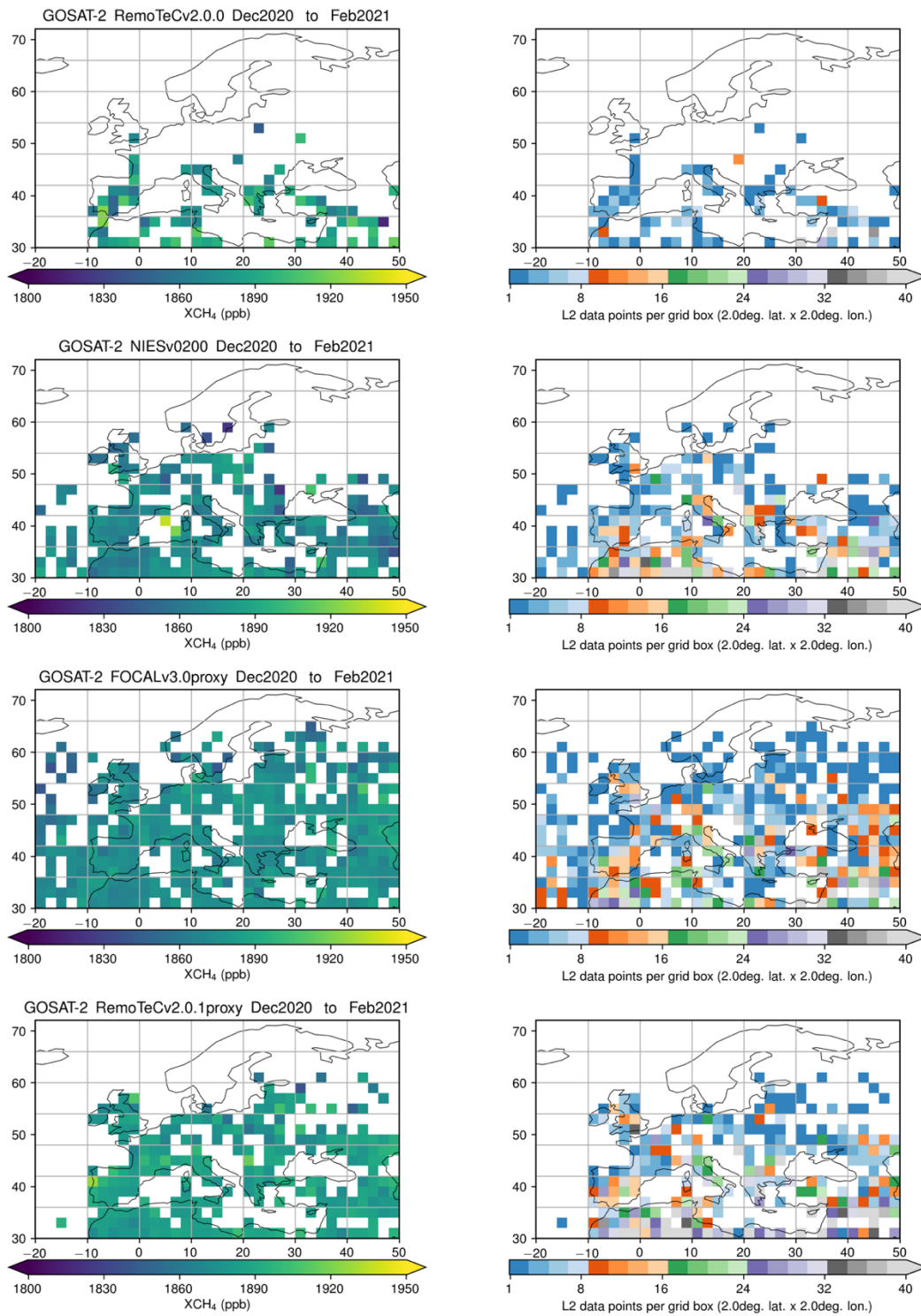


Figure 35: continued



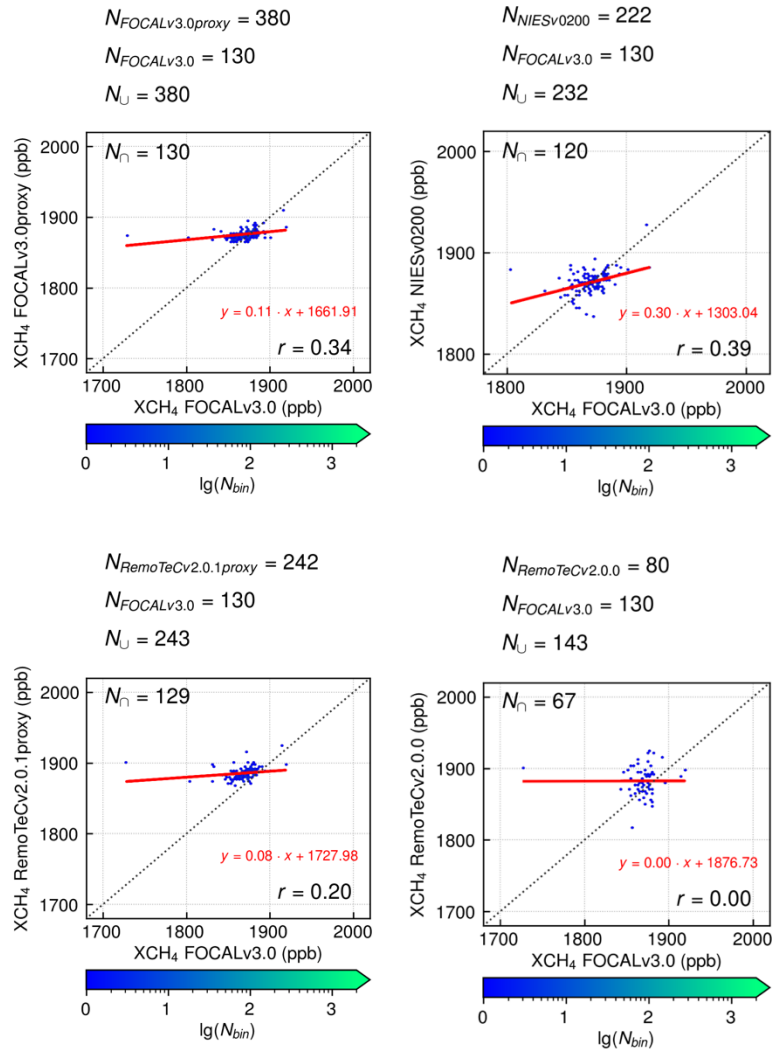


Figure 36: Scatterplots of GOSAT-2 seasonal mean (winter) XCH₄ for Europe. As reference (x-axis), we have chosen the FOCAL FP dataset.

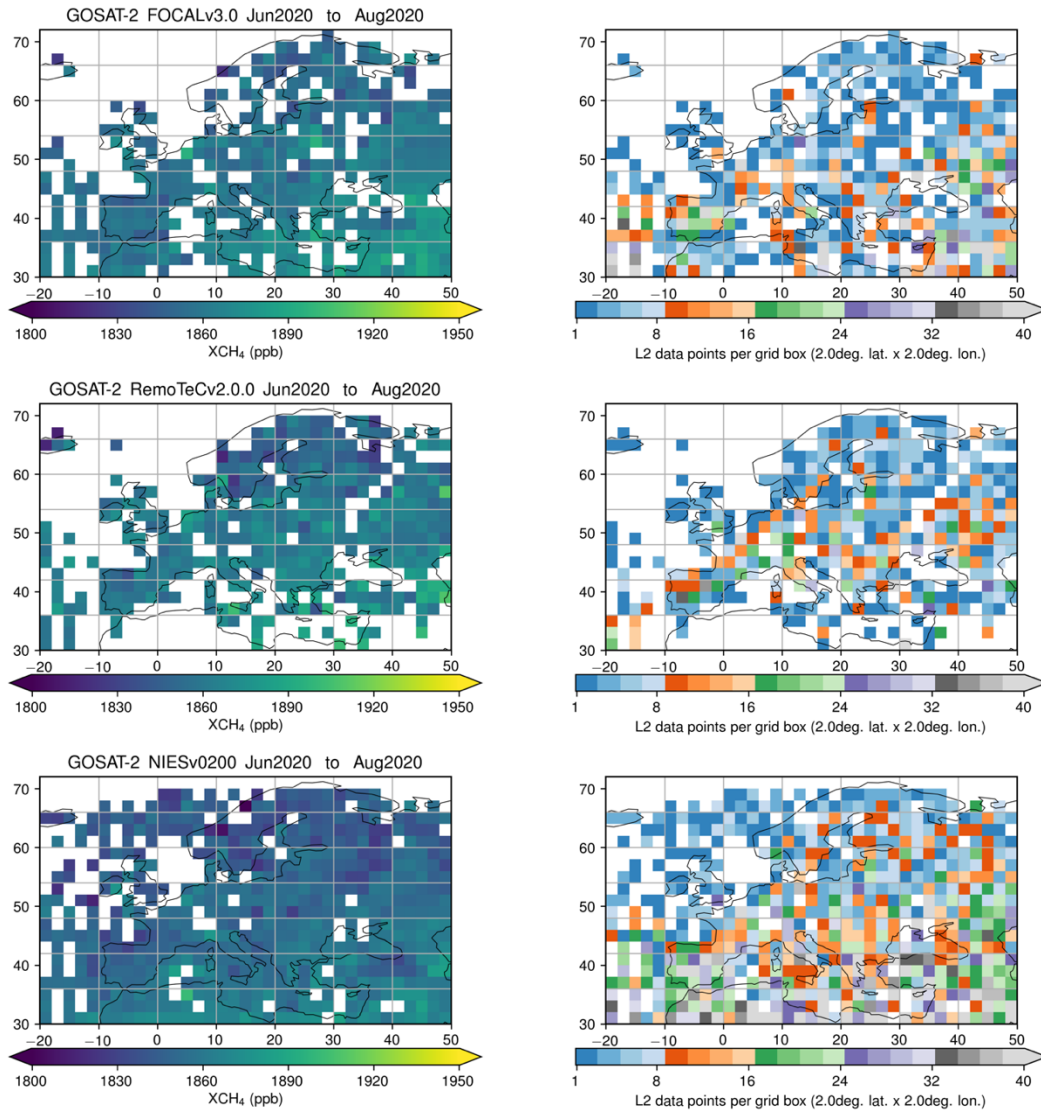


Figure 37: As Figure 35 but for summer 2020.

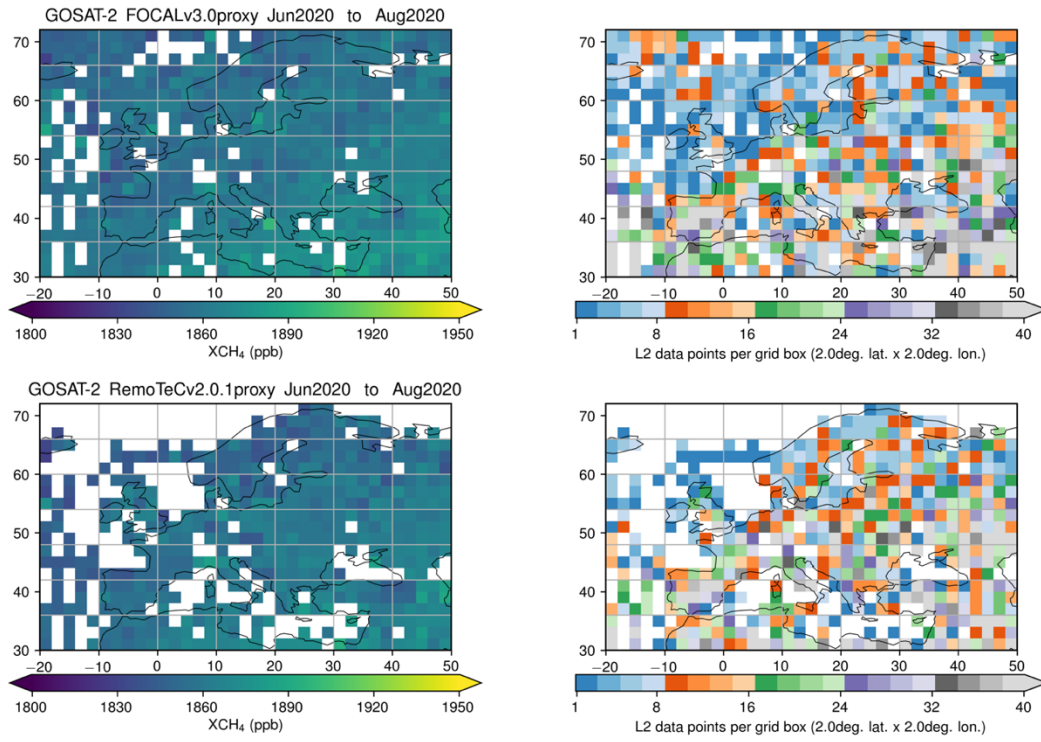


Figure 37: continued

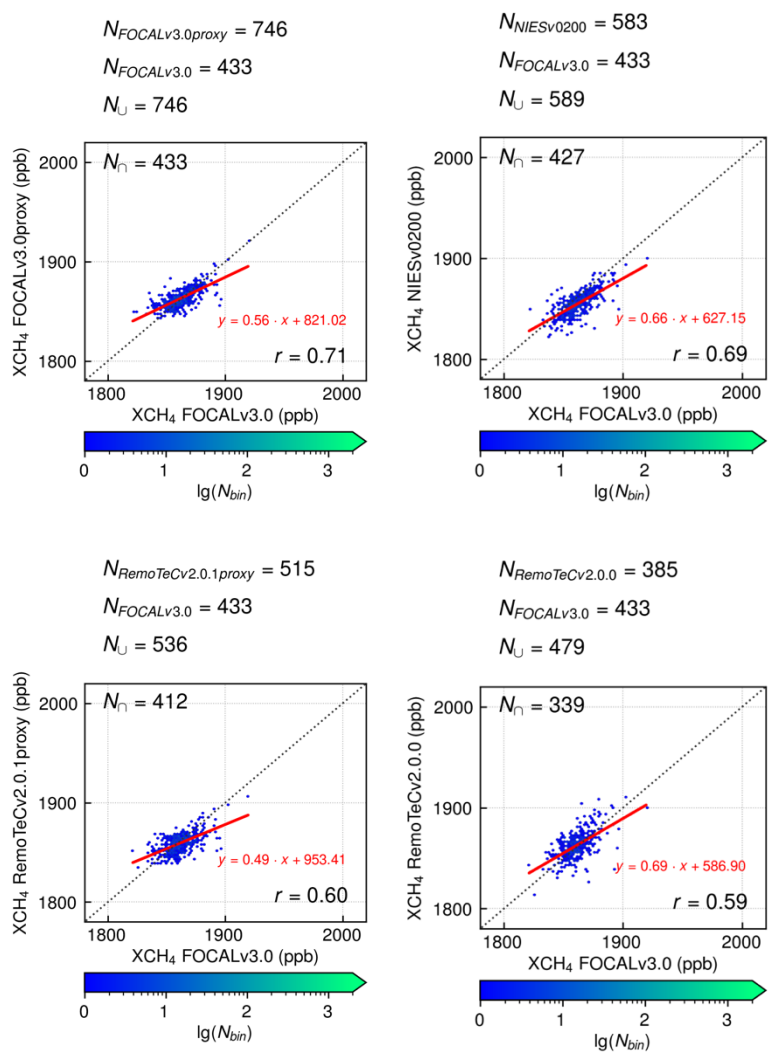


Figure 38: As Figure 36 but for summer 2020.

5. Comparison with TCCON XCH₄

5.1. Methodology

The focus of the comparison to TCCON data is for Europe and only European sites were considered as listed in Table 4. A set of co-location criteria were defined for the comparison: The spatial co-location requires the TROPOMI and GOSAT measurement to be within a radius of 100km around the TCCON station. The altitude collocation is defined by a maximum height difference of 250m. The temporal collocation is set to ± 2 h and TCCON data over this window is averaged.

For a comparison between TCCON and the satellite data, it has to be taken into account that the sensitivities of both instruments differ from each other and that different a priori profiles are used to determine the best estimate of the true atmospheric state, respectively. Therefore, the measurements are adjusted to a common a priori profile to correct for the a priori contribution to the smoothing equation (Schneising et al., 2012; Dils et al., 2014). The TCCON prior is used as the common a priori profile for all measurements (Schneising et al. 2019).

The results are plotted as time series and scatterplots of the individual measurements for the different XCH₄ products in comparison to the TCCON data. We have only included data since 2018 for all satellites to allow better inter-comparability between the results for different satellites.

5.2. Results and Discussion

5.2.1 TROPOMI XCH₄ Comparison

Time series and scatter plots for all selected TCCON sites are given in Figure 39 for the comparison with TROPOMI/WFMD data, in Figure 41 and Figure 42 for the SRON RemoTeC product and in Figure 43 and Figure 44 for the TROPOMI/operational (RPRO) product. The complete set of Figures is available from <https://nc.uni-bremen.de/index.php/s/AZNgkQtrHrZSbgf>.

The comparison of the WFMD datasets to TCCON shows overall good agreement. We find a good correlation ($r \geq 0.7$) and low biases of 6.2 ppb or less for the different sites. The exception is Garmisch where the bias is larger (12.2 ppb) and the correlation is lower ($r = 0.58$). This is likely caused by the difficult location of the site

The comparison for the SRON product shows good agreement with TCCON as well. The obtained correlation coefficients are very similar to those from the WFMD comparison but biases are higher for all sites. This is most pronounced for the Sodankylä site where the bias increases from 2.8 ppb for WFMD to 11.4 ppb for SRON. The number of datapoints available for the TCCON comparison is higher for the WFMD product than for the SRON product, except for Sodankylä where the SRON product has almost 30% more data. This higher data yield at Sodankylä in the SRON product might be related to the increased bias observed for this site as differences in data yield are primarily the result of the applied quality filter and a stricter filter can lead to a lower bias.

The comparison for the operational dataset is, as expected, similar to the SRON comparison with very similar correlation coefficients. The number of data points and the obtained biases are slightly larger for the operational product compared to the SRON product for all sites except for Sodankylä where the bias is comparable.



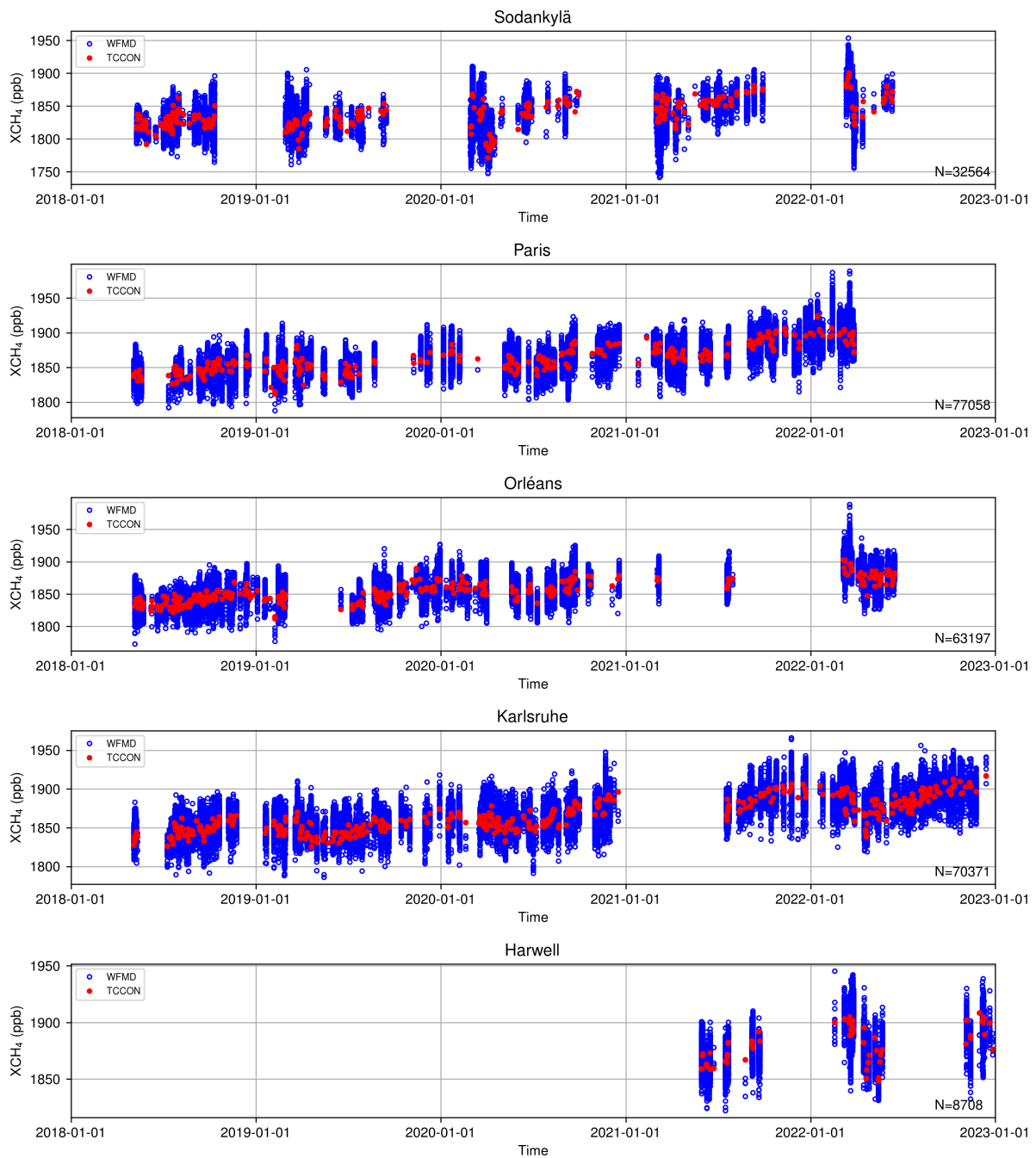


Figure 39: Comparison of the TROPOMI/WFM-DOAS v.1.8 XCH₄ time series (*blue*) with ground-based TCCON measurements (*red*). *N* indicates the number of co-locations.



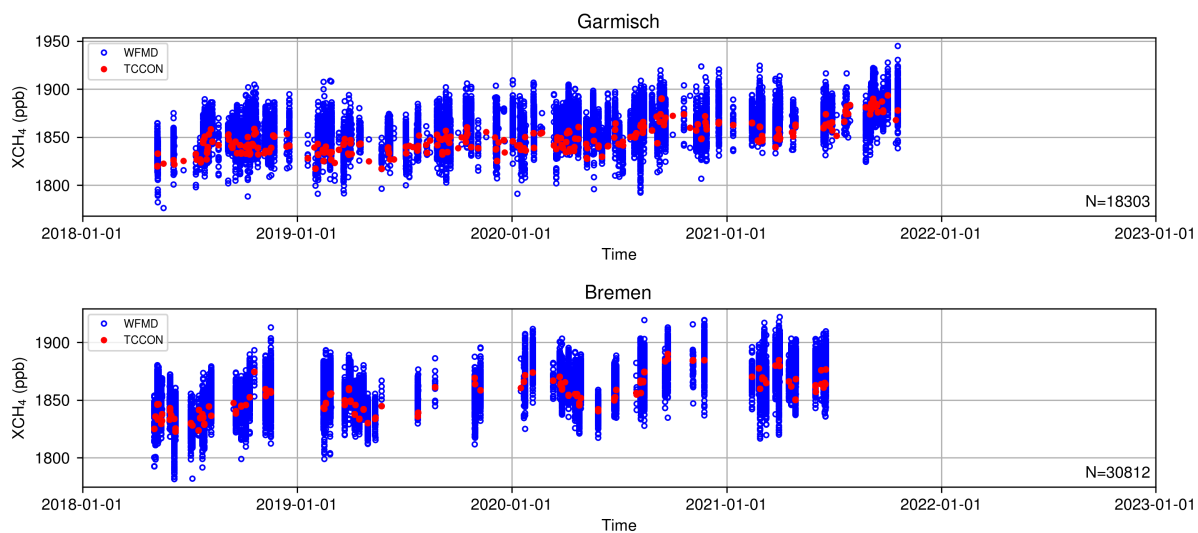


Figure 39: continued 1

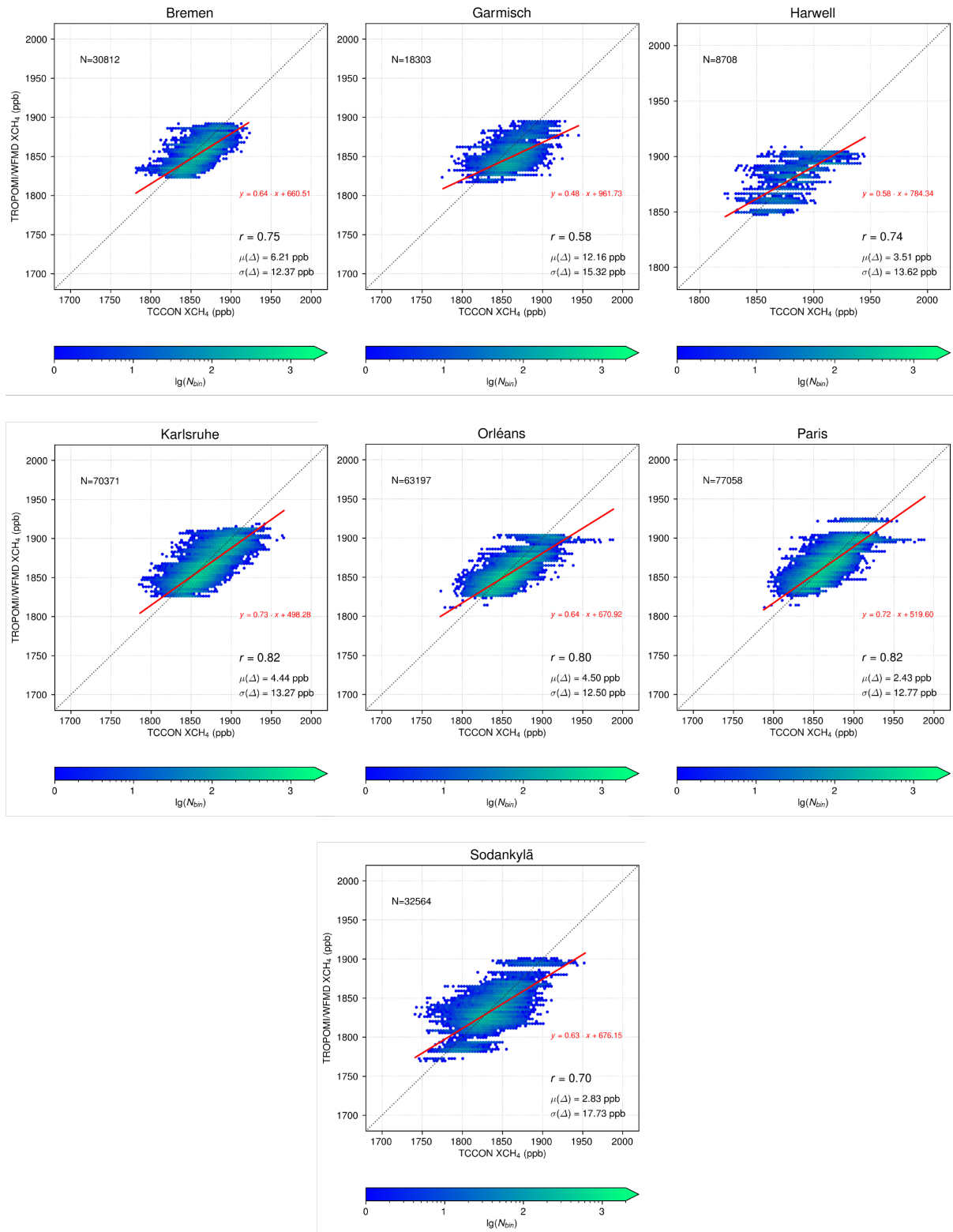


Figure 40: Comparison of TROPOMI/WFMD and TCCON XCH₄ for European sites. The number of co-locations N , the correlation coefficient r , the mean of the difference $\mu(\Delta)$ and the standard deviation $\sigma(\Delta)$ are indicated.



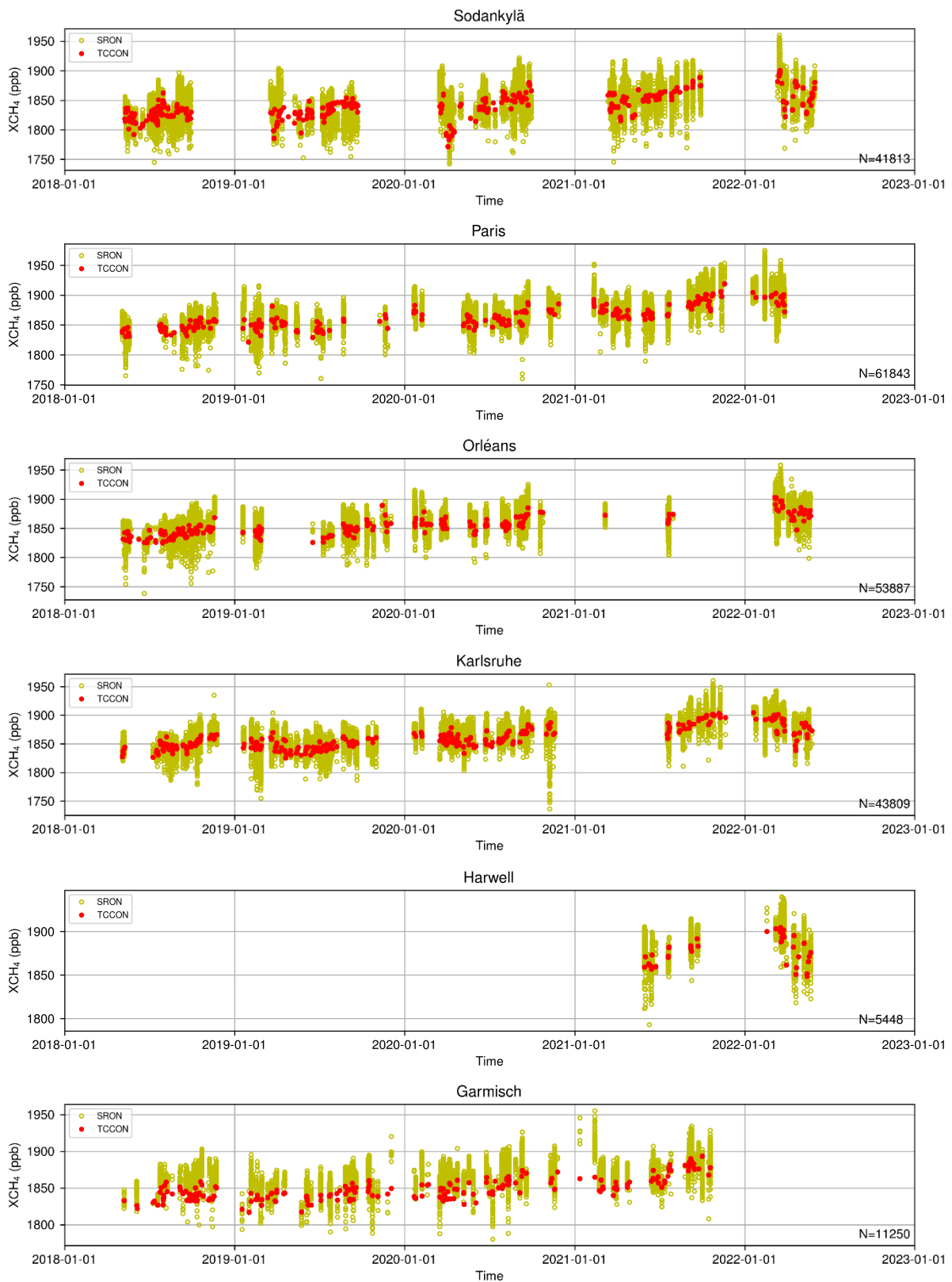


Figure 41: Comparison of the SRON RemoTeC-S5P XCH₄ scientific product version 19.446 time series (yellow) with ground-based TCCON measurements (red). *N* indicates the number of co-locations.



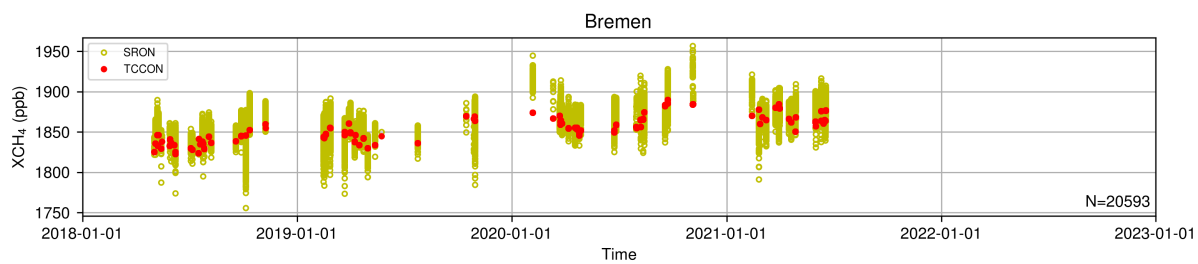


Figure 41: continued

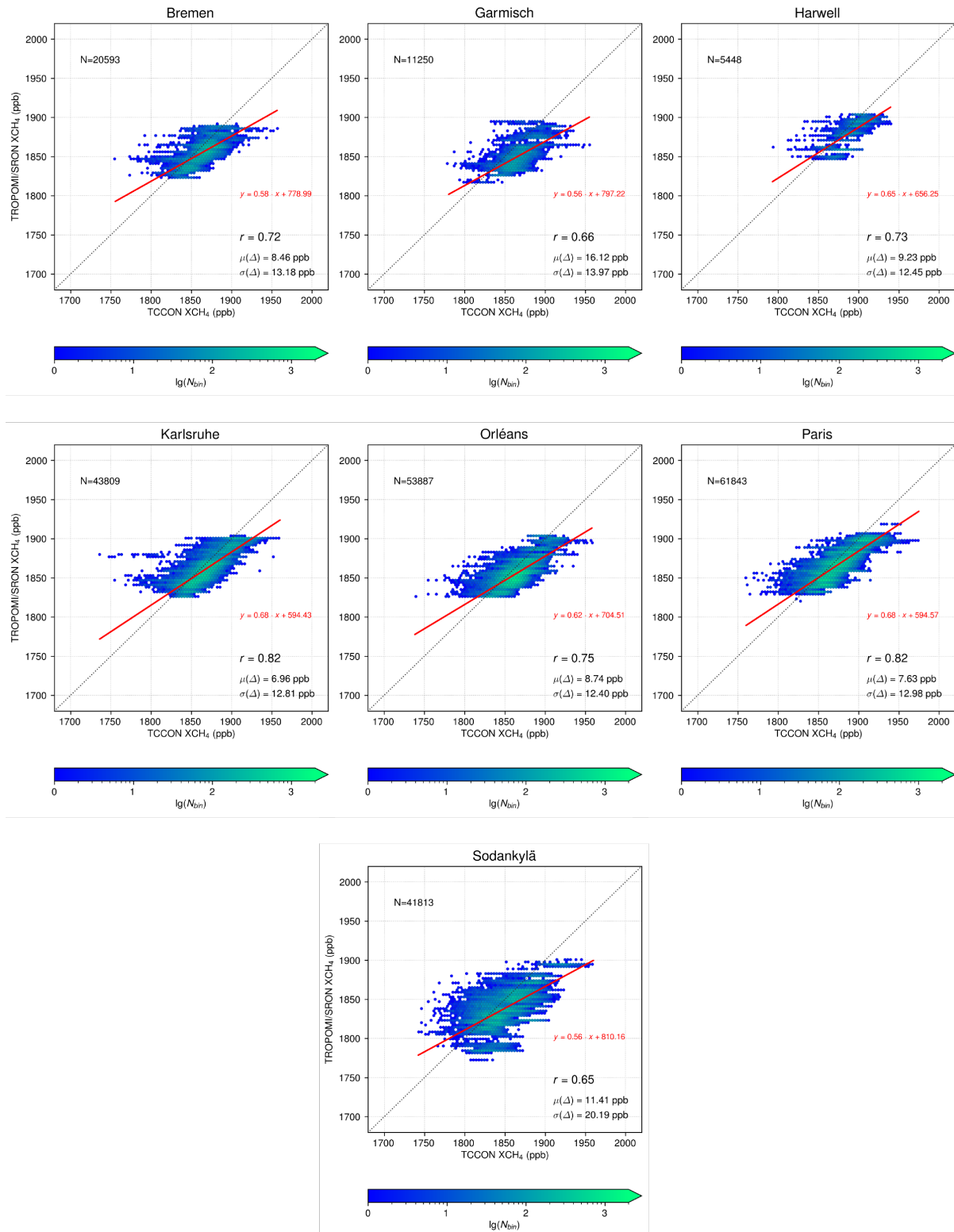


Figure 42: Comparison of RemoTeC-S5P XCH₄ scientific product version 19.446 and TCCON XCH₄ for European sites. The number of collocations N , the correlation coefficient r , the mean of the difference $\mu(\Delta)$ and the standard deviation $\sigma(\Delta)$ are indicated.



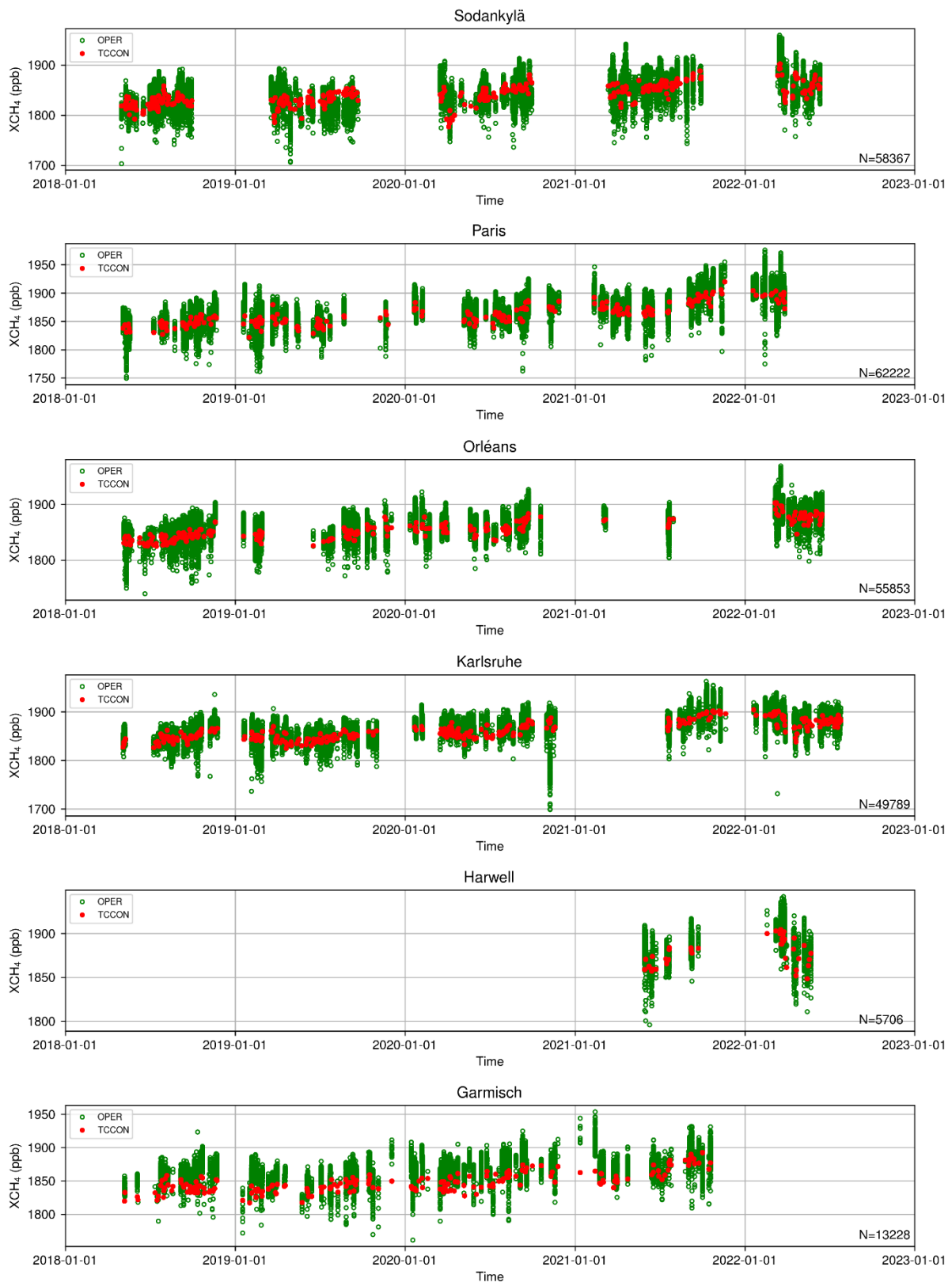


Figure 43: Comparison of the operational (reprocessed) data product RPRO version 02.04.00 time series (*green*) with ground-based TCCON measurements (*red*). *N* indicates the number of collocations.



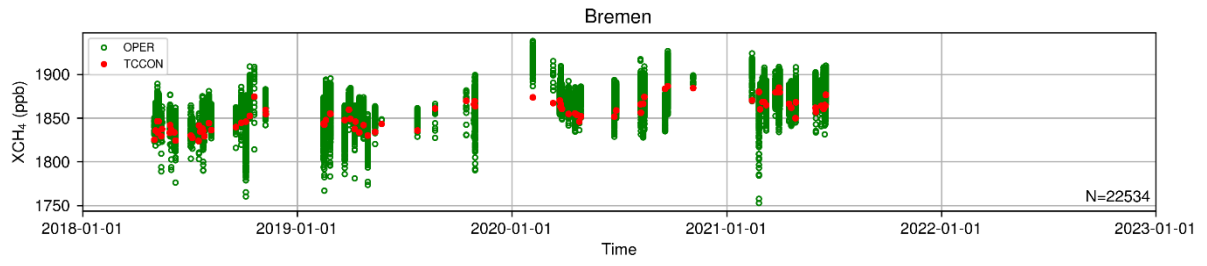


Figure 43: continued



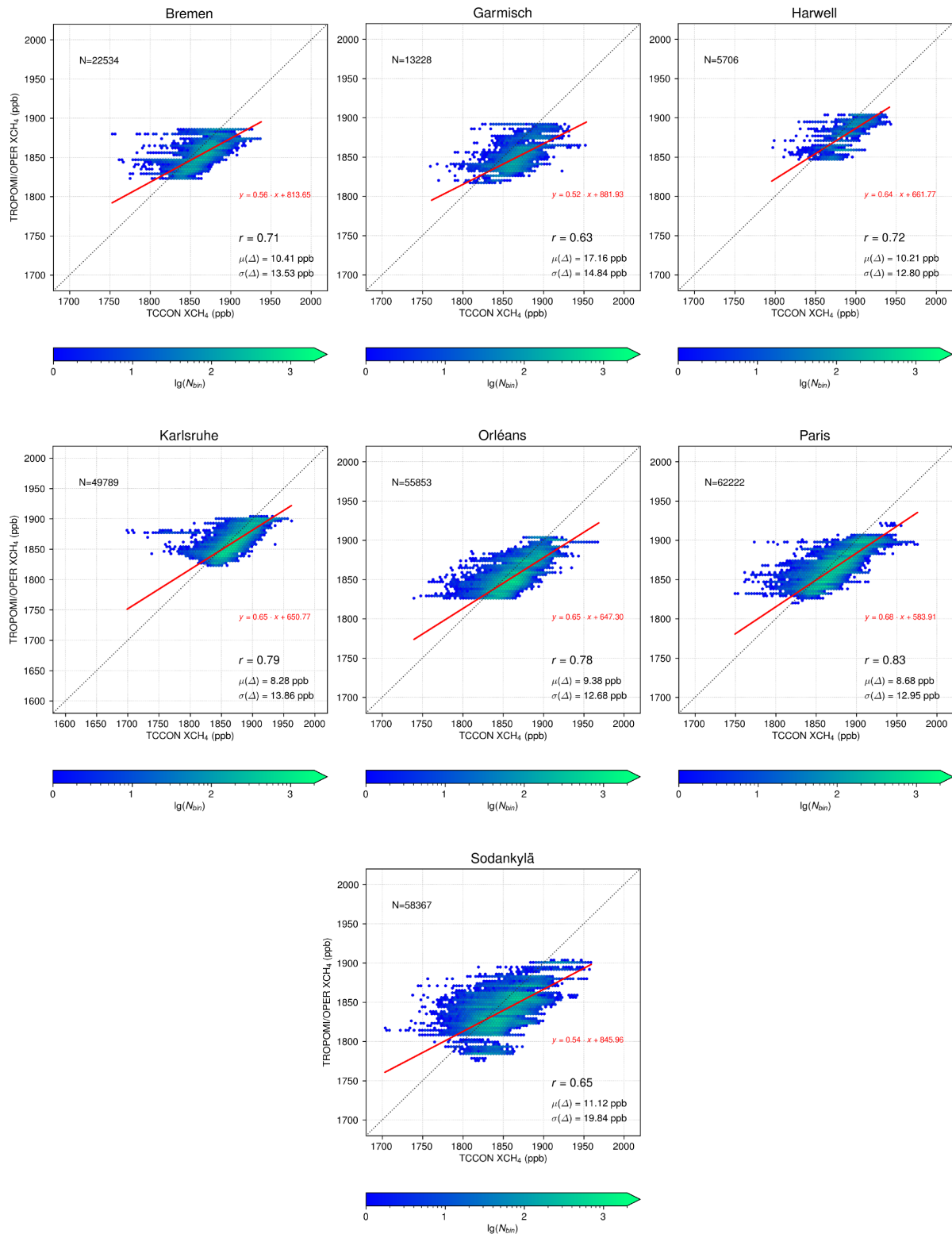


Figure 44: Comparison of TROPOMI/operational (RPRO) and TCCON XCH₄ for European sites. The number of collocations *N*, the correlation coefficient *r*, the mean of the difference $\mu(\Delta)$ and the standard deviation $\sigma(\Delta)$ are indicated.



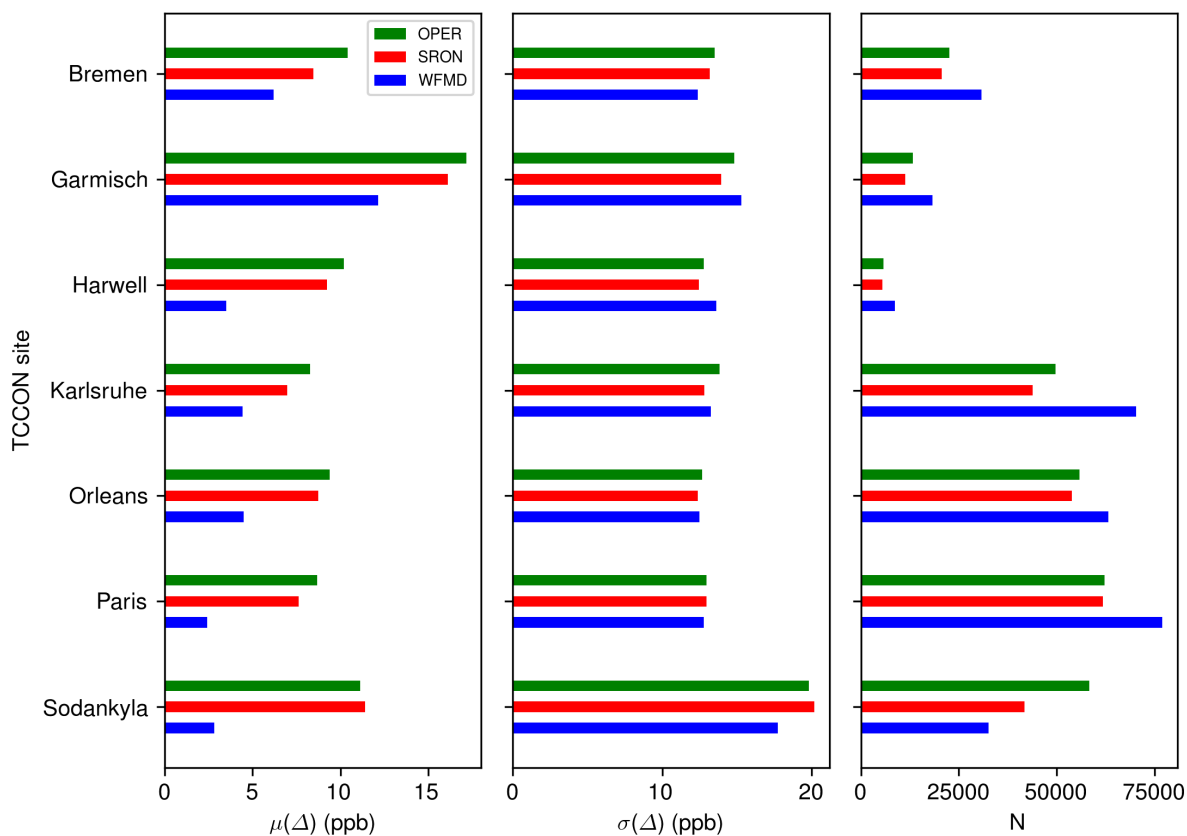


Figure 45: Mean of the difference $\mu(\Delta)$, the standard deviation $\sigma(\Delta)$ and number of soundings (N) of the TCCON and TROPOMI XCH₄ comparison for three different products for European sites.

Figure 45 gives an overview over the obtained biases and scatter obtained from the comparison to TCCON for the three different datasets for all European sites. This shows again the behaviour already described above. For all sites, we find lower biases for the WFMD dataset compared to the SRON and operational datasets with the largest difference being found for Sodankylä. The operational datasets show the largest biases of all three datasets compared to TCCON.

A somewhat different picture is obtained when considering the relative accuracy that is described by the standard-deviation of the biases at the different sites. Here we find similar values of about 3 ppb for all 3 algorithms with a slightly lower value of 3.0 ppb found for the OPER retrieval and a slightly higher value of 3.3 ppb for WFMD. This means that the OPER and SRON dataset have an overall larger offset but the variability of biases across the TCCON sites is similar for all 3 products.

The observed scatter is typically between 12 and 15 ppb and is similar for all three products. Larger scatter is observed for the Sodankylä site. The number of data point is largest for the WFMD dataset, except for Sodankylä where the SRON and operational datasets have significantly more data.

5.2.2. GOSAT XCH₄ Comparison

Time series and scatter plots for all European TCCON sites for the seven GOSAT datasets have been generated. Due to the very large number of generated plots, we only show the time series and scatter plots for the central European site Orleans (Figure 46 and Figure 48) and the high-latitude site Sodankyla (Figure 47 and Figure 49). A summary plot for all European



TCCON sites is given in Figure 50. The complete set of figures is available from <https://nc.uni-bremen.de/index.php/s/3WfGkLfPBMyYarF>.

As expected from the observation pattern of GOSAT, much less data is available for TCCON comparisons for GOSAT compared to TROPOMI. While there had been several thousands of TROPOMI soundings co-located with a TCCON site, this is reduced to few hundred at best for GOSAT. Among the FP retrieval, the FOCAL algorithm has typically the highest number of datapoints. Using the proxy retrieval approach, the number of available GOSAT retrievals can be substantially increased by typically a factor for 3-5 for RemoTeC and UoL-FP and by about 20-50% for FOCAL (FOCAL uses the same retrieval for the FP and proxy approach).

Overall, we find a good level of agreement between the GOSAT satellite datasets and the ground-based TCCON data with values of the correlation coefficient r between 0.5 and 0.8 with the exception of the RemoTeC dataset for Garmisch with a much lower value for r . For sites with higher number of GOSAT data points (Orleans, Paris, Sodankyla), the correlation coefficients vary little between the different datasets.

Biases are below 20 ppb for all sites and algorithms (exception is RemoTeC over Garmisch) and are typically in the range of 5-10 ppb. For the FP retrievals, lowest biases are either found for FOCAL (FP or proxy) and UoL-FP. Among the proxy retrievals, the FOCAL proxy dataset has lowest biases (except for Karlsruhe). Often the proxy retrievals show a higher bias compared to the FP product of the same algorithm. This is most obvious for UoL-FP. However, it needs to be pointed out that for UoL-FP proxy a global bias correction had been determined based on the previous version of the TCCON data which can lead to an offset against the current version of TCCON.

Often the regional accuracy of a dataset is a more important parameter than absolute biases. The regional accuracy can be approximated by the standard-deviation of the biases at all the sites and represents thus the spatial distribution of biases. Here we find the lowest value of 2.0 ppb for the UoL-FP-proxy retrieval which is much better than the value of the UoL-FP full physics product with a value of 4.1 ppb. A similar value of the relative accuracy of 2.4 ppb is found for the FOCAL FP product. For FOCAL, the value of the relative accuracy of the proxy product is higher which is unexpected. The NIES dataset has a value of 3.1 ppb. In case of RemoTeC, the FP datasets has a value of 4.6 ppb which is only slightly reduced to 4.1 ppb in case of the proxy retrieval.

The uncertainty of the datasets can be estimated from the scatter of the data (standard deviation of the individual datapoints). The scatter of the TCCON data will also contribute to this value but this is considered to be a small contribution. We find a value of typically between 5 and 10 ppb for the full physics datasets and between 10 and 18 ppb for the proxy dataset. The scatter of the proxy data is higher, as expected, due to the additional contribution from the additional CO₂ retrieval. In most cases, lowest scatter is found for the FOCAL FP dataset and highest for the RemoTeC proxy data.

Overall, biases are similar between GOSAT and TROPOMI. For some sites high bias values are found for RemoTeC which are not found in the SRON TROPOMI retrieval for the same site. The relative accuracy of the retrievals shows a larger spread for GOSAT compared to TROPOMI with some retrievals having lower values (e.g. UoL-FP proxy) while others (e.g. RemoTeC) have higher values. We find that the scatter in the GOSAT FP datasets is typically similar or lower than in the TROPOMI datasets while the GOSAT proxy datasets can have slightly higher scatter.



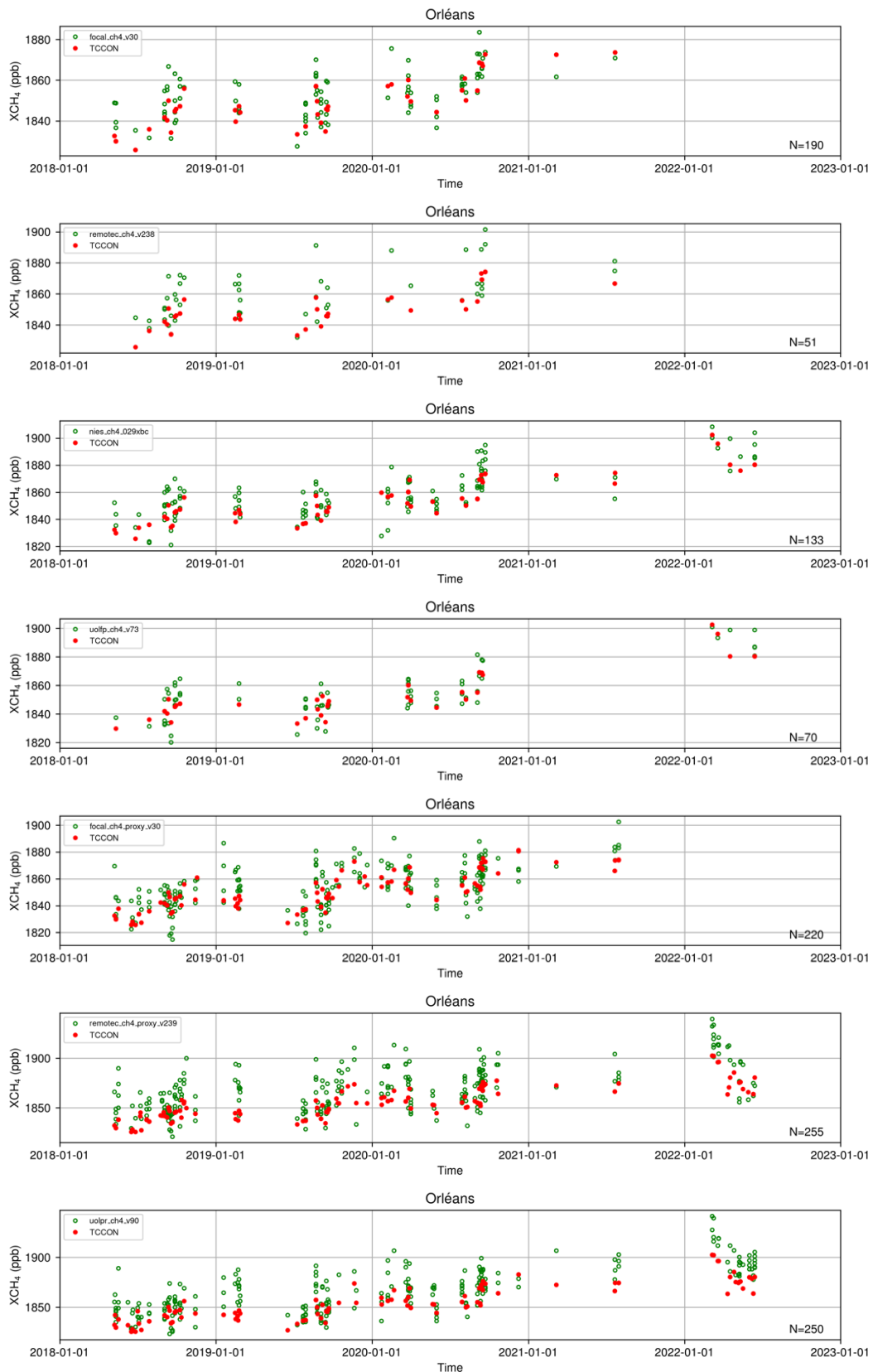


Figure 46: Comparison of the GOSAT retrievals XCH₄ time series (green) with ground-based TCCON measurements (red) at the Orleans site. *N* indicates the number of co-locations.



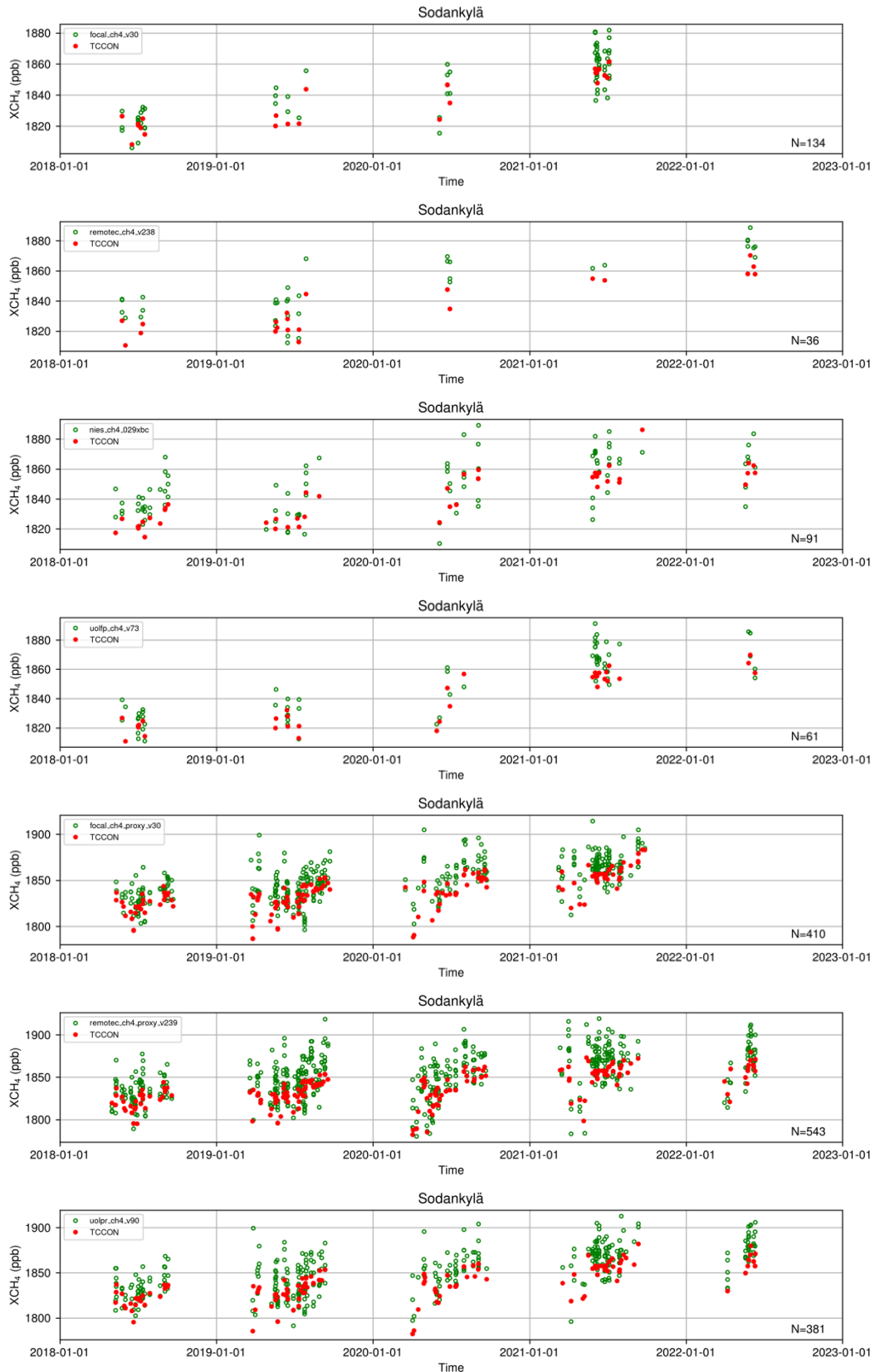


Figure 47: As Figure 46 but for the Sodankyla site.



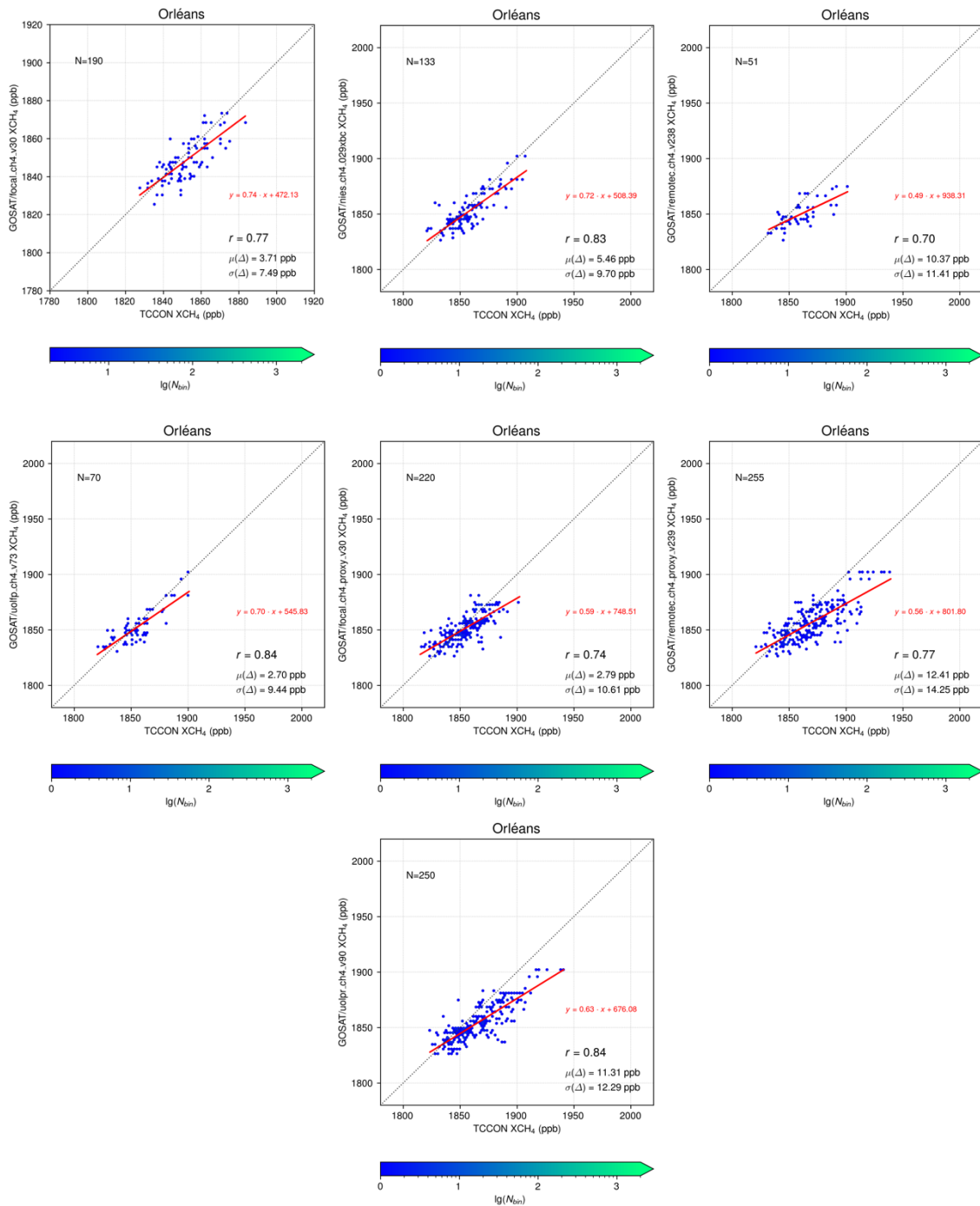


Figure 48: Comparison of GOSAT retrievals and TCCON XCH₄ for the Orleans site. The number of collocations N , the correlation coefficient r , the mean of the difference $\mu(\Delta)$ and the standard deviation $\sigma(\Delta)$ are indicated.

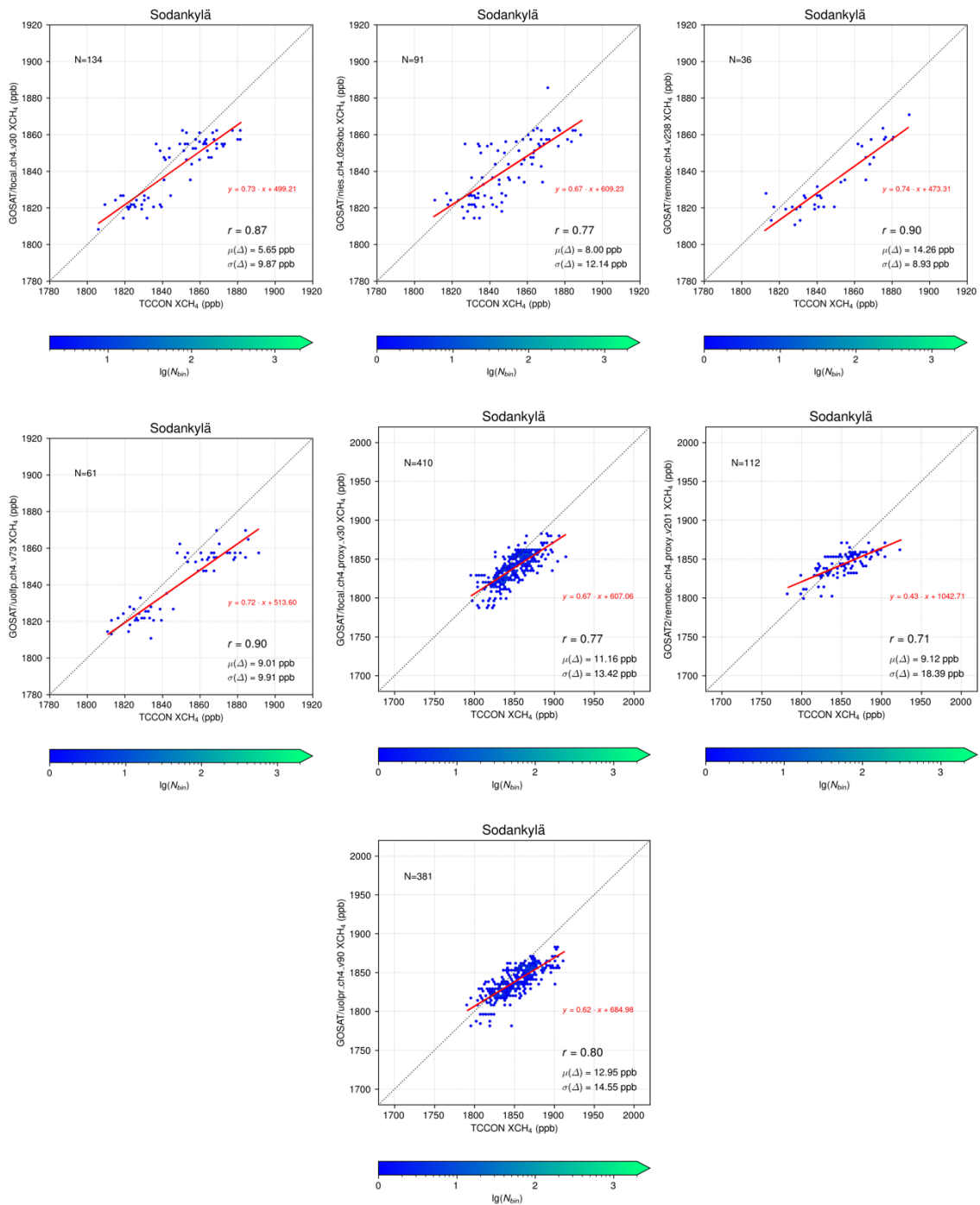


Figure 49: As Figure 48 but for Sodankylä





Figure 50: Upper row: number of soundings (N) and correlation coefficient r of the TCCON and GOSAT XCH₄ comparison for seven different products for European sites. Lower row: Bias (Mean of the difference) and standard deviation of the differences of the TCCON and GOSAT XCH₄ comparison

5.2.3. GOSAT-2 XCH₄ Comparison

Similar time series and scatter plots for all European TCCON sites have been created for the five GOSAT-2 retrievals. As for GOSAT, we show only time series and scatter plots for Orleans (Figure 51 and Figure 53) and Sodankyla (Figure 52 and Figure 54) together with the summary plot in Figure 55. The complete set of Figures is available from <https://nc.uni-bremen.de/index.php/s/3WFgkLFPBMyYarF>.



The number of datapoints of the GOSAT-2 datasets is overall similar compared to GOSAT (but for shorter timeseries for GOSAT-2), but with much fewer datapoints for Sodankyla which points towards a stricter quality filtering for GOSAT-2 for low light and high SZA conditions. A noticeable difference is that now the NIES retrieval has now the highest number of datapoints among the FP retrievals.

The correlation coefficient between the GOSAT-2 datasets and TCCON data shows similar values as for GOSAT with values of r mostly between 0.6 and 0.9.

The observed biases are in a similar range as found for GOSAT. For FOCAL FP, higher biases are found in 4 of 7 sites. In contrast, for the NIES and RemoTeC retrievals biases are substantially lower for GOSAT-2 (except for the Paris site for NIES). Biases for the RemoTeC proxy retrieval are higher than in the respective FP dataset for all sites. For GOSAT-2, the best relative accuracy with a value of 2.8 ppb is found for the NIES retrieval. The value for RemoTeC is about 4 ppb for the FP and the proxy retrieval. The value for FOCAL is slightly higher and around 4.4 ppb for the FP and 4.8 ppb for the proxy product.

The scatter in the GOSAT-2 retrieval has similar values as for GOSAT. FOCAL has lowest scatter while RemoTeC tends to have the highest scatter. For some sites, the scatter in the FOCAL proxy dataset is lower than in the FOCAL FP data which is unusual.

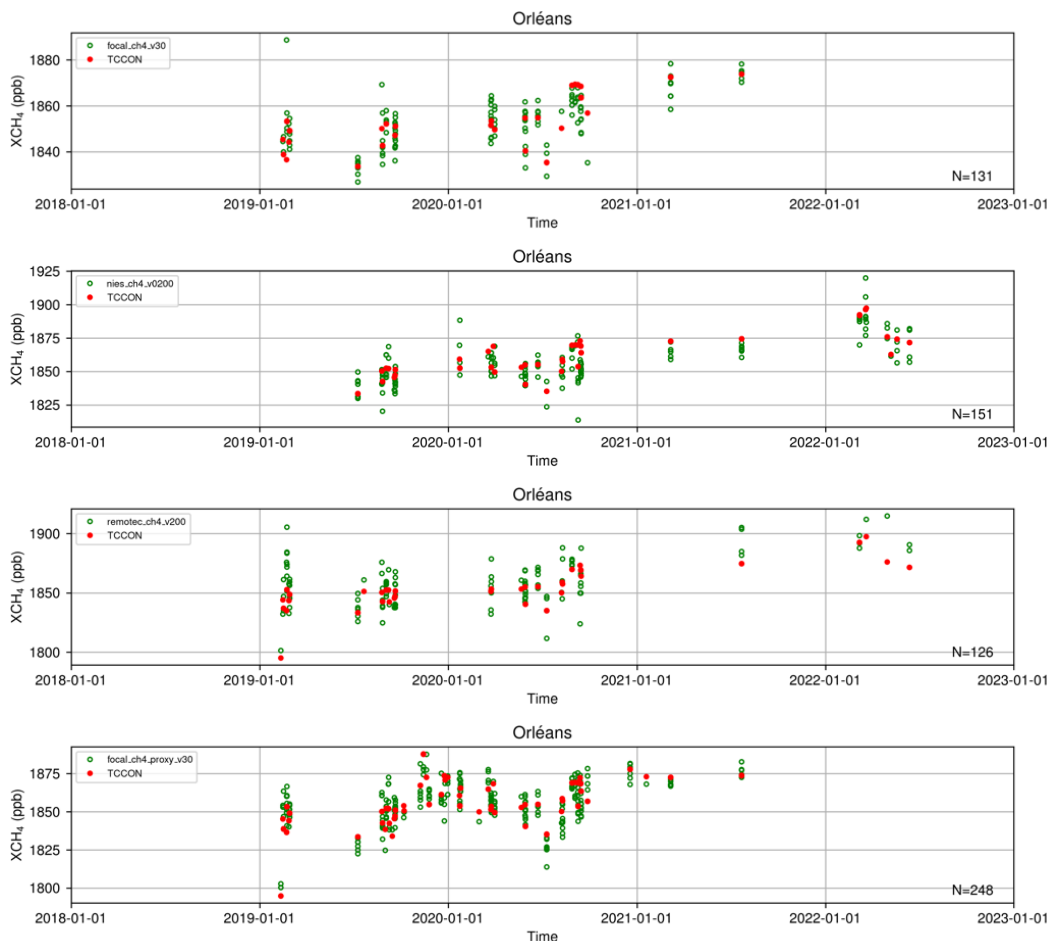


Figure 51: Comparison of the GOSAT-2 retrievals XCH₄ time series (green) with ground-based TCCON measurements (red) at the Orleans site. N indicates the number of co-locations.



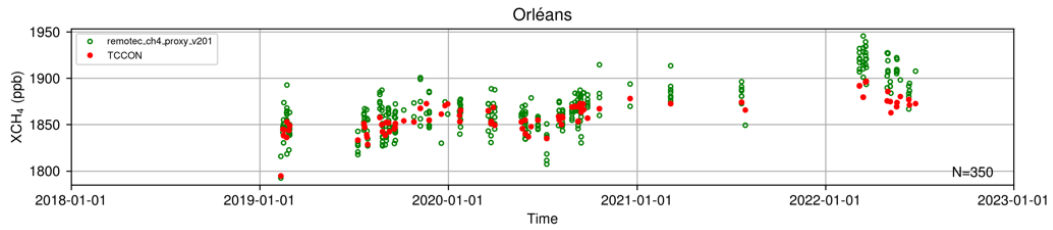


Figure 51: continued

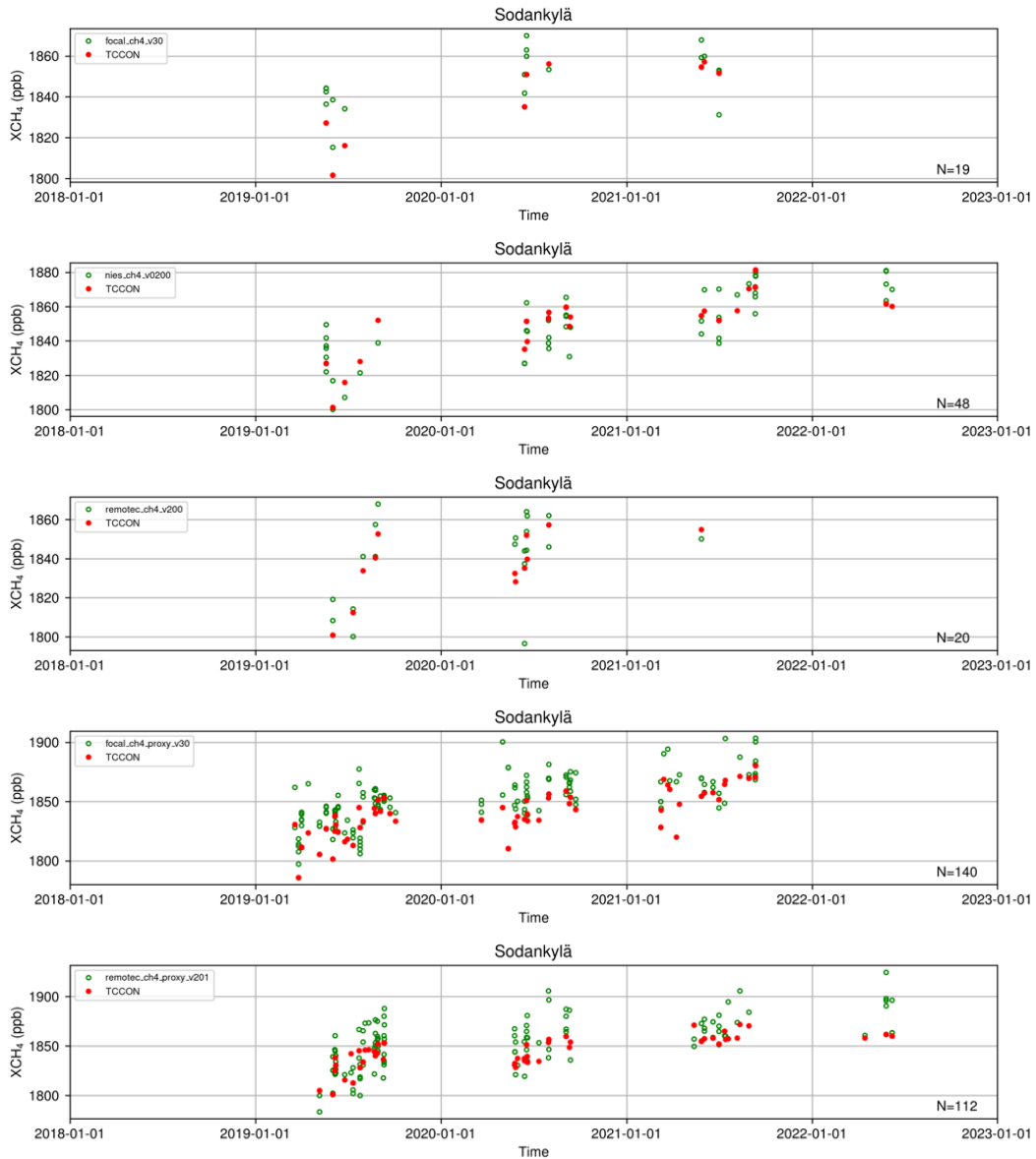


Figure 52: As Figure 51 but for the Sodankyla site.



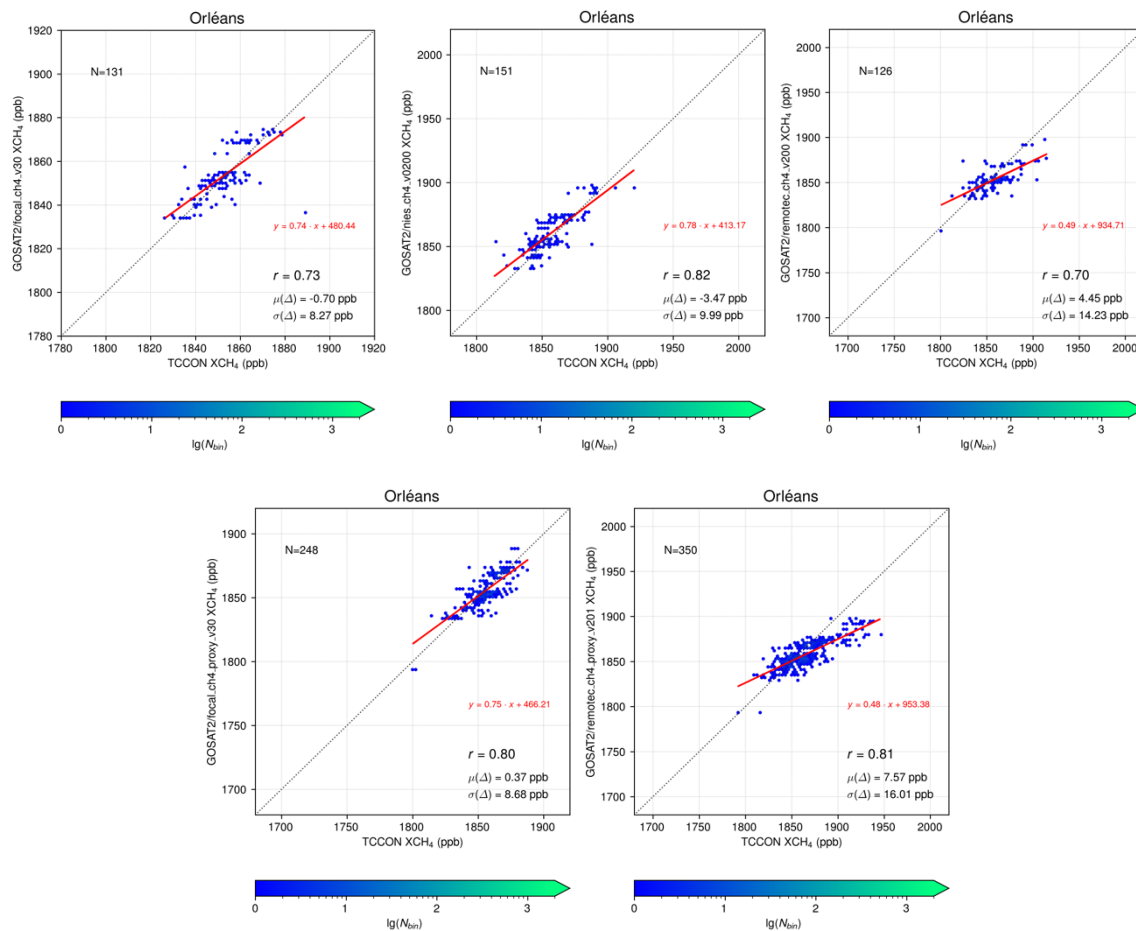


Figure 53: Comparison of GOSAT-2 retrievals and TCCON XCH₄ for the Orleans site. The number of collocations N , the correlation coefficient r , the mean of the difference $\mu(\Delta)$ and the standard deviation $\sigma(\Delta)$ are indicated.

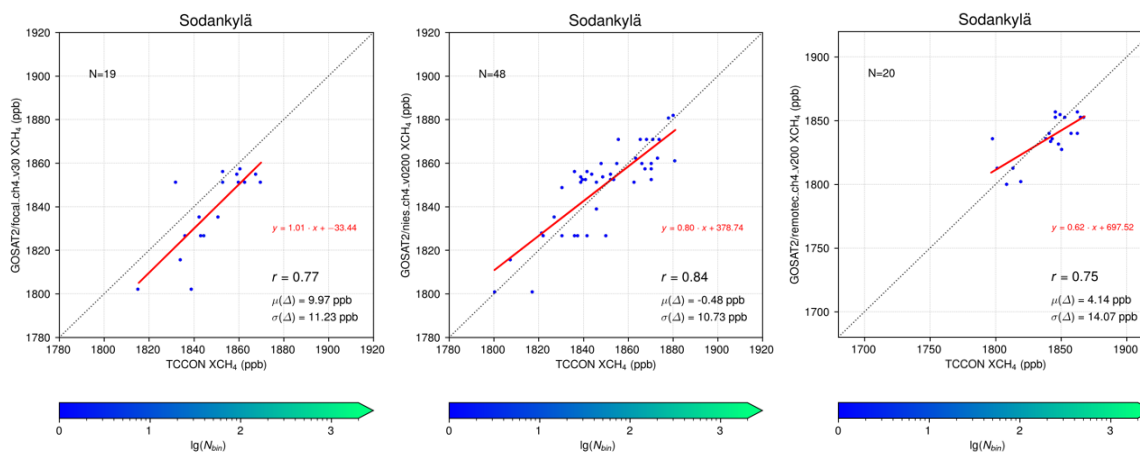


Figure 54: As Figure 53 but for the Sodankylä site



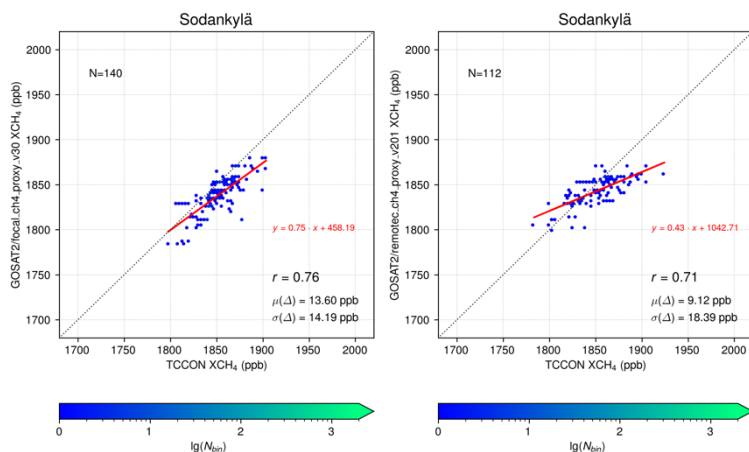


Figure 54: continued

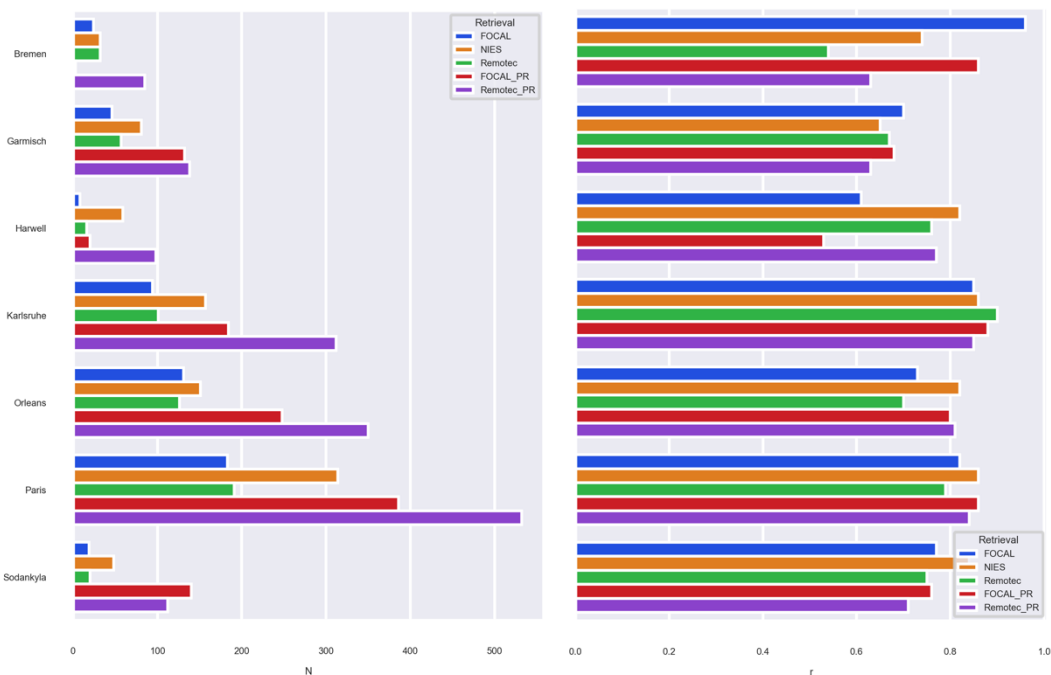


Figure 55: Upper row: number of soundings (N) and correlation coefficient r of the TCCON and GOSAT-2 XCH₄ comparison for five different products for European sites. Lower row: Bias (Mean of the difference) and standard deviation of the differences of the TCCON and GOSAT-2 XCH₄ comparison.

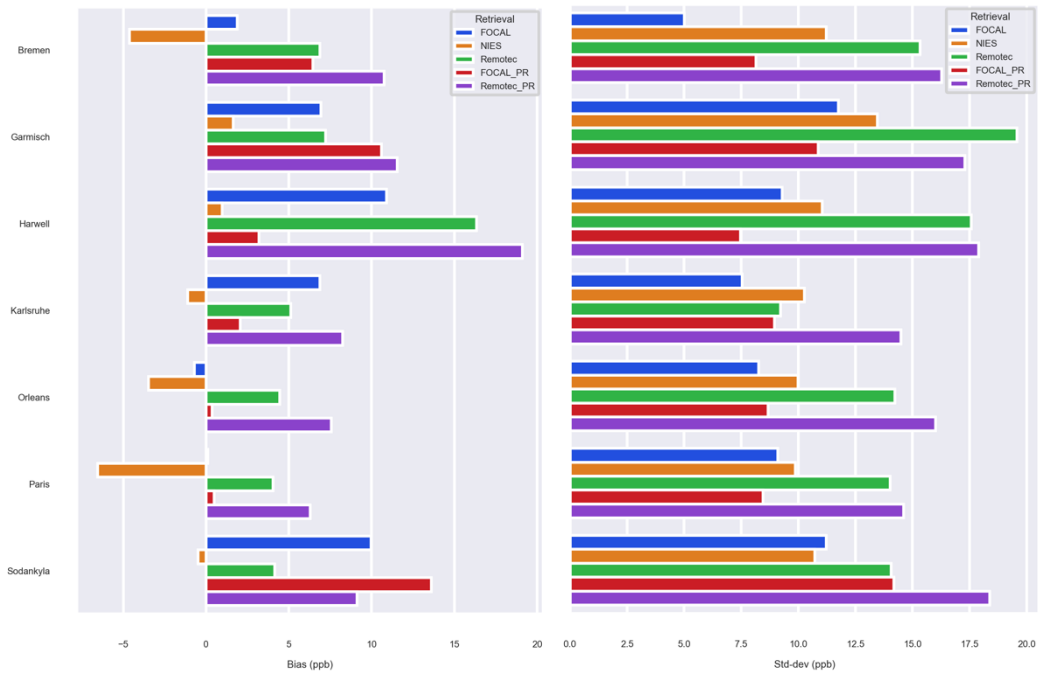


Figure 55: continued



6. Conclusions

Three TROPOMI XCH₄ data products have been inter-compared and assessed against ground-based reference data from the TCCON network. The datasets include the operational, reprocessed data product RPRO version 02.04.00, the SRON RemoTeC-S5P XCH₄ scientific product version 19.446 and the University of Bremen WFM-DOAS data product version 1.8. The assessment has been carried out globally and for the European domain.

As expected, we find that the operational and the SRON data products agree very well with each other. This is expected as both are based on the same retrieval algorithm. The WFMD datasets generated by IUP Bremen shows also good agreement with the two other datasets. There is a pronounced difference in coverage and number of data points with the WFMD product usually showing higher data volume and better coverage. Differences in the retrieved CH₄ values between WFMD and the two other datasets are more pronounced for the European domain than globally. Thus, it can be expected that surface flux inversions on a European domain will differ depending on the chosen dataset.

Differences between the WFMD and the operational dataset are also noticeable when observing emission plumes in single overpasses. Here, the often-better coverage of WFMD offers better opportunities for detection of emission plumes. Also, the magnitude of the CH₄ columns in these single overpasses can differ which can then lead to differences in the quantification of emissions.

The comparison to European TCCON sites of the TROPOMI datasets show high correlation coefficients and low biases for all three datasets, with lowest biases obtained for the WFMD dataset (2.8 to 12.2 ppb) and the highest for the operational dataset (8.3 ppb to 17.2 ppb). Overall, the TCCON comparison demonstrates a high quality of the TROPOMI CH₄ retrievals.

For GOSAT, seven retrievals including 4 full physics (FOCAL, NIES, RemoTeC, UoL-FP) and 3 proxy retrievals (FOCAL, RemoTeC and UoL-FP) have been evaluated and for GOSAT-2 five retrievals (3 full physics: FOCAL, NIES and RemoTeC, and 2 proxy retrievals: FOCAL and RemoTeC). As expected, the coverage and data volume of GOSAT and GOSAT-2 is much lower than for TROPOMI. Differences in coverage are found between different retrievals and especially between full physics and proxy retrievals. Between the GOSAT FP retrievals, FOCAL tends to have highest coverage over the oceans while over land the NIES algorithm tends to have best coverage. For GOSAT-2 better coverage is obtained compared to GOSAT with the NIES retrieval having superior coverage compared to other FP retrievals. For a regional domain such as Europe, the data coverage provided by the FP algorithms, in particular in winter, is very low and might be problematic for a regional inversion so that in terms of coverage, the proxy retrieval datasets might be better suited.

On a global scale, the different GOSAT and GOSAT-2 datasets correlate well. On a European scale, differences are more pronounced and the correlation between datasets can be low. It can be expected that flux results from a European inversion will depend on the chosen dataset.

The assessment of GOSAT data against ground-based TCCON data shows that biases tend to be low for all retrievals with values below 20 ppb and typical values of 5-10 ppb with typically lowest absolute biases observed for FOCAL and UoL-FP (FP) for GOSAT and NIES and FOCAL for GOSAT-2. The regional accuracy (given by the standard deviation of the biases of the different sites) is a measure of the spatial distribution of biases. Here, the UoL-FP proxy retrieval gives the lowest (best) value for GOSAT which is much better compared to the full physics version of UoL-FP. A similar but slightly higher value is found for FOCAL FP.

Results for biases and scatter obtained for GOSAT-2 are overall similar as for GOSAT. For the NIES and RemoTeC FP retrievals we find lower biases for GOSAT-2 compared to GOSAT for almost all sites while for FOCAL FP higher biases are observed in 4 of the 7 sites. In terms of relative accuracy, the best value



is found for the NIES product while the other retrievals have a noticeable higher value for relative accuracy.



Acknowledgements

Acknowledgement of the TCCON science team. The TCCON data were obtained from the TCCON Data Archive, hosted by CaltechDATA, California Institute of Technology (<https://tccondata.org/>).

References

- Barr, A. and T. Borsdorff, Algorithm Theoretical Basis Document (ATBD) ANNEX B for products CO₂_GO₂_SRFP & CH₄_GO₂_SRFP (v2.0.0, 2019-2022), project C3S2_312a_Lot2_DLR – Atmosphere, v7.1b, 2024
- Boesch H. and A. Di Noia , Algorithm Theoretical Basis Document (ATBD) ANNEX A for products CO₂_GOS_OCFP (v7.3), CH₄_GOS_OCFP (v7.3) & CH₄_GOS_OCPR (v9.0) (CDR7,2009-2022), project C3S2_312a_Lot2_DLR – Atmosphere, v7.1b, 2024
- Cogan, A. J., et al., Atmospheric carbon dioxide retrieved from the Greenhouse gases Observing SATellite (GOSAT): Comparison with ground-based TCCON observations and GEOS-Chem model calculations, *J. Geophys. Res.*, 117, D21301, doi:10.1029/2012JD018087, 2012
- Dils, B., et al., The Greenhouse Gas Climate Change Initiative (GHG-CCI): comparative validation of GHG-CCI SCIAMACHY/ENVISAT and TANSO-FTS/GOSAT CO₂ and CH₄ retrieval algorithm products with measurements from the TCCON, *Atmos. Meas. Tech.*, 7, 1723–1744, <https://doi.org/10.5194/amt-7-1723-2014>, 2014
- Duan, M., Q. Min, and J. Li, A fast radiative transfer model for simulating high-resolution absorption bands, *J. Geophys. Res.*, 110, D15201, doi:10.1029/2004JD005590, 2005
- Hase, F., Herkommer, B., Groß, J., Blumenstock, T., Kiel, M. ä ., & Dohe, S. (2023). TCCON data from Karlsruhe (DE), Release GGG2020.R1 (Version R1) [Data set]. CaltechDATA. <https://doi.org/10.14291/tccon.ggg2020.karlsruhe01.R1>
- Hasekamp, O. P., and A. Butz, Efficient calculation of intensity and polarization spectra in vertically inhomogeneous scattering and absorbing atmospheres, *J. Geophys. Res.*, 113, D20309, doi:10.1029/2008JD010379, 2008
- Hasekamp, O., Lorente, A., Hu, H., Butz, A., de Brugh, J., and Landgraf, J.. Algorithm Theoretical Baseline Document for Sentinel-5 Precursor Methane Retrieval. SRON-S5P-LEV2-RP-001, Issue 2.4.0, 2022
- Inoue, M., et al.: Bias corrections of GOSAT SWIR XCO₂ and XCH₄ with TCCON data and their evaluation using aircraft measurement data, *Atmos. Meas. Tech.*, 9, 3491–3512, <https://doi.org/10.5194/amt-9-3491-2016>, 2016.
- Krisna et al., ESA Climate Change Initiative “Plus” (CCI+) Algorithm Theoretical Basis Document (ATBD) Version 1.3 – For the RemoTeC XCO₂ and XCH₄ GOSAT-2 SRON Full Physics Products (CO₂_GO₂_SRFP and CH₄_GO₂_SRFP) Version 2.0.0 for the Essential Climate Variable (ECV) Greenhouse Gases (GHG), https://www.iup.uni-bremen.de/carbon_ghg/docs/GHG-CCIplus/CRDP7/ATBDv3_GHG-CCI_CO2_CH4_GO2_SRFP_v2p0p0.pdf, 2021
- Laughner, J. L., et al., The Total Carbon Column Observing Network's GGG2020 Data Version, *Earth Syst. Sci. Data*, 16, 2197–2260, <https://doi.org/10.5194/essd-16-2197-2024>, 2024 Lorente, A., Borsdorff, T., Landgraf, J., and the SRON L2 team, SRON RemoTeC-S5P scientific XCH₄ data product Product User Guide. 2022
- Kivi, R., Heikkinen, P., & Kyrö, E. (2022). TCCON data from Sodankylä (FI), Release GGG2020.R0 (Version R0) [Data set]. CaltechDATA. <https://doi.org/10.14291/tccon.ggg2020.sodankyla01.R0>



- Lunt et al., Rain-fed pulses of methane from East Africa during 2018–2019 contributed to atmospheric growth rate, *Environ. Res. Lett.*, 16, 024021, 2021
- Noël, S., et al. Retrieval of greenhouse gases from GOSAT and GOSAT-2 using the FOCAL algorithm, *Atmos. Meas. Tech.*, 15, 3401–3437, <https://doi.org/10.5194/amt-15-3401-2022>, 2022.
- Maasackers, J.D. *et al.*, Using satellites to uncover large methane emissions from landfills, *Sci. Adv.* **8**, DOI:[10.1126/sciadv.abn9683](https://doi.org/10.1126/sciadv.abn9683), 2022
- Notholt, J., Petri, C., Warneke, T., & Buschmann, M. (2022). TCCON data from Bremen (DE), Release GGG2020.R0 (Version R0) [Data set]. CaltechDATA. <https://doi.org/10.14291/tccon.ggg2020.bremen01.R0>
- O'Dell, C. W., Acceleration of multiple-scattering, hyperspectral radiative transfer calculations via low-streams interpolation, *J. Geophys. Res.*, 115, D10206, doi:10.1029/2009JD012803, 2010
- Parker, R. J., et al.: A decade of GOSAT Proxy satellite CH₄ observations, *Earth Syst. Sci. Data*, 12, 3383–3412, <https://doi.org/10.5194/essd-12-3383-2020>, 2020
- Reuter, M., Buchwitz, M., Schneising, O., Noël, S., Bovensmann, H., and Burrows, J. P.: A Fast Atmospheric Trace Gas Retrieval for Hyperspectral Instruments Approximating Multiple Scattering – Part 2: Application to XCO₂ Retrievals from OCO-2, *Remote Sens.*, 9, 1102, <https://doi.org/10.3390/rs9111102>, 2017a
- Reuter, M., Buchwitz, M., Schneising, O., Noël, S., Rozanov, V., Bovensmann, H., and Burrows, J. P.: A Fast Atmospheric Trace Gas Retrieval for Hyperspectral Instruments Approximating Multiple Scattering – Part 1: Radiative Transfer and a Potential OCO-2 XCO₂ Retrieval Setup, *Remote Sens.*, 9, 1159, <https://doi.org/10.3390/rs9111159>, 2017b
- Reuter, M., et al.: Ensemble-based satellite-derived carbon dioxide and methane column-averaged dry-air mole fraction data sets (2003–2018) for carbon and climate applications, *Atmos. Meas. Tech.*, 13, 789–819, <https://doi.org/10.5194/amt-13-789-2020>, 2020
- Rodgers, C.D., *Inverse Methods For Atmospheric Sounding: Theory And Practice*, World Scientific, 2000
- Schepers, D., et al., Methane retrievals from Greenhouse Gases Observing Satellite (GOSAT) shortwave infrared measurements: Performance comparison of proxy and physics retrieval algorithms, *J. Geophys. Res.*, 117, D10307, doi:[10.1029/2012JD017549](https://doi.org/10.1029/2012JD017549), 2012
- Schneising, O. (2022), Algorithm Theoretical Basis Document (ATBD) - TROPOMI WFM-DOAS (TROPOMI/WFMD) XCH₄. https://www.iup.uni-bremen.de/carbon_ghg/products/tropomi_wfmd/atbd_wfmd.pdf.
- Schneising, O., et al., Atmospheric greenhouse gases retrieved from SCIAMACHY: comparison to ground-based FTS measurements and model results, *Atmos. Chem. Phys.*, 12, 1527–1540, <https://doi.org/10.5194/acp-12-1527-2012>, 2012
- Schneising, O., et al., A scientific algorithm to simultaneously retrieve carbon monoxide and methane from TROPOMI onboard Sentinel-5 Precursor, *Atmos. Meas. Tech.*, 12, 6771–6802, <https://doi.org/10.5194/amt-12-6771-2019>, 2019
- Schneising, O., Buchwitz, M., Reuter, M., Vanselow, S., Bovensmann, H., and Burrows, J. P., Remote sensing of methane leakage from natural gas and petroleum systems revisited, *Atmos. Chem. Phys.*, 20, 9169–9182, <https://doi.org/10.5194/acp-20-9169-2020>, 2020
- Schneising, O., Buchwitz, M., Hachmeister, J., Vanselow, S., Reuter, M., Buschmann, M., Bovensmann, H., and Burrows, J. P. Advances in retrieving XCH₄ and XCO from Sentinel-5 Precursor: improvements in the scientific TROPOMI/WFMD algorithm, *Atmos. Meas. Tech.*, 16, 669–694, <https://doi.org/10.5194/amt-16-669-2023>, 2023



- Sussmann, R., & Rettinger, M. (2023). TCCON data from Garmisch (DE), Release GGG2020.R0 (Version R0) [Data set]. CaltechDATA. <https://doi.org/10.14291/tcon.ggg2020.garmisch01.R0>
- Té, Y., Jeseck, P., & Janssen, C. (2022). TCCON data from Paris (FR), Release GGG2020.R0 (Version R0) [Data set]. CaltechDATA. <https://doi.org/10.14291/tcon.ggg2020.paris01.R0>
- Wunch, D., Toon, G. C., Blavier, J.-F. L., Washenfelder, R. A., Notholt, J., Connor, B. J., Griffith, D. W. T., Sherlock, V., and Wennberg, P. O.: The Total Carbon Column Observing Network, *Philos. T. R. Soc. A*, 369, 2087–2112, <https://doi.org/10.1098/rsta.2010.0240>, 2011.
- Tsuruta A, Kivimäki E, Lindqvist H, Karppinen T, Backman L, Hakkarainen J, Schneising O, Buchwitz M, Lan X, Kivi R, et al., CH₄ Fluxes Derived from Assimilation of TROPOMI XCH₄ in CarbonTracker Europe-CH₄: Evaluation of Seasonality and Spatial Distribution in the Northern High Latitudes. *Remote Sensing*. 15(6):1620. <https://doi.org/10.3390/rs15061620>, 2023
- Warneke, T., Petri, C., Notholt, J., & Buschmann, M. (2022). TCCON data from Orléans (FR), Release GGG2020.R0 (Version R0) [Data set]. CaltechDATA. <https://doi.org/10.14291/tcon.ggg2020.orleans01.R0>
- Weidmann, D., Brownsword, R., & Doniki, S. (2023). TCCON data from Harwell, Oxfordshire (UK), Release GGG2020.R0 (Version R0) [Data set]. CaltechDATA. <https://doi.org/10.14291/tcon.ggg2020.harwell01.R0>
- Wunch, D., G. C. Toon, J.-F. L. Blavier, R. A. Washenfelder, J. Notholt, B. J. Connor, D. W. T. Griffith, V. Sherlock, and P. O. Wennberg (2011), The Total Carbon Column Observing Network, *Philos. Trans. R. Soc. A Math. Phys. Eng. Sci.*, 369(1943), 2087–2112, [doi:10.1098/rsta.2010.0240](https://doi.org/10.1098/rsta.2010.0240).
- Wunch, D., G. C. Toon, V. Sherlock, N. M. Deutscher, C. Liu, D. G. Feist, and P. O. Wennberg (2015), The Total Carbon Column Observing Network's GGG2014 Data Version, Pasadena, California
- Yoshida, Y., et al., Improvement of the retrieval algorithm for GOSAT SWIR XCO₂ and XCH₄ and their validation using TCCON data, *Atmos. Meas. Tech.*, 6, 1533–1547, <https://doi.org/10.5194/amt-6-1533-2013>, 2013.
- Yoshida, Y., Y. Someya, H. Ohyama, I. Morino, T. Matsunaga, N. M. Deutscher, D. W. T. Griffith, F. Hase, L. T. Iraci, R. Kivi, J. Notholt, D. F. Pollard, Y. Té, V. A. Velasco, and D. Wunch, Quality evaluation of the column-averaged dry air mole fractions of carbon dioxide and methane observed by GOSAT and GOSAT-2. *SOLA*, 19, 173–184, [doi:10.2151/sola.2023-023](https://doi.org/10.2151/sola.2023-023), 2023
- Yoshida and Oshio, 2020: Y. Yoshida and H. Oshio: GOSAT-2 TANSO-FTS-2 SWIR L2 Retrieval Algorithm Theoretical Basis Document, National Institute for Environmental Studies, GOSAT-2 Project https://prdct.gosat-2.nies.go.jp/documents/pdf/ATBD_FTS-2_L2_SWL2_en_00.pdf, 2020



<https://eyeclima.eu>

BRUSSELS, 19 09 2024

Funded by the European Union. Views and opinions expressed are however those of the author(s) only and do not necessarily reflect those of the European Union. Neither the European Union nor the granting authority can be held responsible for them.



This project has received funding from the European Union's Horizon Europe research and innovation programme under grant agreement No 101081395